

Updated CPUE standardizations for bigeye and yellowfin tuna caught by Taiwanese longline fishery in the Indian Ocean using generalized linear model

Yu-Min Yeh¹, Simon Hoyle² and Shu-Ting Chang³

¹Department of Tourism Management and Master Program of Leisure Environment Management, Nanhua University, 55, Sec. 1, Nanhu Rd. Chung Keng Li, Dalin, Chiayi 62248, Taiwan

²IOTC consultant, New Zealand. Email: simon.hoyle@gmail.com.

³Overseas Fisheries Development Council of the Republic of China, 3F, No, 14, Wenzhou St., Da'an Dist., Taipei 106, Taiwan (R.O.C.)

Abstract

Updated Taiwanese longline fishery data to 1979-2017 were used in this analysis. We used cluster analysis to classify longline sets into groups based on the species composition of the catch, to understand whether cluster analysis could identify distinct fishing strategies. Bigeye and yellowfin tuna CPUE were then standardized. All analyses were based on the approaches used by the collaborative workshop of longline data and CPUE standardization for bigeye and yellowfin tuna held in June 2018 in Taipei.

Introduction

The Working Party on Tropical Tunas (WPTT) and the Scientific Committee of the Indian Ocean Tuna Commission (IOTC) have noted that the CPUE trends from longline fisheries for bigeye tuna in the Indian Ocean differ considerably between Taiwan and Japan (Anonymous 2013a). Much effort has been devoted to dealing with this issue from various point of views, considering data quality, data management systems, analytical methods, etc. (Anonymous, 1998; OFDC, 2013; Hoyle S., 2014; Okamoto H., 2014; Yeh, 2014). In June 2018, several collaborative studies were conducted between national scientists with expertise in Japanese, Taiwanese, Korean fleets, Seychelles longline fleets, an IOTC scientist, and an independent scientist, Dr. Simon Hoyle. The workshops addressed Terms of Reference covering several important and longstanding issues related to the albacore, bigeye and yellowfin tuna CPUE indices in the Indian Ocean.

In this analysis, a framework analysis suggested by the collaborative study was conducted using updated Taiwanese operational data.

Materials and methods

In this analysis, operational catch and effort data with 1 degree by 1 degree resolution from the

logbooks of Taiwanese longline fishery from 1979-2017 were used, as provided by Overseas Fisheries Development Council (OFDC). From 2013, the Taiwanese Fisheries Agency has supported the Taiwanese pelagic longline fishery industry in submitting logbook data via an E-logbook system. In 2015 the E-logbook coverage rate reached over 80%, and attained 100% after 2016. Therefore, data were compiled from E-logbooks after 2015.

Data preparation and cleaning were performed by adopting the suggestions made by the collaborative work (IOTC, 2015). Each set was allocated to a bigeye region and a yellowfin region (Figure 1). Basically, the region definitions conformed to the 2017 joint work (Hoyle et al, 2017). Except for the conventional region 2 of the region structure used to estimate yellowfin CPUE indices, the region was divided into region 2N and region 2S along latitude 0° conforming to the 2015 bigeye assessment model.

Cluster analysis

We adopted the hierarchical clustering method Ward hclust (IOTC, 2015) to identify effort associated with different fishing strategies. The cluster analysis was performed separately for regions for both bigeye and yellowfin. Analyses used species composition to group the data. The data were transformed by centering and scaling, so as to reduce the dominance of species with higher average catches. For this analysis, we aggregated the data by vessel-month to reduce the variability, and therefore reduce misallocation of sets. The assumption is that we believe individual vessels tend to follow a consistent fishing strategy in a month period. More detailed information can be referred to the collaborative work report (IOTC, 2017).

CPUE standardization

CPUE standardization methods adopted the suggestions made from the collaborative work (IOTC, 2017) for Taiwanese fleet to include year-quarter, vessel id, and five by five $^{\circ}$ latitude and longitude grids as main effects. Cluster is also included as a main effect in the model. Analyses were conducted separately for each region, and for bigeye and yellowfin. CPUE Indices were estimated using two approaches, delta lognormal and lognormal + constant, but the primary approach was the delta lognormal. More detailed information can be obtained from the collaborative work report (IOTC, 2018).

The effects of covariates were examined using the package *influ* (Bentley *et al.* 2011) to show the influence of each covariate. For the final analyses, data were prepared by selecting operational data by region, for vessels that had fished for 8 quarters in that region. Data in GLM were 'area-weighted', with the weights of the sets adjusted so that the total weight per year-quarter in each 5 degree square would sum to 1. For both species for the GLMs, model fits were examined by plotting the residual densities and using Q-Q plots.

The operational data were standardized using generalized linear models in R. All analyses were performed using R source code freely shared by Simon Hoyle in the collaborative work.

Results and Discussions

The recent status of Taiwanese tuna longline fisheries

Figure 2 ~ 6 showed the historical evolution of Taiwanese tuna longline fishing effort and number of hooks between floats (NHBF), bigeye and yellowfin catch and nominal CPUE by 5 degree square from 1979 to 2017. Overall speaking, recent years, the scope of fishing grounds by Taiwanese tuna longline vessels had been shrinking. Large NHBF is more common, even in the temperate Indian Ocean, since more vessels equipped with American style rolling machine which can be setting and hauling more faster.

Cluster analysis

The aims of the cluster analysis were to identify whether cluster analysis could identify distinct fishing strategies in each region; secondly to use the cluster analysis to identify these fishing strategies in the data for each region, and so to better understand the fishing practices.

In BET region 1N, 1S and 2, we identified 5 clusters as the number with the most support (Figure 4), However, using cluster analysis to identify bigeye and yellowfin targeting is challenging, since targeting is probably less an either/or strategy than a mixture of variables that shift the species composition one way or the other (Table 1).

In BET region 3, we identified 4 clusters as the number with the most support (Figure 5), we found that species composition averaging 82% 'other' in one cluster, suggesting that oilfish targeting can represent the majority of the catch, 84% albacore in another cluster, a mix of bigeye, yellowfin and albacore in a third cluster, and a mix of swordfish, albacore, bigeye in a fourth cluster were identified at the trip level by hcltrip (Table 1).

In BET region 4, we identified 4 clusters as the number with the most support (Figure 5), we found that species composition averaging 84% albacore in one cluster, a mix of 58% albacore and 30% 'other' in another cluster, a mix of bigeye, yellowfin, albacore and swordfish in a third cluster, and a mix of 52% albacore, 26% southern Bluefin tuna and 12% other fish in a fourth cluster, were identified at the trip level by hcltrip (Table 1).

For BET regions, for each cluster in every region, the corresponding fishing strategies were revealed by the various distribution of fishing year, month, number of hooks between floats, location, number of hooks associated with sets in each cluster (Figure 9 ~18).

In YFT region 2N, we identified 5 clusters as the number with the most support (Figure 19). Also, except one cluster with 24% other fish, using cluster analysis to identify bigeye and yellowfin targeting is challenging, since targeting is probably less an either/or strategy than a mixture of variables that shift the species composition one way or the other (Table 2).

In YFT region 2S, we identified 5 clusters as the number with the most support (Figure 19). Also, except one cluster with 30% other fish, using cluster analysis to identify bigeye and yellowfin targeting is challenging, since targeting is probably less an either/or strategy than a mixture of variables that shift the species composition one way or the other (Table 2).

In YFT region 3, we identified 5 clusters as the number with the most support (Figure 19). We found that species composition averaged 92% ‘other’ in one cluster, suggesting that oilfish targeting can represent the majority of the catch; 80% albacore in another cluster; a mix of bigeye, yellowfin, albacore and swordfish in a third cluster; and a mix of albacore, bigeye, yellowfin in a fourth cluster were identified at the trip level by hcltrip (Table 2).

In YFT region 4, we identified 5 clusters as the number with the most support (Figure 20), we found that species composition averaging 87% albacore in one cluster, 70% albacore in another cluster, a mix of 59% albacore and 28% ‘other fish’ in third cluster, a mix of bigeye, yellowfin, albacore and swordfish in a fourth cluster, and a mix of 52% albacore, 22% southern Bluefin tuna and 12% bigeye in a fifth cluster, were identified at the trip level by hcltrip (Table 2).

In YFT region 5, we identified 5 clusters as the number with the most support (Figure 20). we found that species composition averaging 83% albacore in one cluster, 78% bigeye and 10% yellowfin in another cluster, 27% bigeye and 44% yellowfin in a third cluster, and 53% bigeye and 27% ‘other’ in a fourth cluster were identified at the trip level by hcltrip (Table 2).

For YFT regions, for each cluster in every region, the corresponding fishing strategies were revealed by the various distribution of fishing year, month, number of hooks between floats, location, number of hooks associated with sets in each cluster (Figure 21 ~29).

CPUE indices

Vessel effects for the Taiwanese fleets operating in region 1S and region 4 of BET region (Figure 31 and Figure 34) showed increasing catchability of bigeye tuna, while for other regions, there was little apparent change in catchability through time (Figure 30, 32 ~ 33) Vessel effects for the Taiwanese fleets operating in region 4 of YFT region (Figure 37) showed increasing catchability of yellowfin tuna, while for other regions, there was little apparent change in catchability through time (Figure 35~36, 38).

For covariate effects, we present an example result for bigeye in region 1N. The coefficients for each vessel (bottom right, Figure 30) show much variation and there are changes in the distribution of records among vessels, resulting in variable changes in annual influence (right panel). The high influence in 1979 arises because there was a greater than usual proportion of effort from vessels with higher coefficients. The spatial distributions of fishing sets (latlong effect) were fairly stable through time with some exceptions. The high influence in around 2012 arises because there was a greater than usual proportion of effort occurred in the Somalia area with the highest coefficients. The coefficients for each cluster (bottom left, Figure 30) show there was one cluster (TW2) with much higher catchability than the other three clusters. There were changes in the distribution of records among clusters, resulting in variable changes in annual influence.

We excluded low-target clusters from the dataset and included the cluster effect in the model. For bigeye tuna the western tropical indices in regions 1N and 1S (blue line, the top two plots in Figure 39) show no strong trend through time. There was a spike in 2012 followed by a moderate decline in the latest 6 years. In the eastern tropical area (region 2) and temperate area there was also no strong trend

through time with relatively lower signal in the last two years. For yellowfin tuna, indices in the western tropical region 2N and 2S CPUE (Figure 40) increased from 1979 to 1987 and then declined until 1989, fluctuated during 1990-2006 then declined to 2010, and then increased to a spike in 2012. After that time it remained close to the lowest level observed. The eastern tropical region 5 from 1989 declined steadily to 2006, and declined more dramatically to 2016. It was also close to the lowest level in the time series by 2016.

Yellowfin in western temperate region 3 CPUE declined steadily to 2011, and then remained but with significant variability (Figure 40). Increased showed a followed a similar pattern to the western tropical indices, with a decline until the mid-1970s followed by an increase until the late 1980s, and subsequently a slow decline with significant variability (Figure 40). In eastern temperate region 4, it seems that more data was excluded in this analysis which led to many jumps. Based on earlier analysis, from 1995 CPUE showed a decline pattern with significant variability and reached their lowest observed levels by 2016.

For both species for the delta lognormal models, model fits were presented by using Q-Q plots (Figure 41 and Figure 42) and plotting the residual densities plots (Figure 43 - 52).

References

- Anonymous (1998). Critical review of the data collection and processing system of Chinese Taipei, and revision of statistics for its LL fleet (Taipei, July 1997). SCRS/97/017, ICCAT: 141-204.
- Bentley, N., T. H. Kendrick, P. J. Starr and P. A. Breen (2011). "Influence plots and metrics: tools for better understanding fisheries catch-per-unit-effort standardizations." *ICES Journal of Marine Science* 69(1): 84-88.
- Hoyle S. (2014). Spatial considerations in bigeye and yellowfin CPUE from Japanese and Taiwan,China longline fisheries in the Indian Ocean (Hoyle S). Working Party on Tropical Tuna, Indian Ocean Tuna Commission. IOTC–2014–WPTT16–25.
- Hoyle, S. D., and H. Okamoto. 2015. Descriptive analyses of the Japanese Indian Ocean longline fishery, focusing on tropical areas. Indian Ocean Tuna Commission Working Party on Tropical Tunas.
- Hoyle, S. D., H. Okamoto, Y.-m. Yeh, Z. G. Kim, S. I. Lee, and R. Sharma. 2015b. IOTC–CPUEWS02 2015: Report of the 2nd CPUE Workshop on Longline Fisheries, 30 April – 2 May 2015. Indian Ocean Tuna Commission.
- Hoyle, S. D., Y.-M. Yeh, S.-T. Chang, and R.-F. Wu. 2015c. Descriptive analyses of the Taiwanese Indian Ocean longline fishery, focusing on tropical areas. Indian Ocean Tuna Commission Working Party on Tropical Tunas.

- Hoyle, S. D., C. Assan, , S.-T. Chang, F. Dan, R. Govinden, D.M. Kim, T. Kitakado, S. I. Lee, J. Lucas, T. Matsumoto, and Y.-M Yeh¹. Collaborative study of tropical tuna CPUE from multiple Indian Ocean longline fleets in 2017.
- IOTC (2015). Report of the 2nd CPUE Workshop on Longline Fisheries. IOTC–2015–CPUEWS02–R[E]
- Indian Ocean. Working Party on Tropical Tuna, Indian Ocean Tuna Commission. IOTC–2014–WPTT16–28.
- Langley, A., M. Herrera and J. Million (2012). Stock assessment of yellowfin tuna in the Indian Ocean using MULTIFAN-CL. Working Party on Tropical Tuna, Indian Ocean Tuna Commission. IOTC–2012–WPTT14–38 Rev_1.
- Langley, A. 2016. Stock assessment of bigeye tuna in the Indian Ocean for 2016-model development and evaluation. IOTC Proceedings, volume IOTC-2016-WPTT18-20, page 98p, Victoria, Seychelles:11-13.
- Lee, Y.-C. and H.-C. Liu (1996). The tuna statistics procedures of Taiwan longline and gillnet Fisheries in the Indian Ocean." IPTP Collective Volumes(9): 368-369.
- Okamoto H (2014). Provisional analysis on comparison of CPUE trend of bigeye and yellowfin tuna between Japanese and Taiwan-China longline fisheries based on whole and shared strata in the Overseas Fisheries Development Council (2013). Data Collection and Processing System of Statistics for the Taiwanese Deep-Sea Longline Fishery. IOTC Working Party on Tropical Tunas (WPTT) 15. San Sebastian, Spain. IOTC–2013–WPTT15–40 Rev_1.
- Simon D. Hoyle, Doo Nam Kim, Sung Il Lee, Takayuki Matsumoto, Kaisuke Satoh, and Yu-Min Yeh. (2016). Collaborative study of tropical tuna CPUE from multiple Indian Ocean longline fleets in 2016. IOTC-2016-WPTT18-14.
- Simon D. Hoyle, Cindy Assan, Shu-Ting Chang, Dan Fu, Rodney Govinden, Doo Nam Kim, Sung Il Lee, Juliette Lucas, Takayuki Matsumoto, Kaisuke Satoh, Yu-Min Yeh, and Toshihide Kitakado. (2017). Collaborative study of tropical tuna CPUE from multiple Indian Ocean longline fleets in 2017. IOTC-2017-WPTT19-32.
- Simon D. Hoyle , Emmanuel Chassot , Dan Fu , Doo Nam Kim , Sung Il Lee, Takayuki Matsumoto, Kaisuke Satoh, Sheng-Ping Wang, Yu-Min Yeh, and Toshihide Kitakado. (2018). Collaborative study of tropical tuna CPUE from multiple Indian Ocean longline fleets in 2018. IOTC-2018-WPTT20-XX.
- Yeh, Y.-M. (2014). Preliminary analysis of Taiwanese longline fisheries based on operational catch and effort data for bigeye and yellowfin tuna in the Indian Ocean. Working Party on Tropical Tuna, Indian Ocean Tuna Commission. IOTC–2014–WPTT16–42.
- R Core Team. 2016. R: A Language and Environment for Statistical Computing. R Foundation for Statistical Computing, Vienna, Austria.

¹ Nanhua University, invited Taiwanese expert.

Table 1. For Taiwanese effort in the BET region 1N, 1S, 2, 3, and 4, average percentage of each species per set, by cluster, as estimated by cluster analysis.

Region	Cluster	Albacore	Bigeye tuna	Yellowfin tuna	Swordfish	Strip marlin	Blue marlin	Other fishes	Southern Bluefin tuna
1N	1	0.1%	30.8%	20.9%	26.2%	6.5%	9.7%	5.7%	0.0%
	2	0.7%	64.7%	16.1%	9.2%	1.7%	3.2%	4.5%	0.0%
	3	0.2%	39.6%	46.0%	7.4%	1.6%	2.4%	2.9%	0.0%
	4	0.3%	36.4%	20.6%	11.5%	1.4%	3.9%	25.8%	0.0%
	5	0.4%	54.3%	18.5%	13.7%	2.9%	4.1%	0.4%	5.7%
1S	1	51.2%	18.6%	15.2%	2.4%	0.7%	1.5%	10.3%	0.0%
	2	1.5%	36.2%	26.2%	16.6%	4.1%	6.7%	7.1%	1.6%
	3	2.2%	39.1%	43.0%	6.2%	1.1%	2.6%	5.7%	0.0%
	4	2.4%	42.9%	17.2%	6.0%	0.8%	2.8%	27.9%	0.0%
	5	1.3%	67.5%	15.6%	6.7%	1.0%	2.2%	5.6%	0.0%
2	1	0.9%	77.0%	12.6%	4.2%	2.1%	2.2%	1.0%	0.0%
	2	0.7%	38.9%	24.3%	9.7%	18.5%	5.8%	0.9%	1.2%
	3	66.5%	15.8%	11.7%	2.4%	1.1%	1.1%	1.5%	0.0%
	4	2.5%	53.5%	29.6%	5.8%	3.5%	3.2%	1.8%	0.0%
	5	1.9%	58.5%	8.3%	4.9%	0.7%	2.9%	22.9%	0.0%
3	1	84.2%	5.0%	4.2%	1.5%	0.3%	0.3%	3.8%	0.7%
	2	24.4%	36.2%	18.4%	10.5%	1.3%	1.0%	5.2%	3.0%
	3	17.5%	17.2%	10.5%	48.5%	1.3%	0.8%	4.0%	0.3%
	4	8.6%	3.8%	1.8%	3.0%	0.2%	0.1%	82.2%	0.2%
4	1	84.4%	7.8%	2.7%	1.3%	0.5%	0.2%	1.6%	1.4%
	2	24.2%	37.0%	16.8%	11.0%	1.7%	1.0%	3.7%	4.6%
	3	57.5%	4.9%	1.4%	1.3%	0.0%	0.0%	29.7%	5.1%
	4	51.9%	7.6%	1.2%	1.5%	0.1%	0.1%	11.8%	25.9%

Table 2. For Taiwanese effort in the YFT region 2N, 2S, 3, 4, and 5, average percentage of each species per set, by cluster, as estimated by cluster analysis.

Region	Cluster	Albacore	Bigeye tuna	Yellowfin tuna	Swordfish	Strip marlin	Blue marlin	Other fishes	Southern Bluefin tuna
2N	1	0.1%	70.5%	12.5%	8.4%	1.5%	3.3%	3.6%	0.0%
	2	1.0%	53.8%	27.8%	10.5%	1.5%	2.6%	2.7%	0.0%
	3	0.2%	37.8%	18.4%	22.3%	6.0%	9.1%	5.0%	1.3%
	4	0.3%	40.9%	18.2%	11.2%	1.3%	3.8%	24.3%	0.0%
	5	0.1%	25.5%	58.4%	6.8%	2.1%	2.4%	4.7%	0.0%
2S	1	6.2%	35.6%	26.3%	15.5%	3.1%	5.2%	7.3%	0.9%
	2	0.8%	50.0%	32.3%	6.9%	1.5%	3.4%	5.2%	0.0%
	3	1.4%	40.9%	16.4%	7.1%	0.9%	3.5%	29.7%	0.0%
	4	1.1%	69.2%	15.7%	5.7%	0.8%	1.8%	5.8%	0.0%
	5	1.2%	24.8%	60.4%	5.0%	0.9%	2.0%	5.7%	0.0%
3	1	80.4%	5.1%	7.5%	1.7%	0.3%	0.5%	4.4%	0.1%
	2	13.0%	27.1%	37.3%	7.0%	2.5%	2.2%	9.0%	1.9%
	3	11.2%	57.8%	13.0%	5.6%	0.7%	1.3%	9.8%	0.7%
	4	4.2%	1.4%	0.7%	1.0%	0.0%	0.0%	92.4%	0.2%
	5	17.0%	22.3%	11.2%	44.1%	1.2%	0.6%	3.3%	0.3%
4	1	87.0%	6.6%	2.7%	1.2%	0.4%	0.2%	1.3%	0.6%
	2	58.6%	5.9%	1.9%	1.4%	0.1%	0.1%	28.5%	3.5%
	3	20.6%	38.4%	20.9%	12.9%	1.5%	1.3%	3.4%	1.0%
	4	51.9%	12.1%	2.6%	2.3%	0.2%	0.2%	8.5%	22.3%
5	1	2.5%	60.4%	23.2%	5.8%	3.3%	3.0%	1.4%	0.2%
	2	0.5%	26.9%	43.6%	8.1%	12.2%	5.5%	3.2%	0.0%
	3	83.2%	5.6%	6.6%	2.1%	0.9%	0.8%	0.7%	0.0%
	4	2.1%	53.0%	9.2%	5.2%	0.7%	2.9%	26.9%	0.0%

5

1.3%

78.3%

9.8%

4.2%

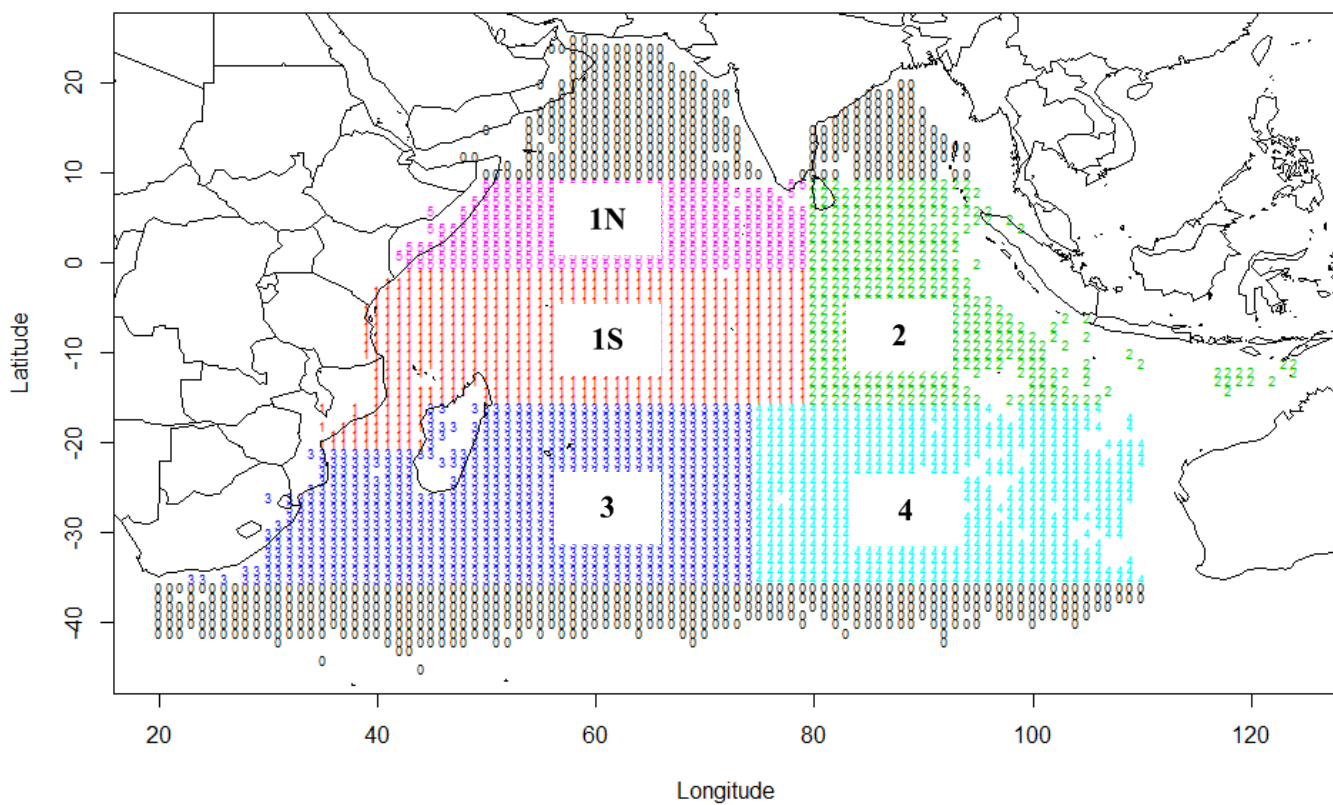
1.6%

1.8%

3.0%

0.0%

regB3



regY2

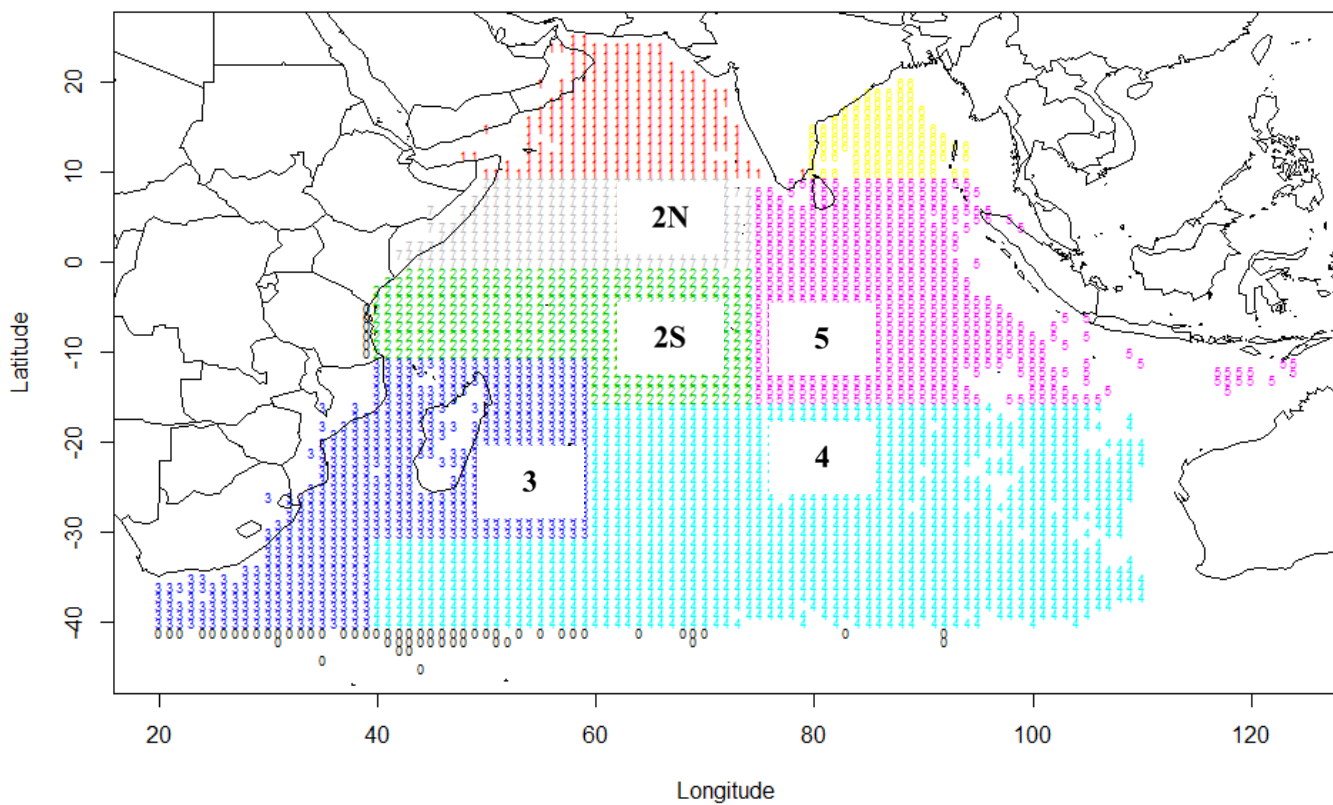


Figure 1. Spatial stratification of the Indian Ocean for this analysis.

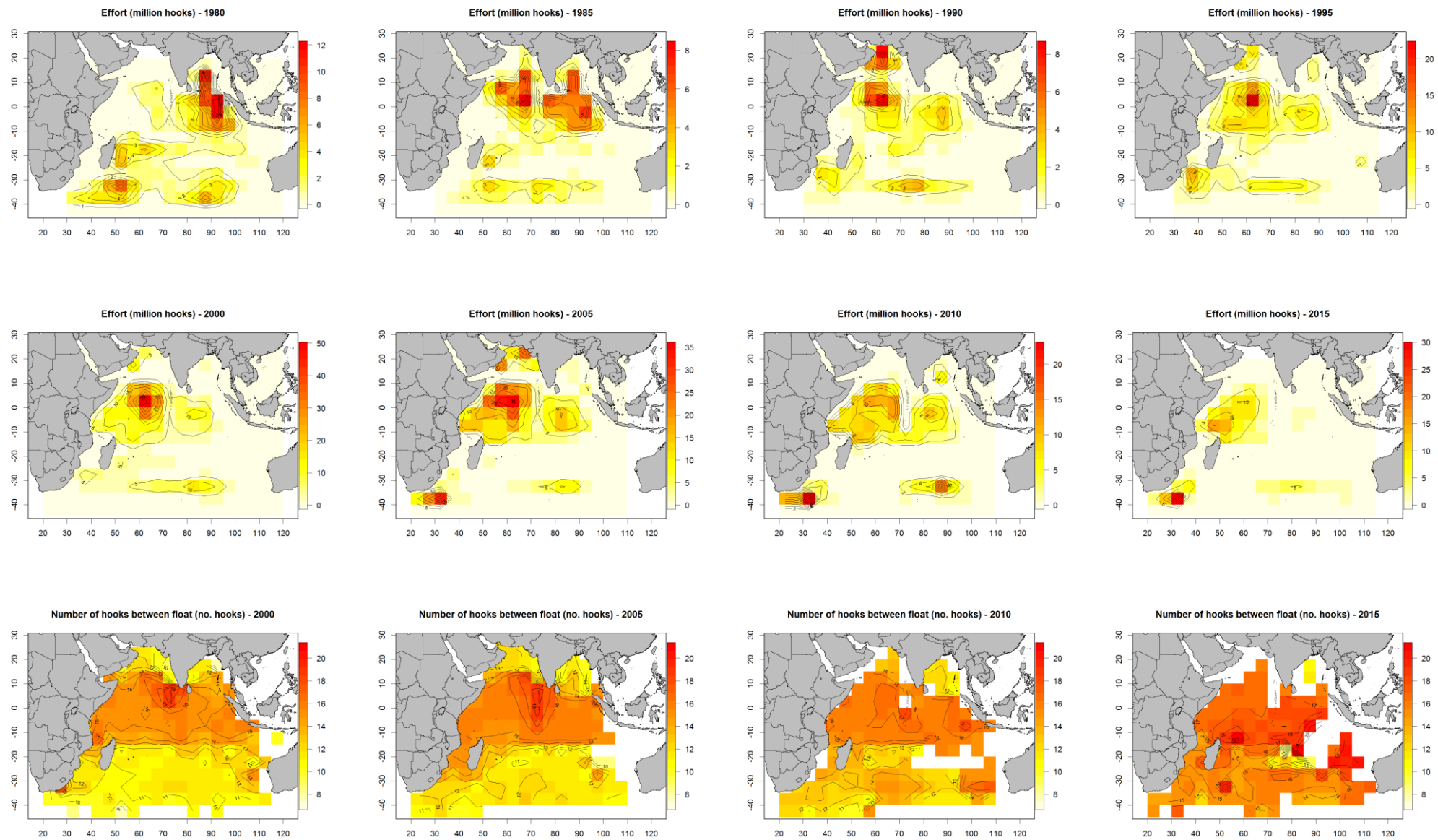


Figure 2. Maps of Taiwanese longline effort (top two rows) and number of hooks between floats (bottom row) by 5x5 grids for per five years from 1979 to 2017.

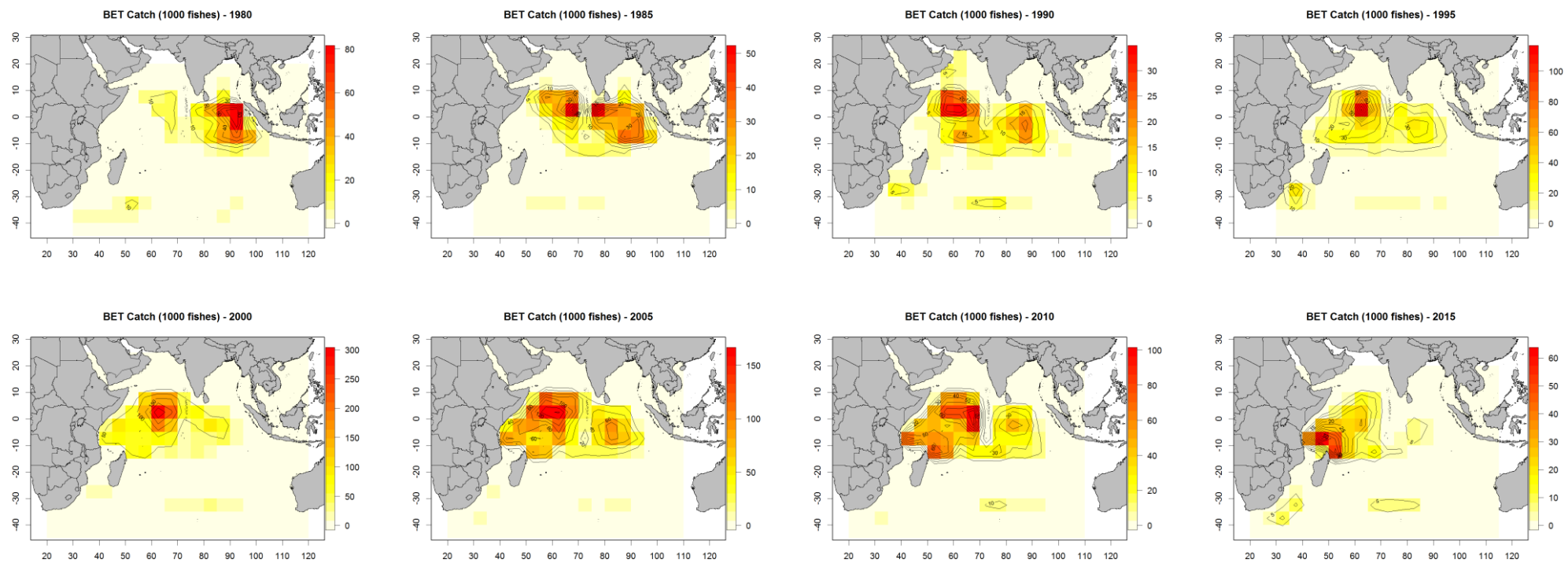


Figure 3. Maps of Taiwanese longline bigeye catch by 5x5 grids for per five years from 1979 to 2017.

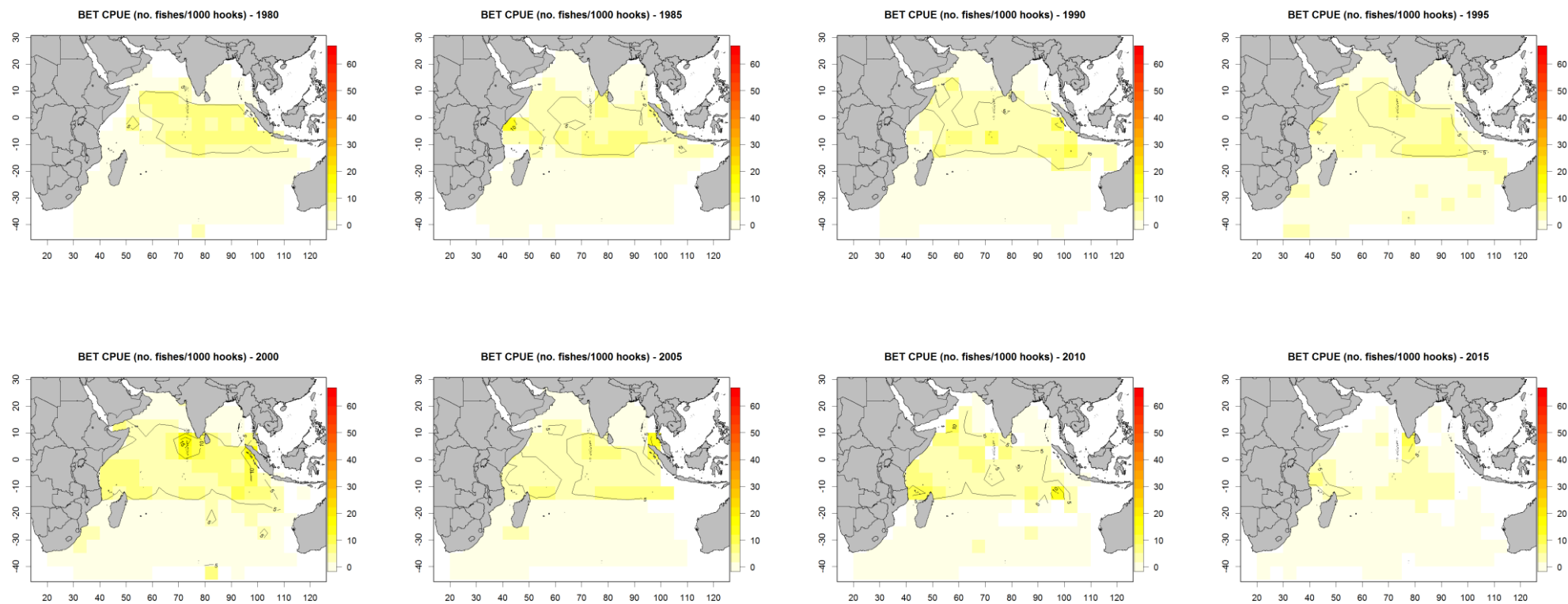


Figure 4. Maps of Taiwanese longline bigeye CPUE by 5x5 grids for per five years from 1979 to 2017.

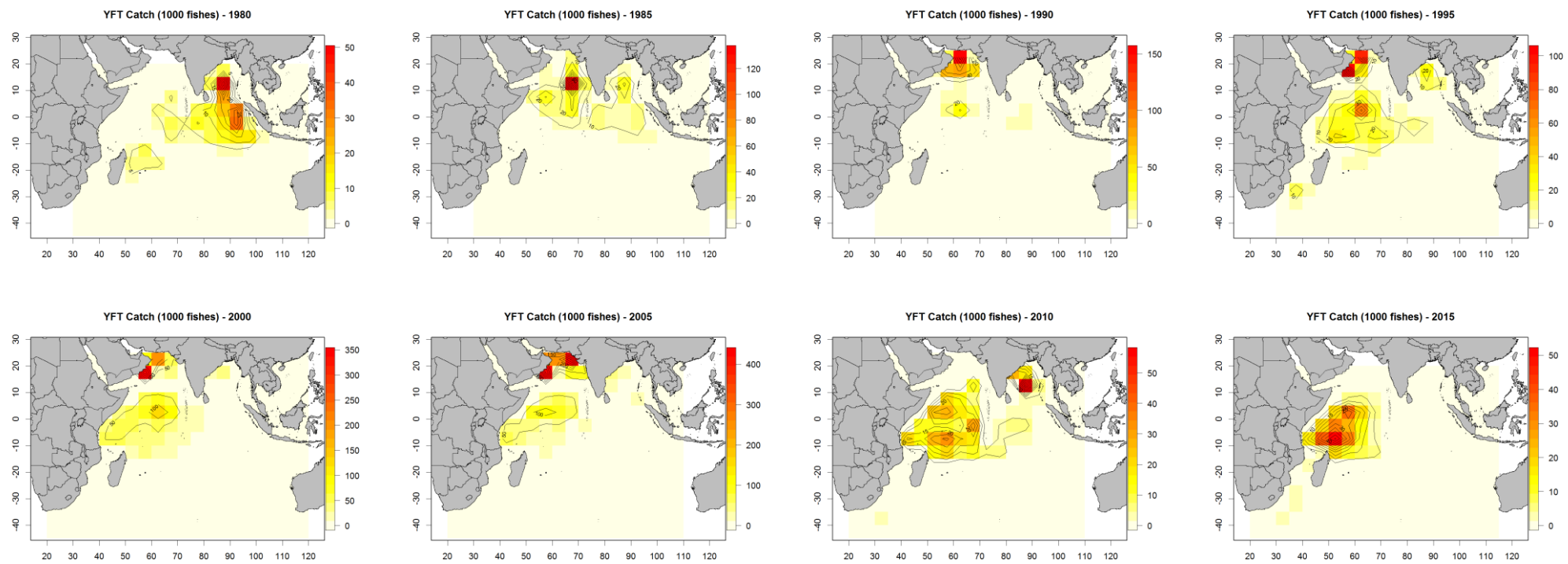


Figure 5. Maps of Taiwanese longline yellowfin catch by 5x5 grids for per five years from 1979 to 2017.

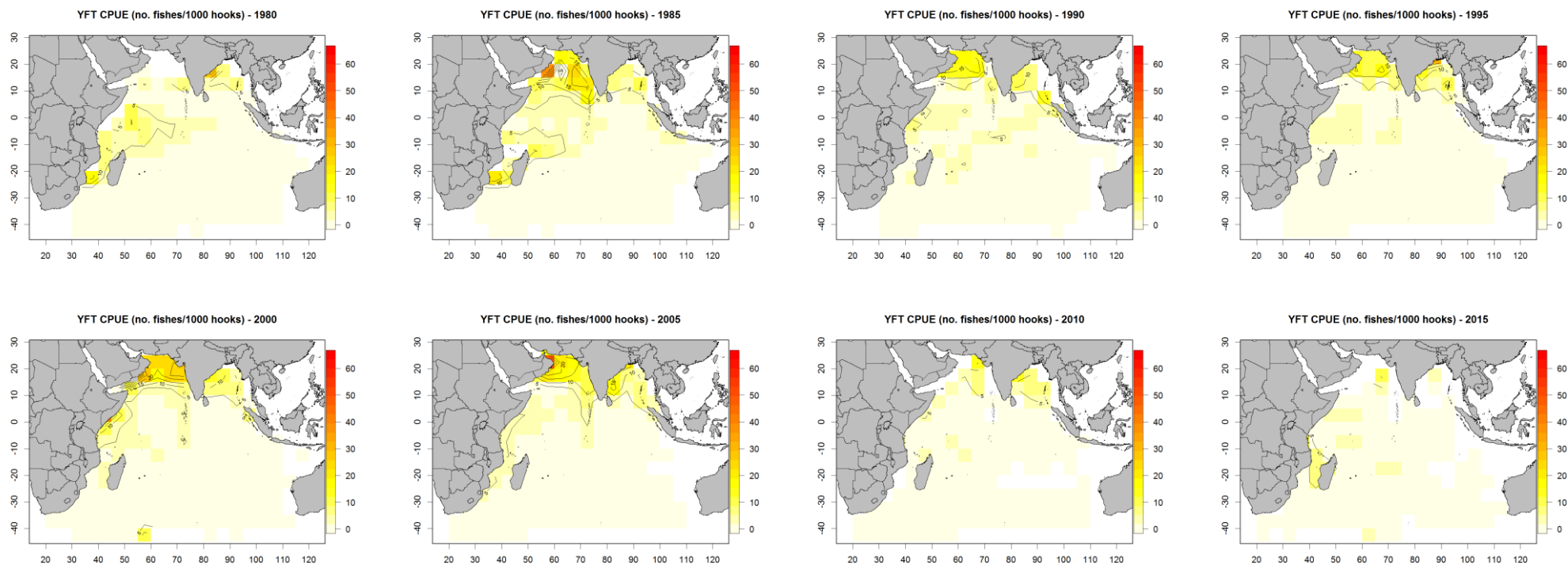


Figure 6. Maps of Taiwanese longline yellowfin CPUE by 5x5 grids for per five years from 1979 to 2017.

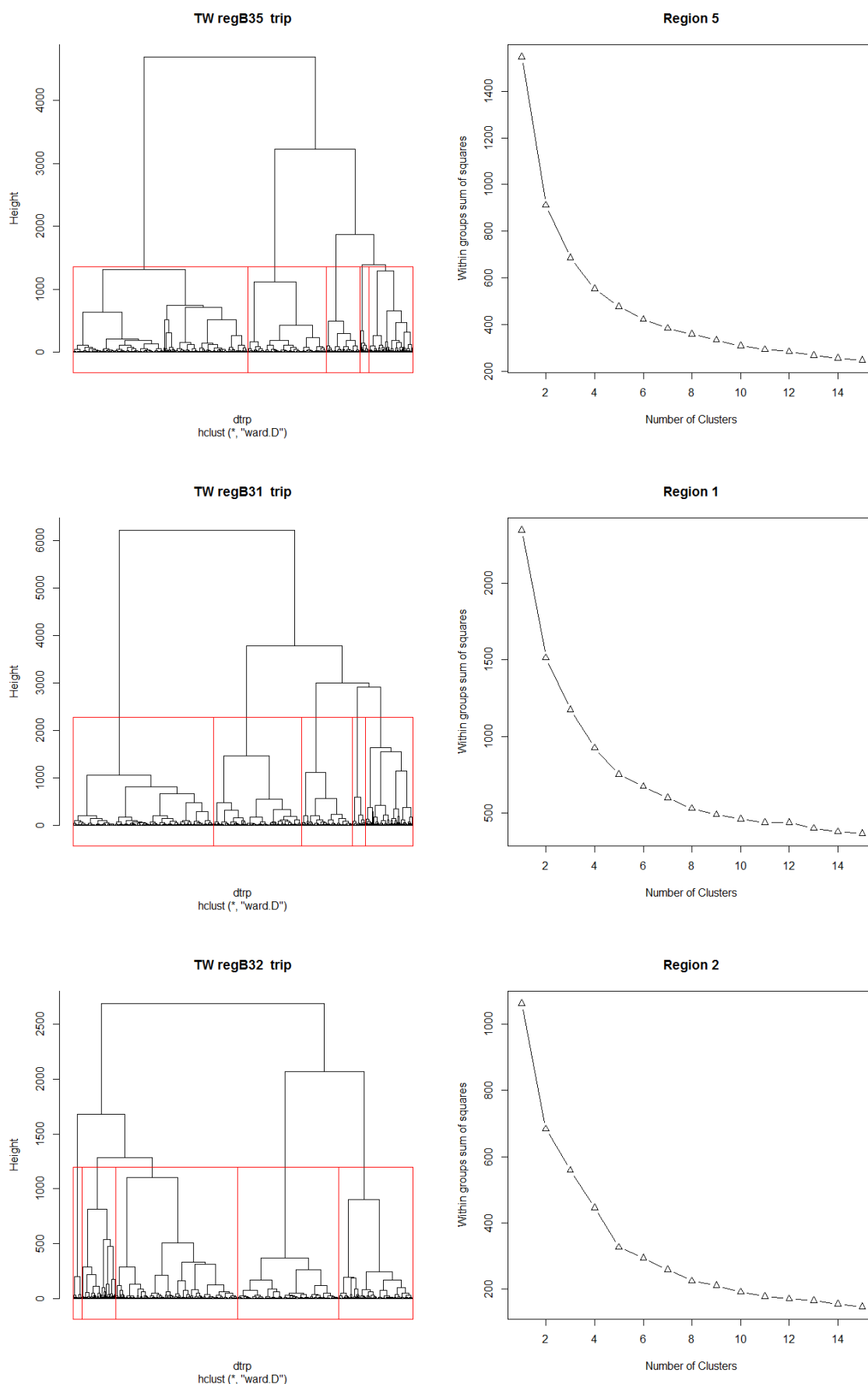


Figure 7. Plots showing analyses to estimate the number of distinct classes of species composition in Taiwanese region 1N, 1S, 2 of B3. These are based on a hierarchical Ward clustering analysis of trip-level data (top left); within-group sums of squares from kmeans analyses with a range of numbers of clusters (top right); and analyses

of the numbers of components to retain from a principal component analysis of trip-level (bottom left) data.

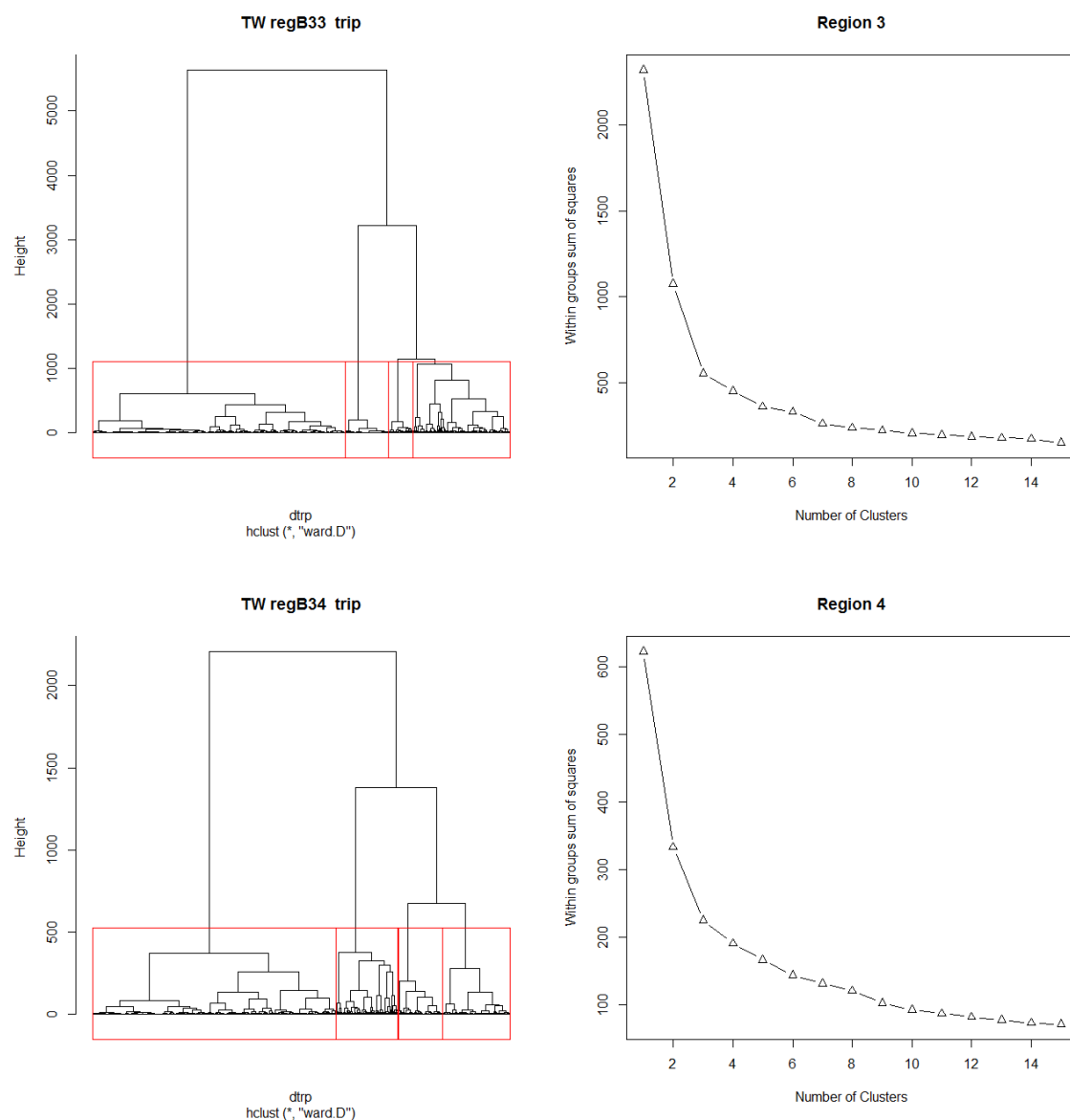


Figure 8. Plots showing analyses to estimate the number of distinct classes of species composition in Taiwanese region 3 and 4 of B3. These are based on a hierarchical Ward clustering analysis of trip-level data (top left); within-group sums of squares from kmeans analyses with a range of numbers of clusters (top right); and analyses of the numbers of components to retain from a principal component analysis of trip-level (bottom left) data.

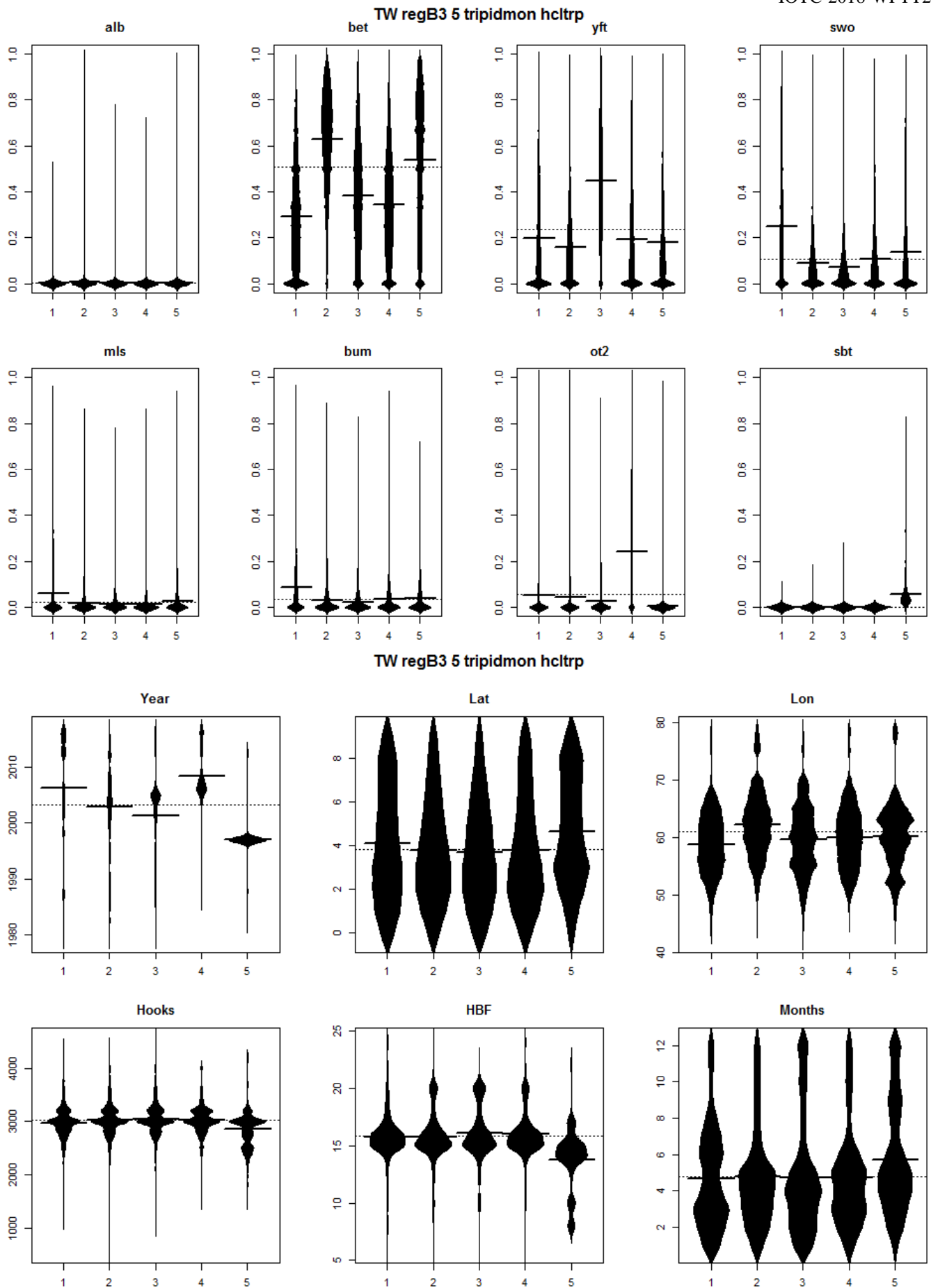


Figure 9. For Taiwanese effort in region 1N of B3 for the period 1979-2017, for each species, boxplot of the proportion of the species in the trip versus the cluster. The widths of the boxes are proportional to the numbers of trips in each cluster (above). Boxplot showing the distributions of variables associated with sets in each hcltrp

cluster (below). Clustering was performed using a hierarchical Ward clustering analysis of trip-level data.

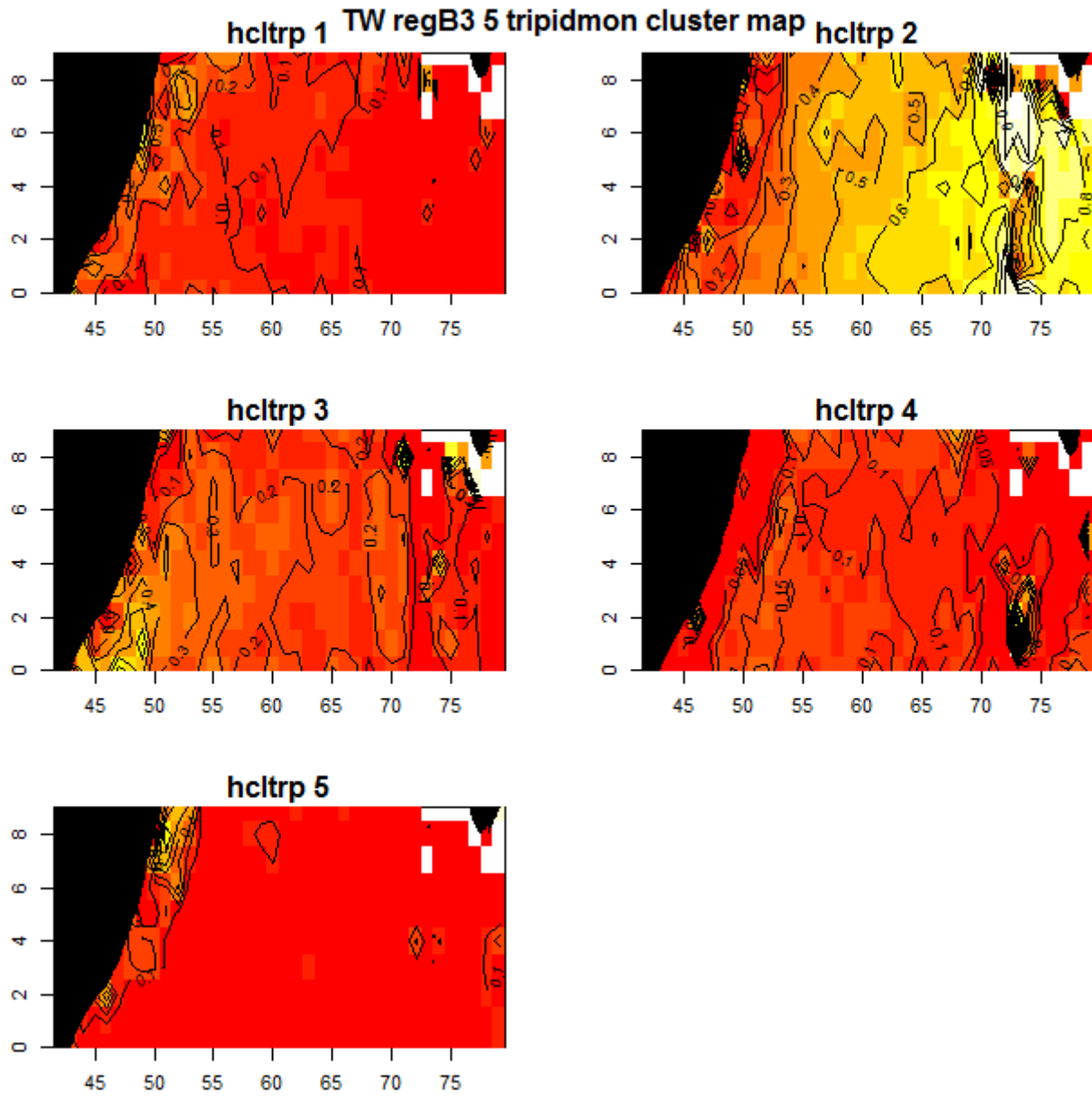


Figure 10. Maps of the spatial distributions of clusters in region 1N of B3 for Taiwanese effort.

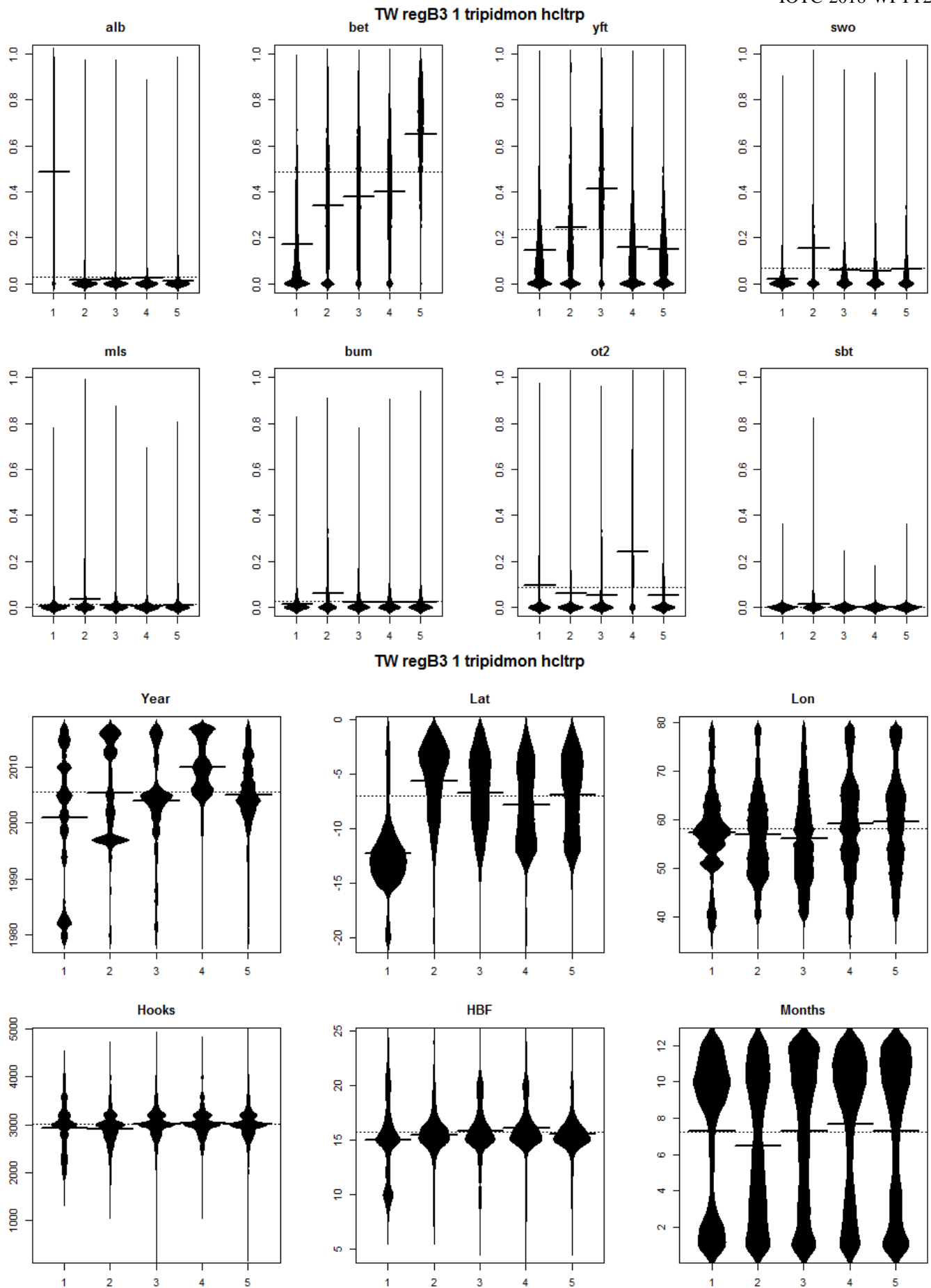


Figure 11. For Taiwanese effort in region 1S of B3 for the period 1979-2017, for each species, boxplot of the proportion of the species in the trip versus the cluster. The widths of the boxes are proportional to the numbers of trips in each cluster (above). Boxplot showing the distributions of variables associated with sets in each hcltrp

cluster (below). Clustering was performed using a hierarchical Ward clustering analysis of trip-level data.

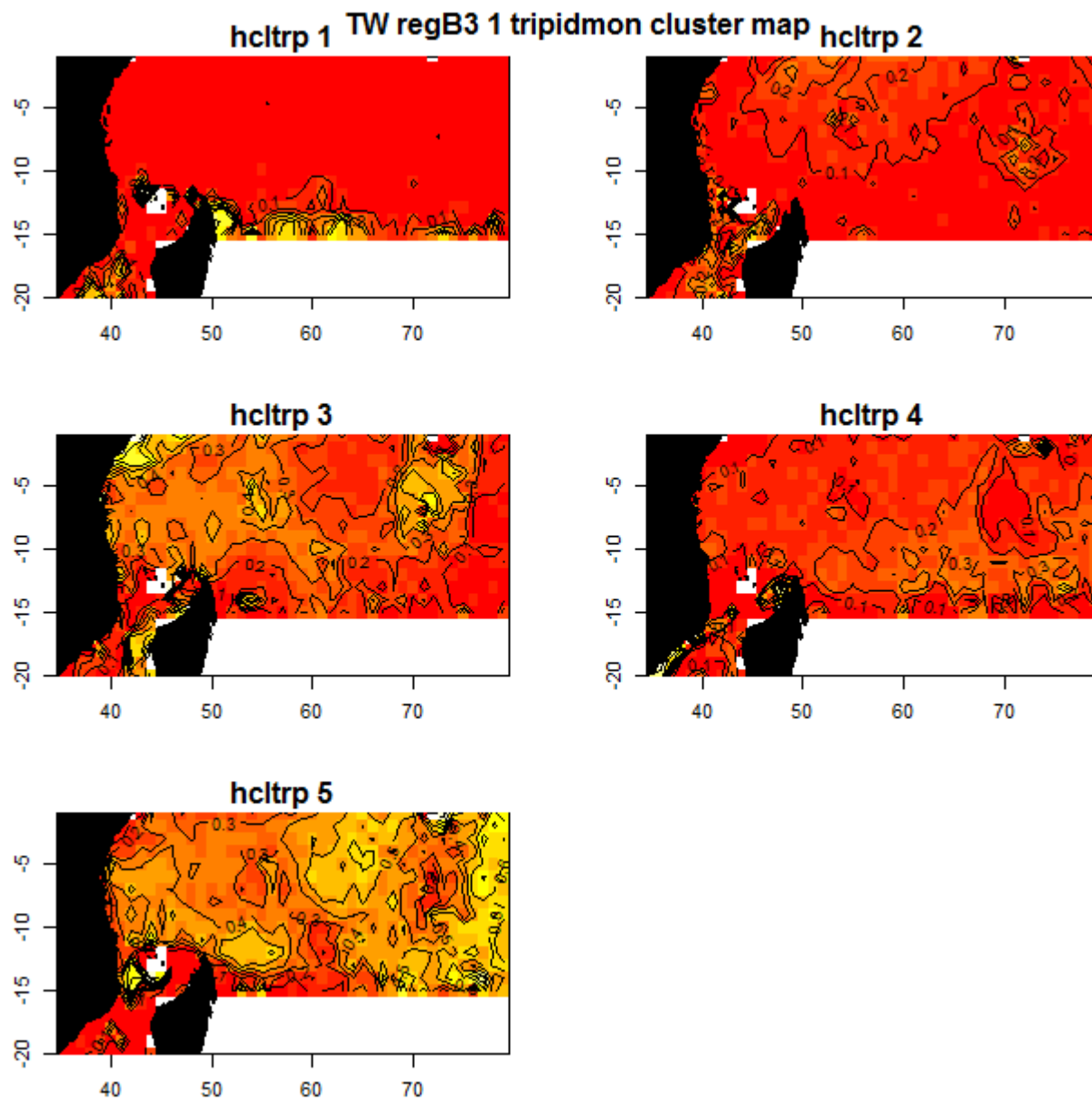


Figure 12. Maps of the spatial distributions of clusters in region 1S of B3 for Taiwanese effort.

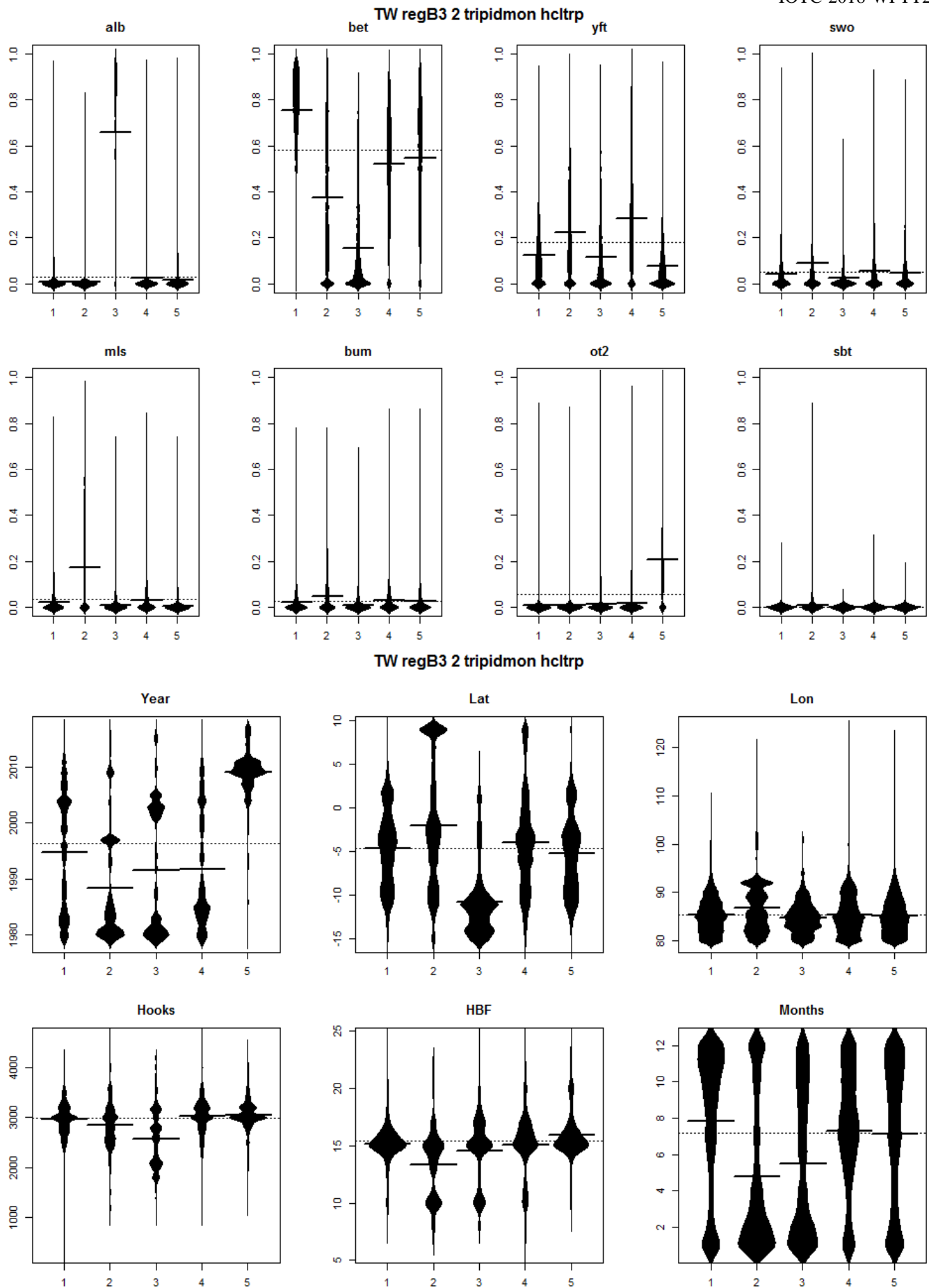


Figure 13. For Taiwanese effort in region 2 of B3 for the period 1979-2017, for each species, boxplot of the proportion of the species in the trip versus the cluster. The widths of the boxes are proportional to the numbers of trips in each cluster (above). Boxplot showing the distributions of variables associated with sets in each hcltrp cluster (below). Clustering was performed using a hierarchical Ward clustering analysis of trip-level data.

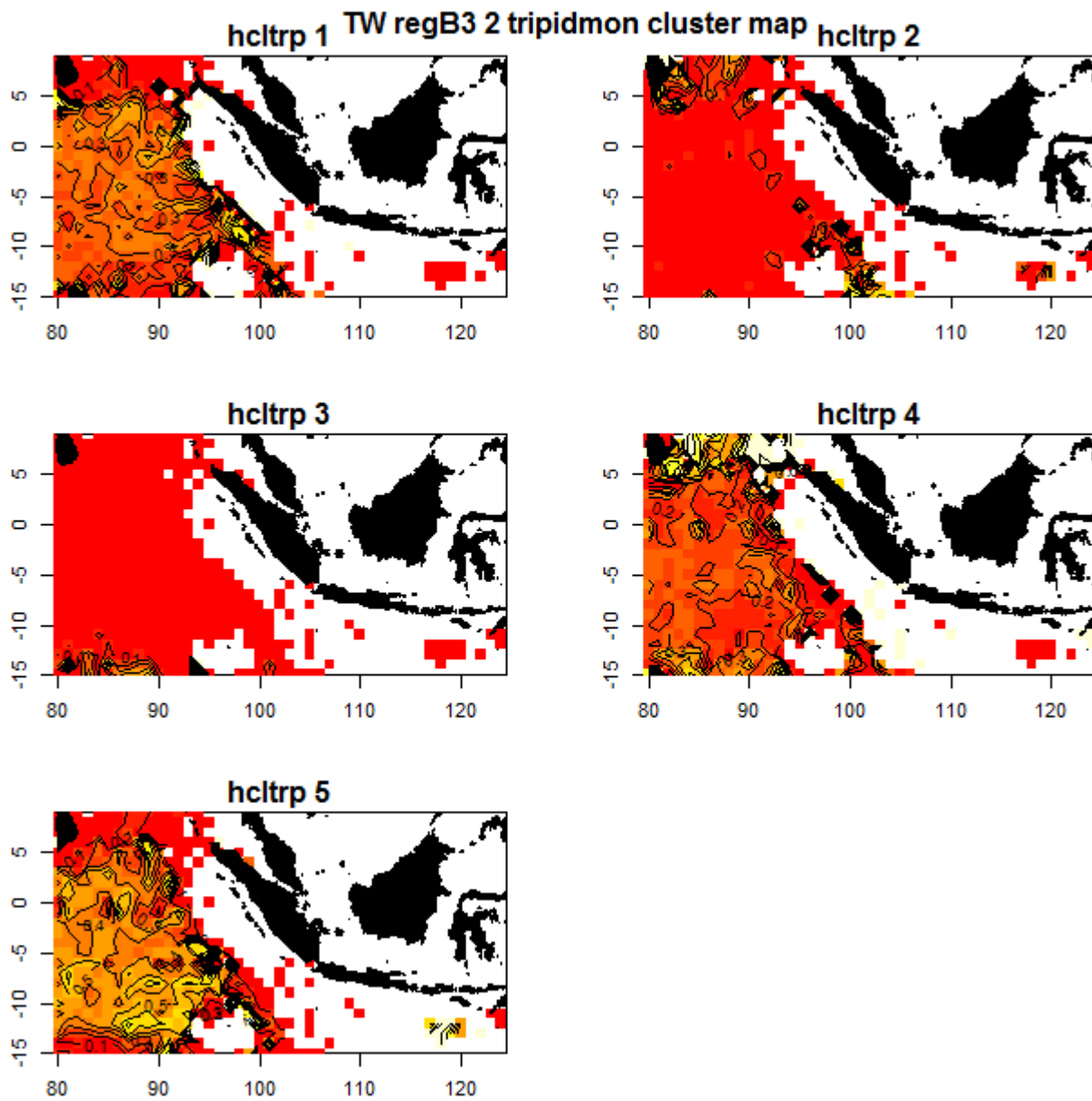


Figure 14. Maps of the spatial distributions of clusters in region 2 of B3 for Taiwanese effort.

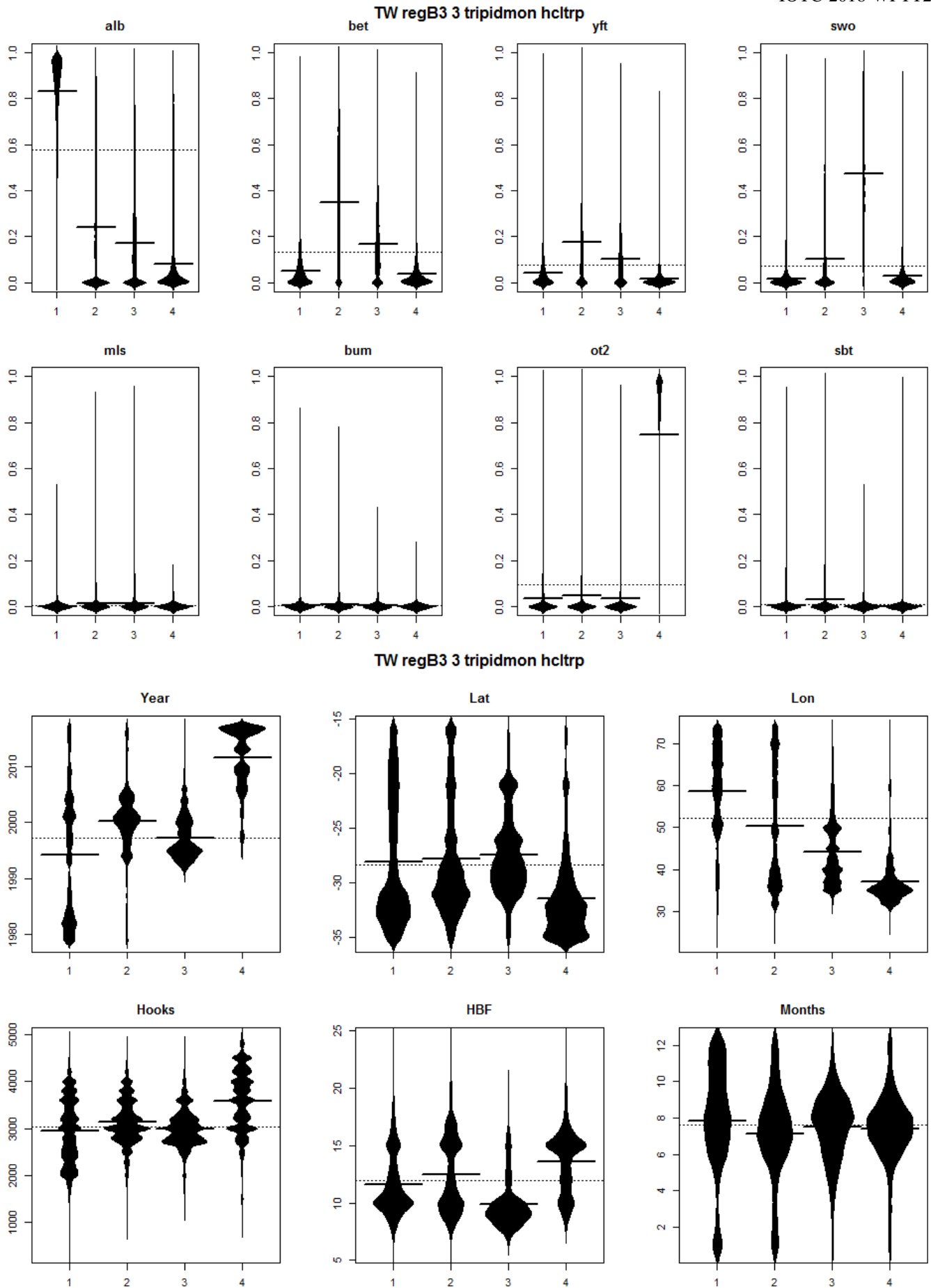


Figure 15. For Taiwanese effort in region 3 of B3 for the period 1979-2017, for each species, boxplot of the proportion of the species in the trip versus the cluster. The widths of the boxes are proportional to the numbers of trips in each cluster (above). Boxplot showing the distributions of variables associated with sets in each hcltrp

cluster (below). Clustering was performed using a hierarchical Ward clustering analysis of trip-level data.

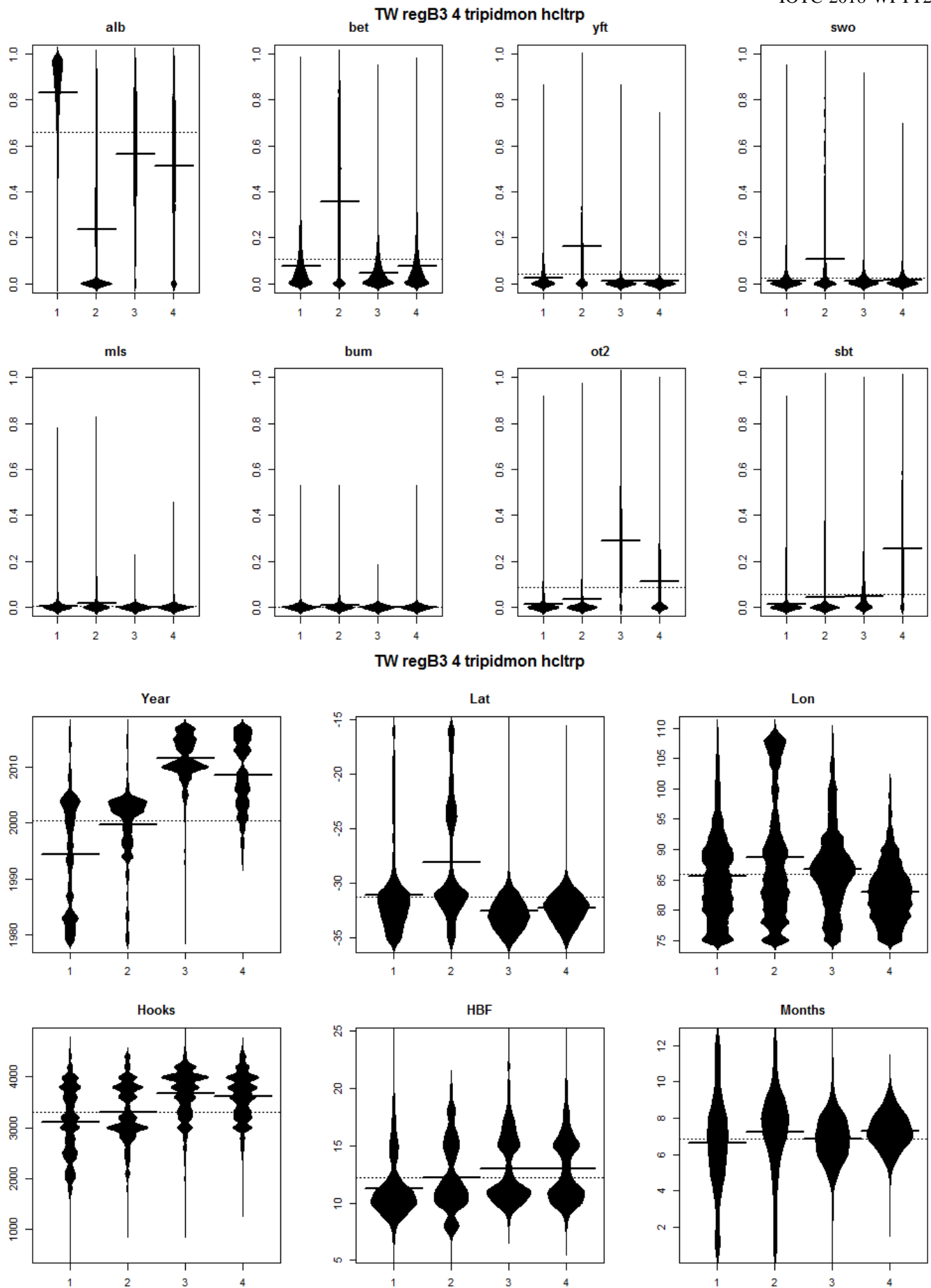


Figure 17. For Taiwanese effort in region 4 of B3 for the period 1979-2017, for each species, boxplot of the proportion of the species in the trip versus the cluster. The widths of the boxes are proportional to the numbers of trips in each cluster (above). Boxplot showing the distributions of variables associated with sets in each hcltrp

cluster (below). Clustering was performed using a hierarchical Ward clustering analysis of trip-level data.

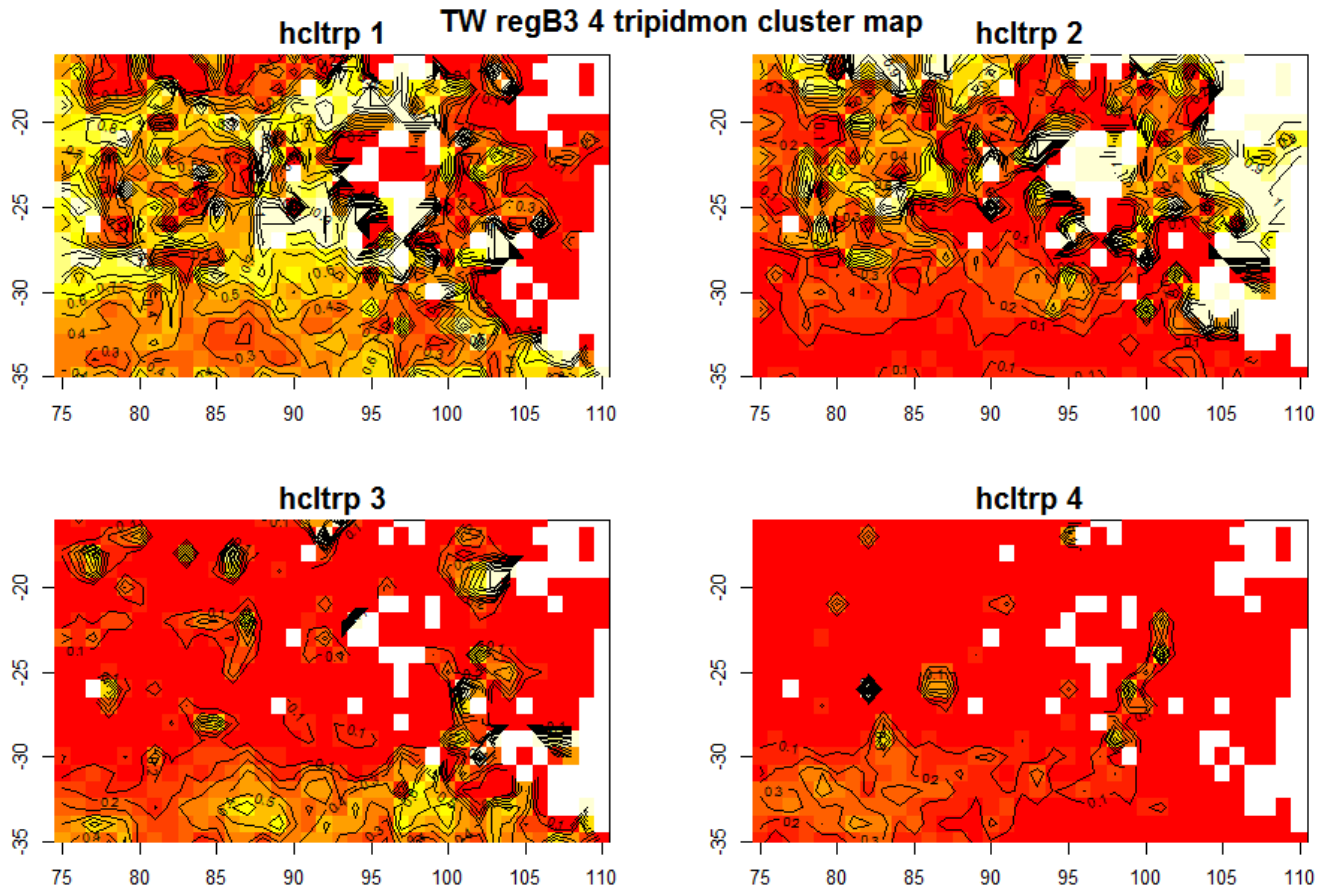


Figure 18. Maps of the spatial distributions of clusters in region 4 of B3 for Taiwanese effort.

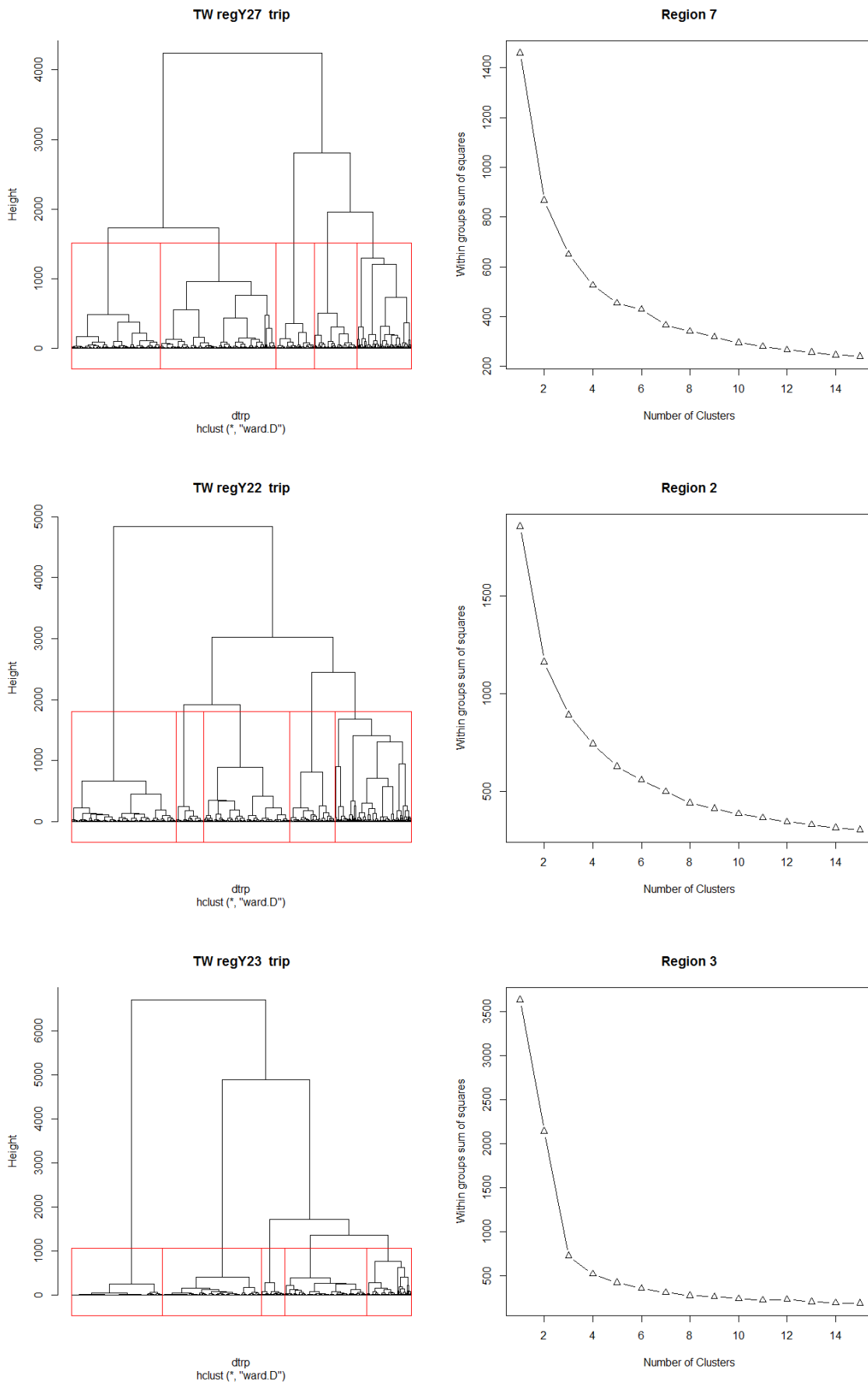


Figure 19. Plots showing analyses to estimate the number of distinct classes of species composition in Taiwanese region 2N, 2S & 3 of Y2. These are based on a hierarchical Ward clustering analysis of trip-level data (top left); within-group sums of squares from kmeans analyses with a range of numbers of clusters (top right); and analyses

of the numbers of components to retain from a principal component analysis of trip-level (bottom left) data.

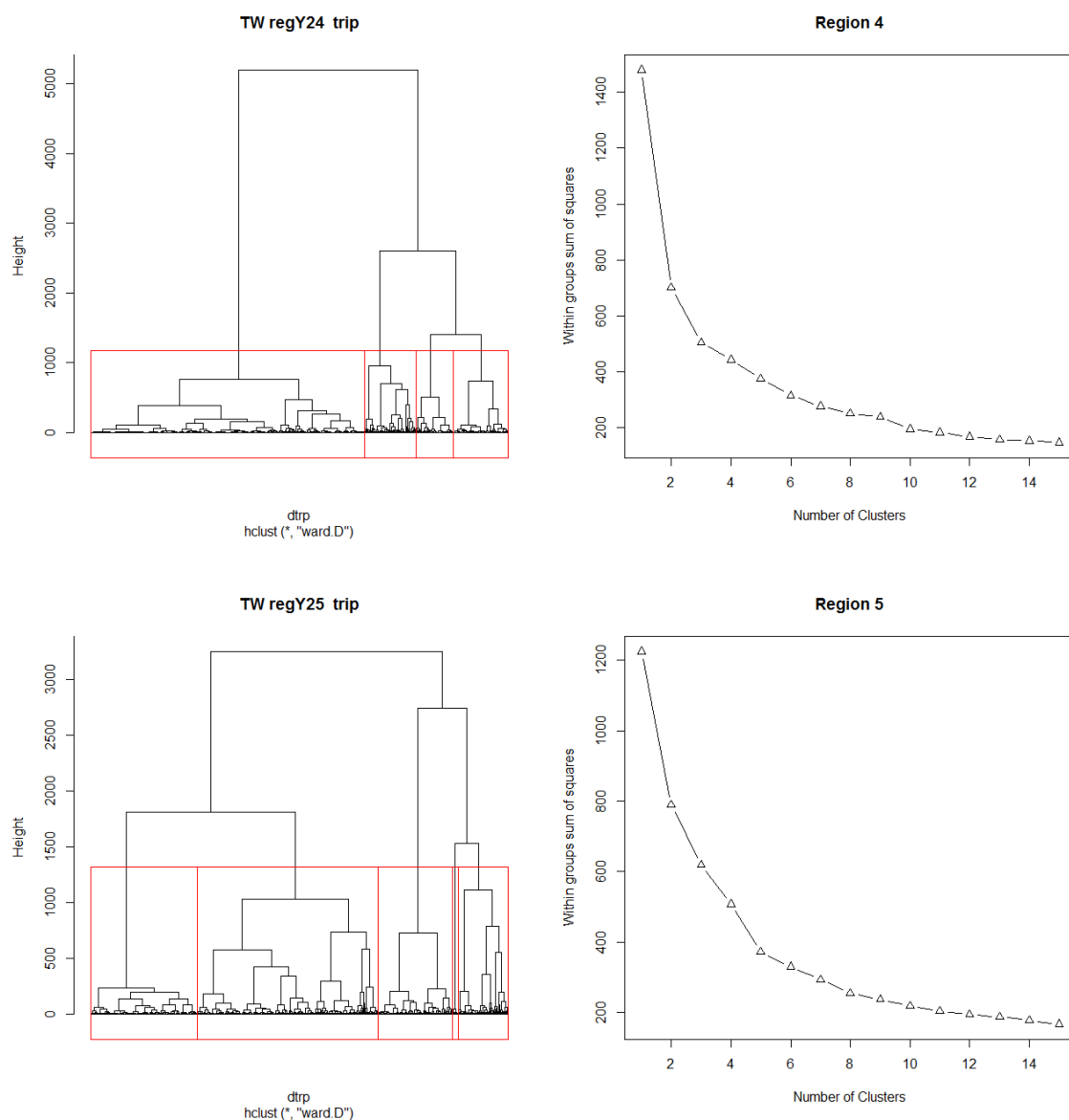


Figure 20. Plots showing analyses to estimate the number of distinct classes of species composition in Taiwanese region 4 & 5 of Y2. These are based on a hierarchical Ward clustering analysis of trip-level data (top left); within-group sums of squares from kmeans analyses with a range of numbers of clusters (top right); and analyses of the numbers of components to retain from a principal component analysis of trip-level (bottom left) data.

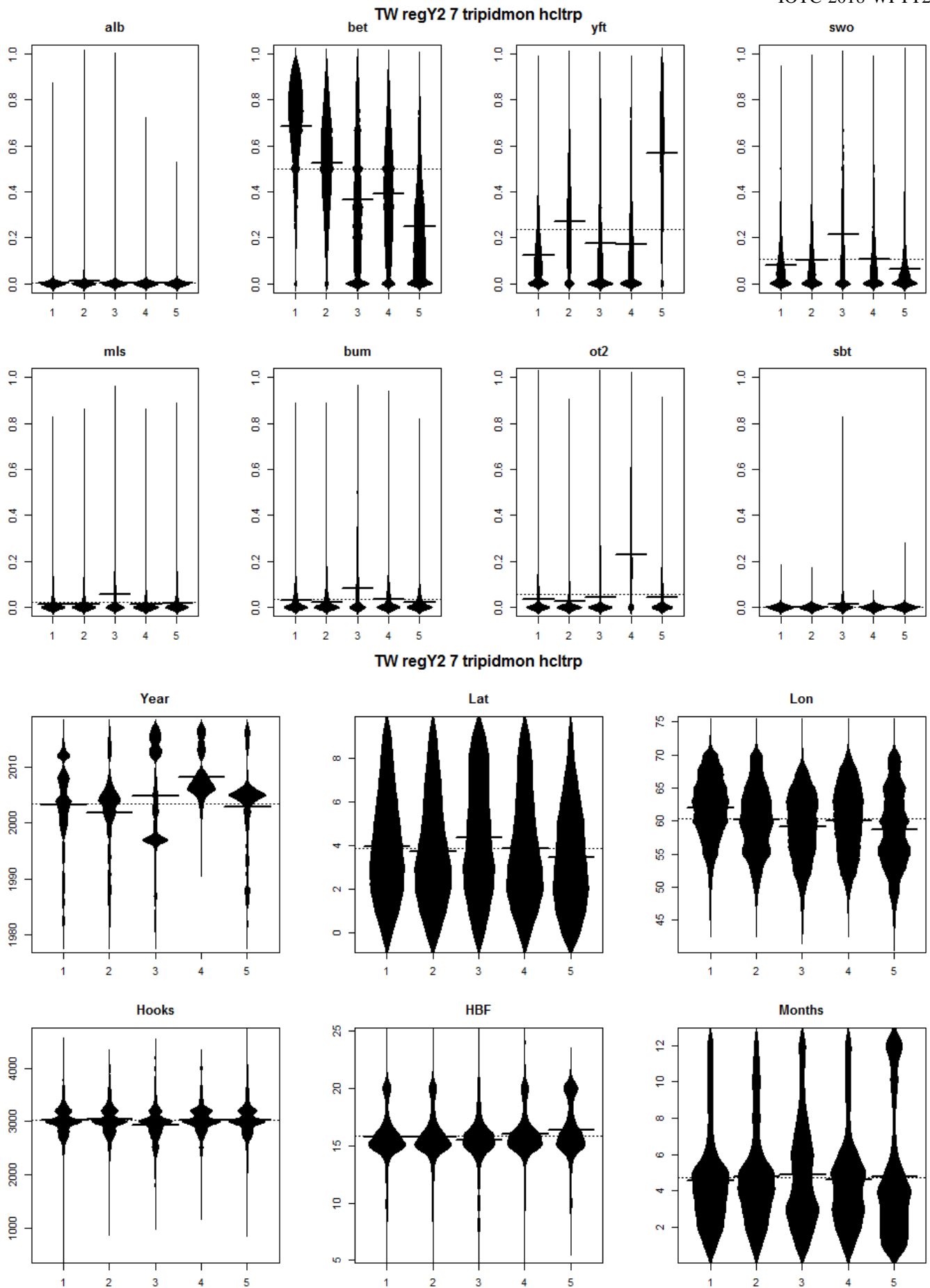


Figure 21. . For Taiwanese effort in region 2N of Y for the period 1979-2017, for each species, boxplot of the proportion of the species in the trip versus the cluster. The widths of the boxes are proportional to the numbers of trips in each cluster (above). Boxplot showing the distributions of variables associated with sets in each hcltrp

cluster (below). Clustering was performed using a hierarchical Ward clustering analysis of trip-level data.

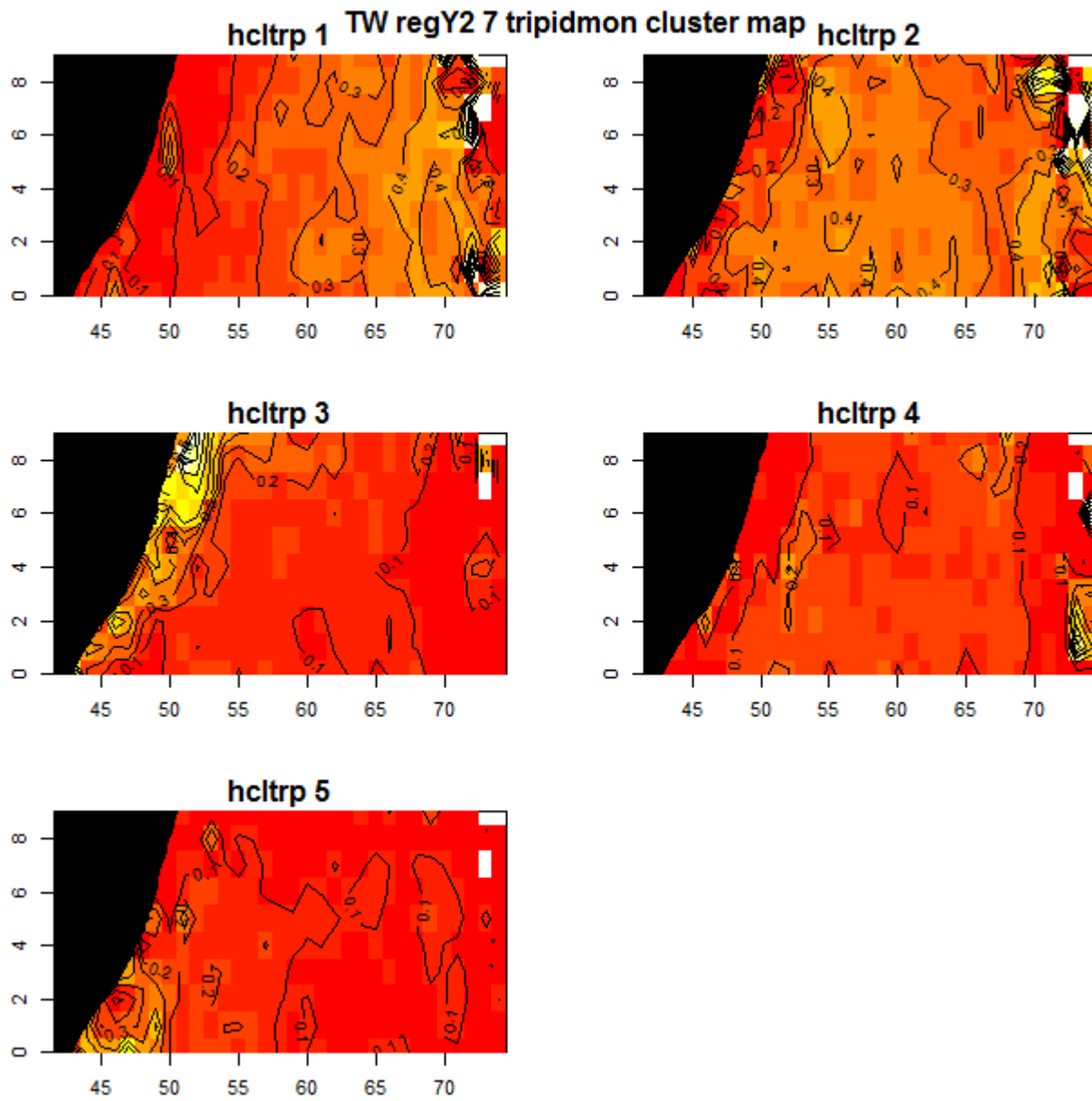


Figure 22. Maps of the spatial distributions of clusters in region 2N of Y for Taiwanese effort.

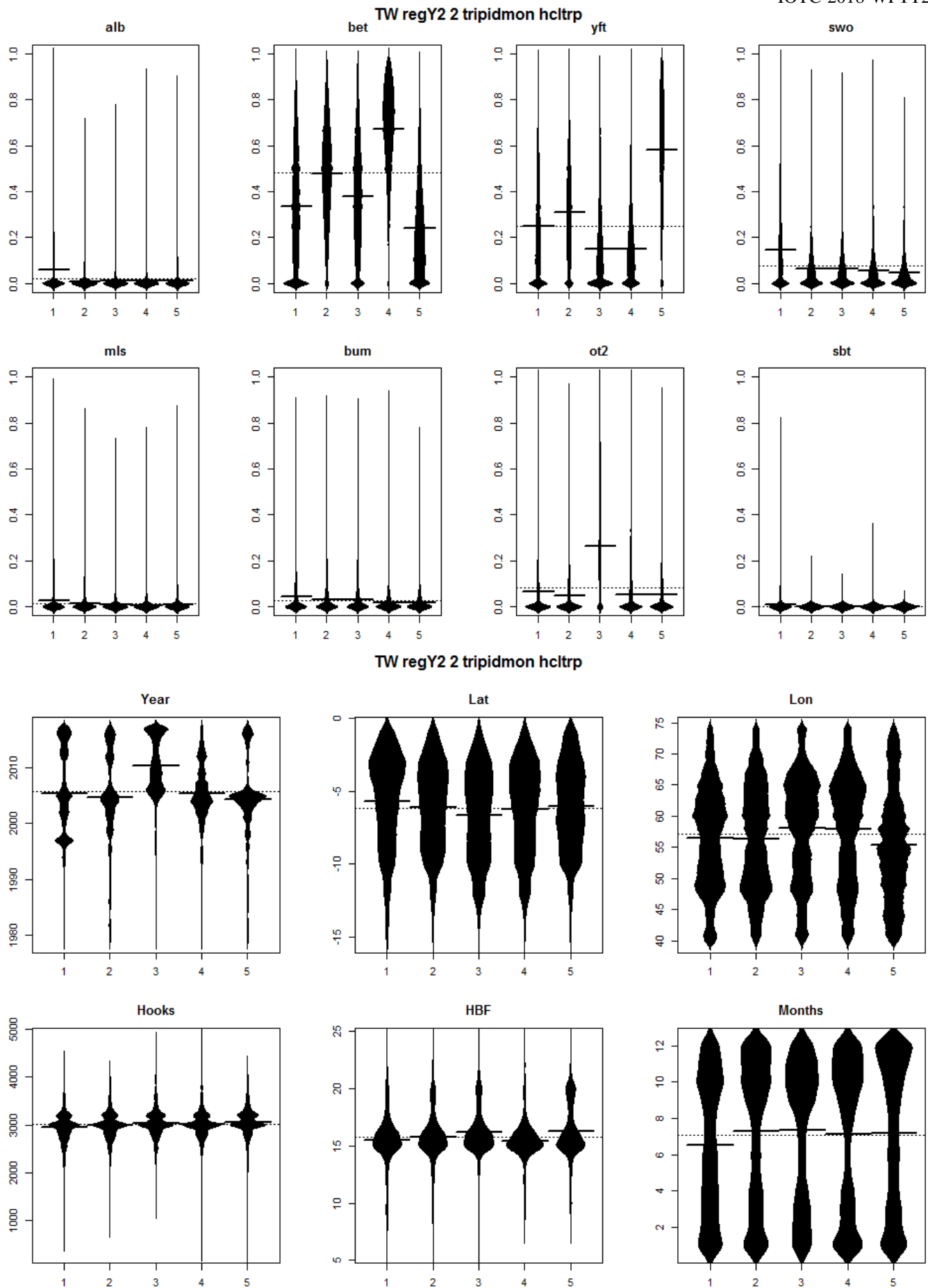


Figure 23. For Taiwanese effort in region 2S of Y for the period 1979-2017, for each species, boxplot of the proportion of the species in the trip versus the cluster. The widths of the boxes are proportional to the numbers of trips in each cluster (above). Boxplot showing the distributions of variables associated with sets in each hcltrp cluster (below). Clustering was performed using a hierarchical Ward clustering analysis of trip-level data.

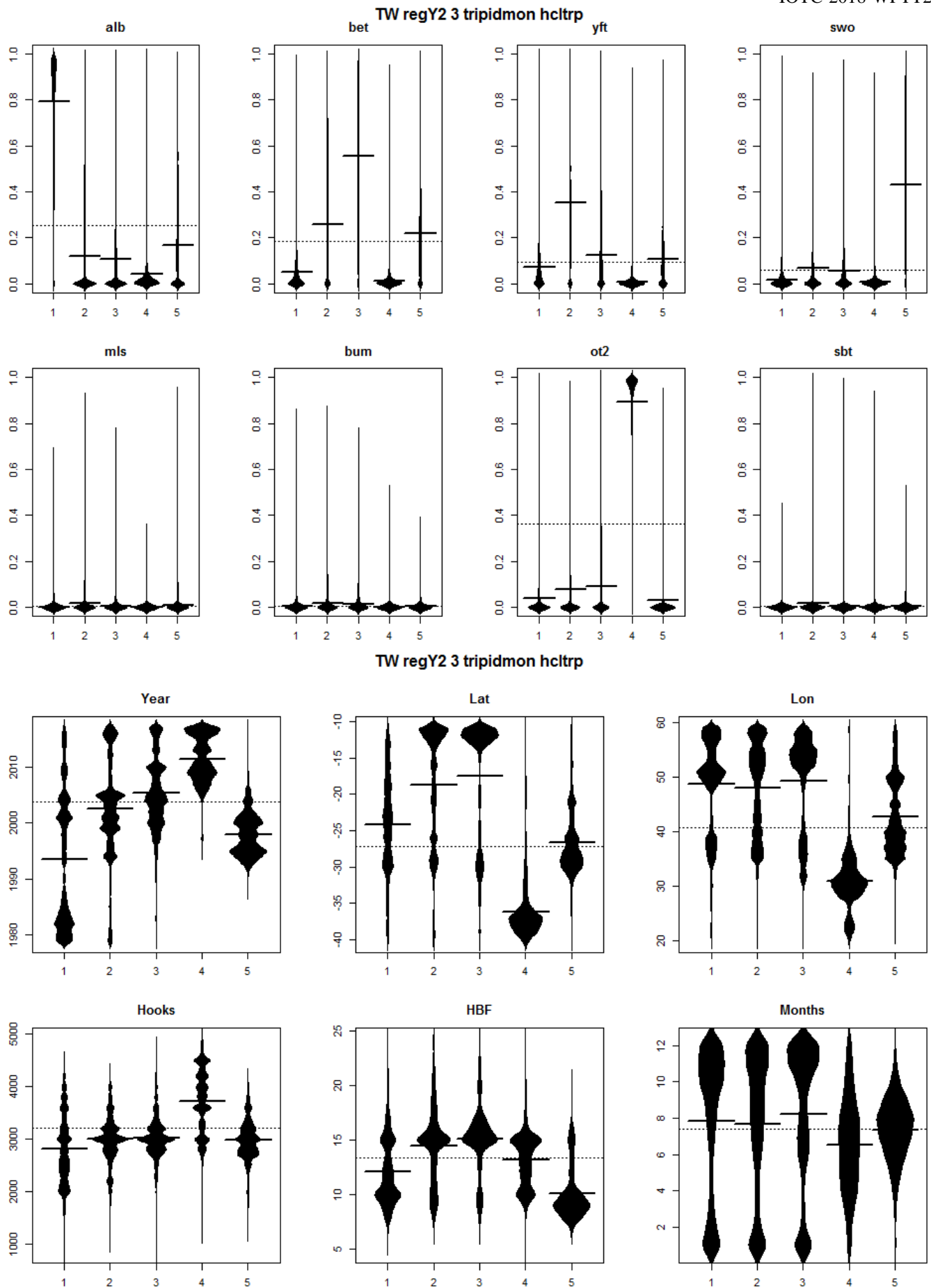


Figure 24. For Taiwanese effort in region 3 of Y2 for the period 1979-2017, for each species, boxplot of the proportion of the species in the trip versus the cluster. The widths of the boxes are proportional to the numbers of trips in each cluster (above). Boxplot showing the distributions of variables associated with sets in each hcltrp

cluster (below). Clustering was performed using a hierarchical Ward clustering analysis of trip-level data.

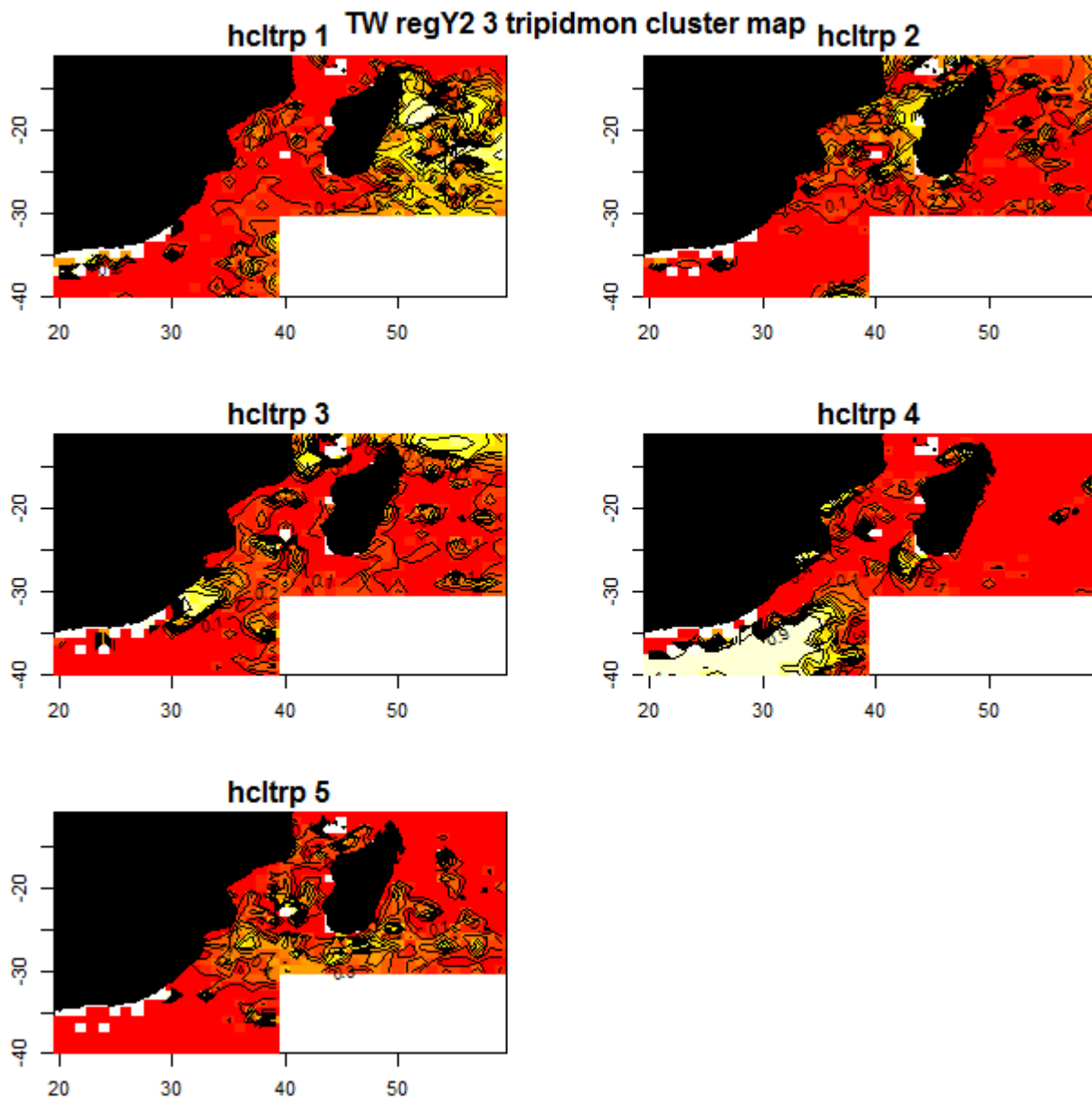


Figure 25. Maps of the spatial distributions of clusters in region 3 of Y2 for Taiwanese effort.

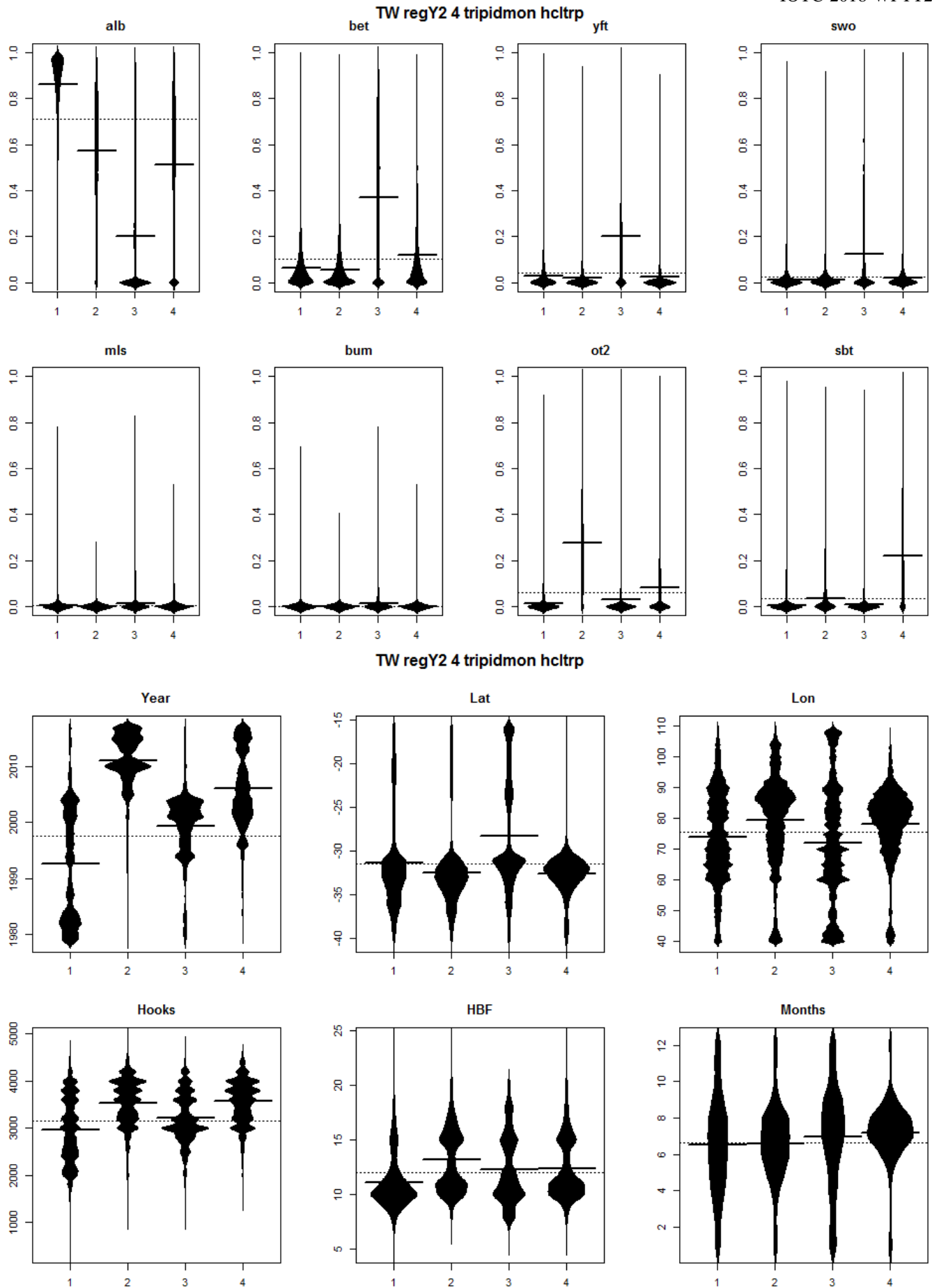


Figure 26. For Taiwanese effort in region 4 of Y2 for the period 1979-2017, for each species, boxplot of the proportion of the species in the trip versus the cluster. The widths of the boxes are proportional to the numbers of trips in each cluster (above). Boxplot showing the distributions of variables associated with sets in each hcltrp

cluster (below). Clustering was performed using a hierarchical Ward clustering analysis of trip-level data.

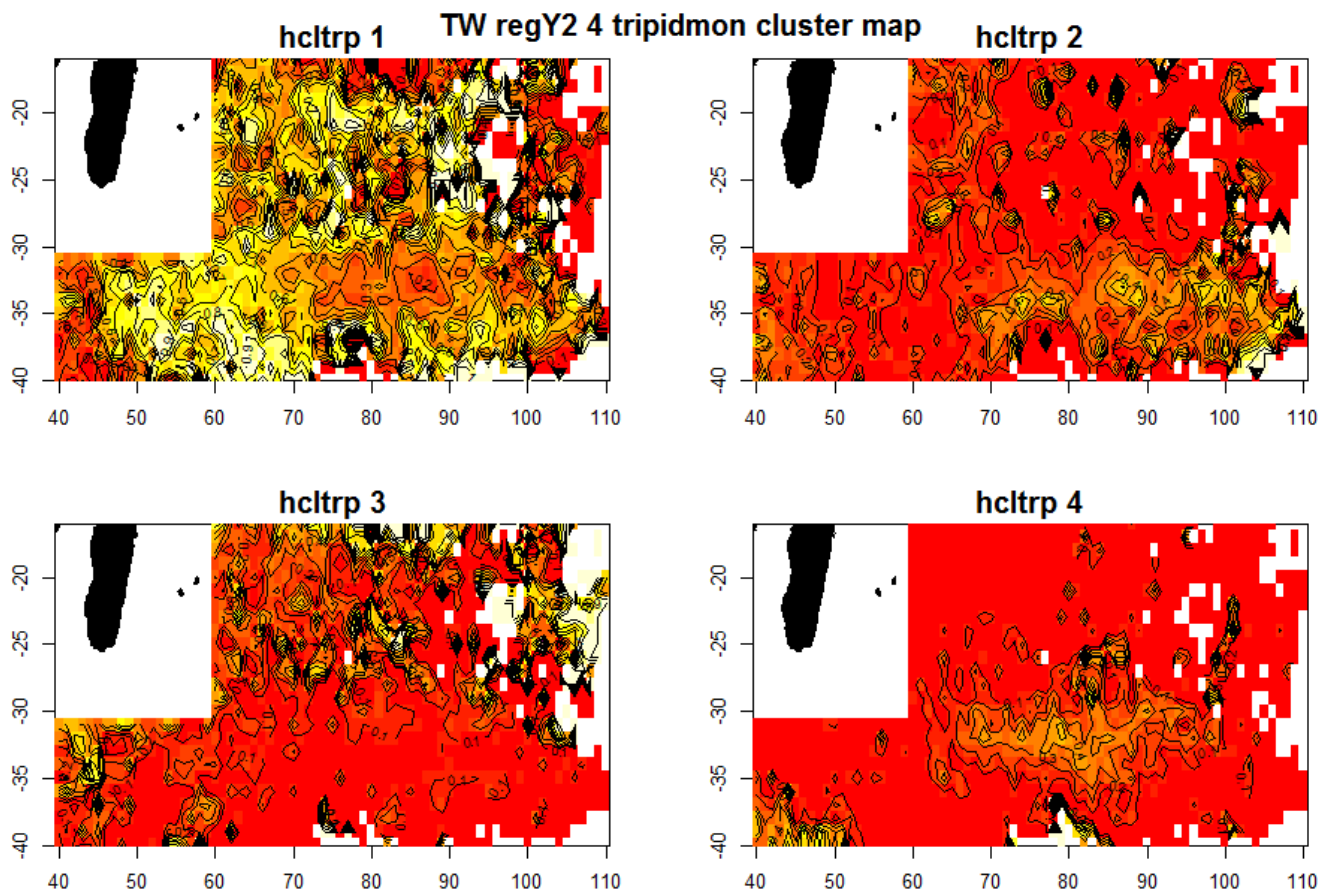


Figure 27. Maps of the spatial distributions of clusters in region 4 of Y2 for Taiwanese effort.

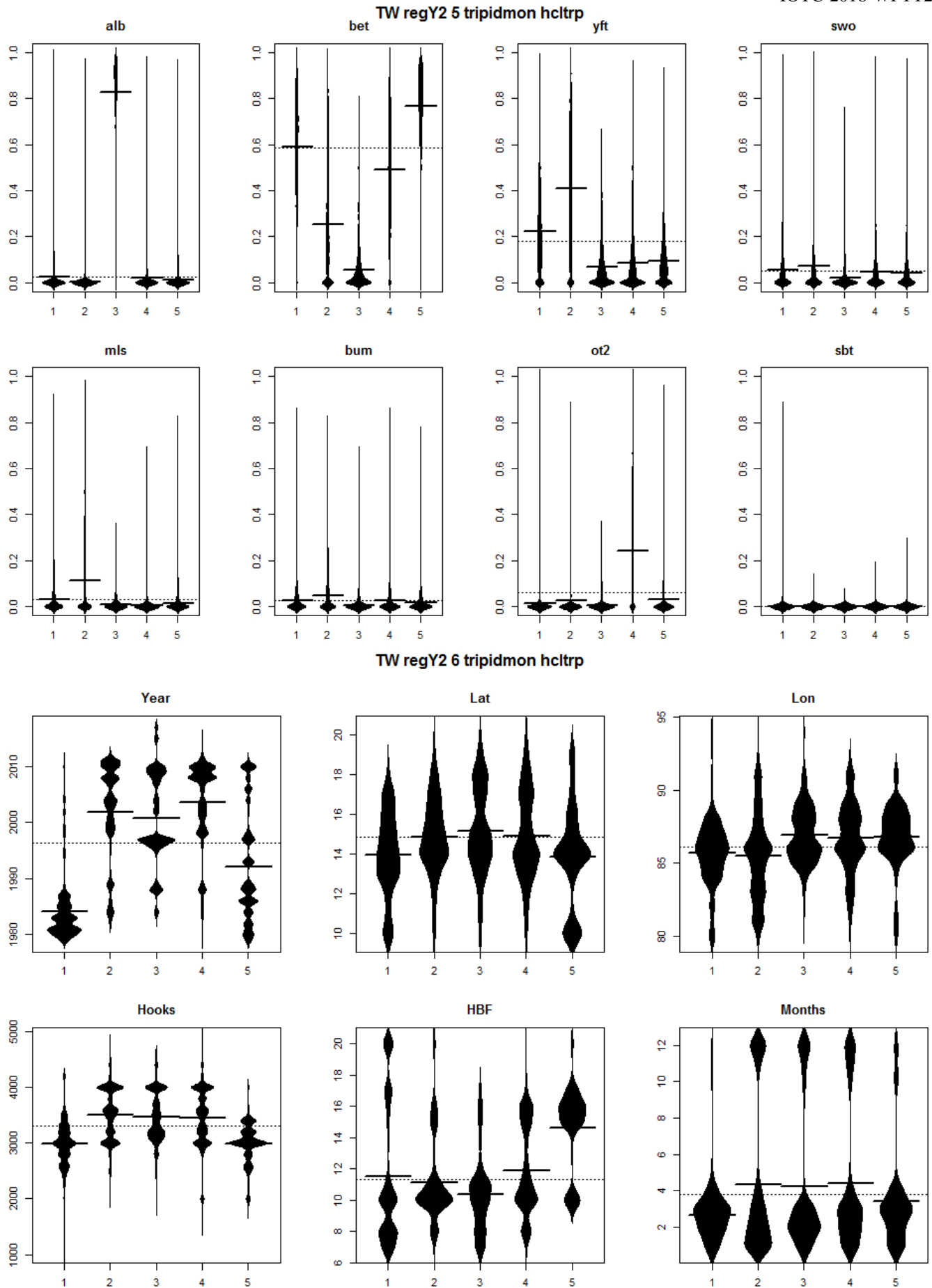


Figure 28. For Taiwanese effort in region 5 of Y2 for the period 1979-2017, for each species, boxplot of the proportion of the species in the trip versus the cluster. The widths of the boxes are proportional to the numbers of trips in each cluster (above). Boxplot showing the distributions of variables associated with sets in each hcltrp

cluster (below). Clustering was performed using a hierarchical Ward clustering analysis of trip-level data.

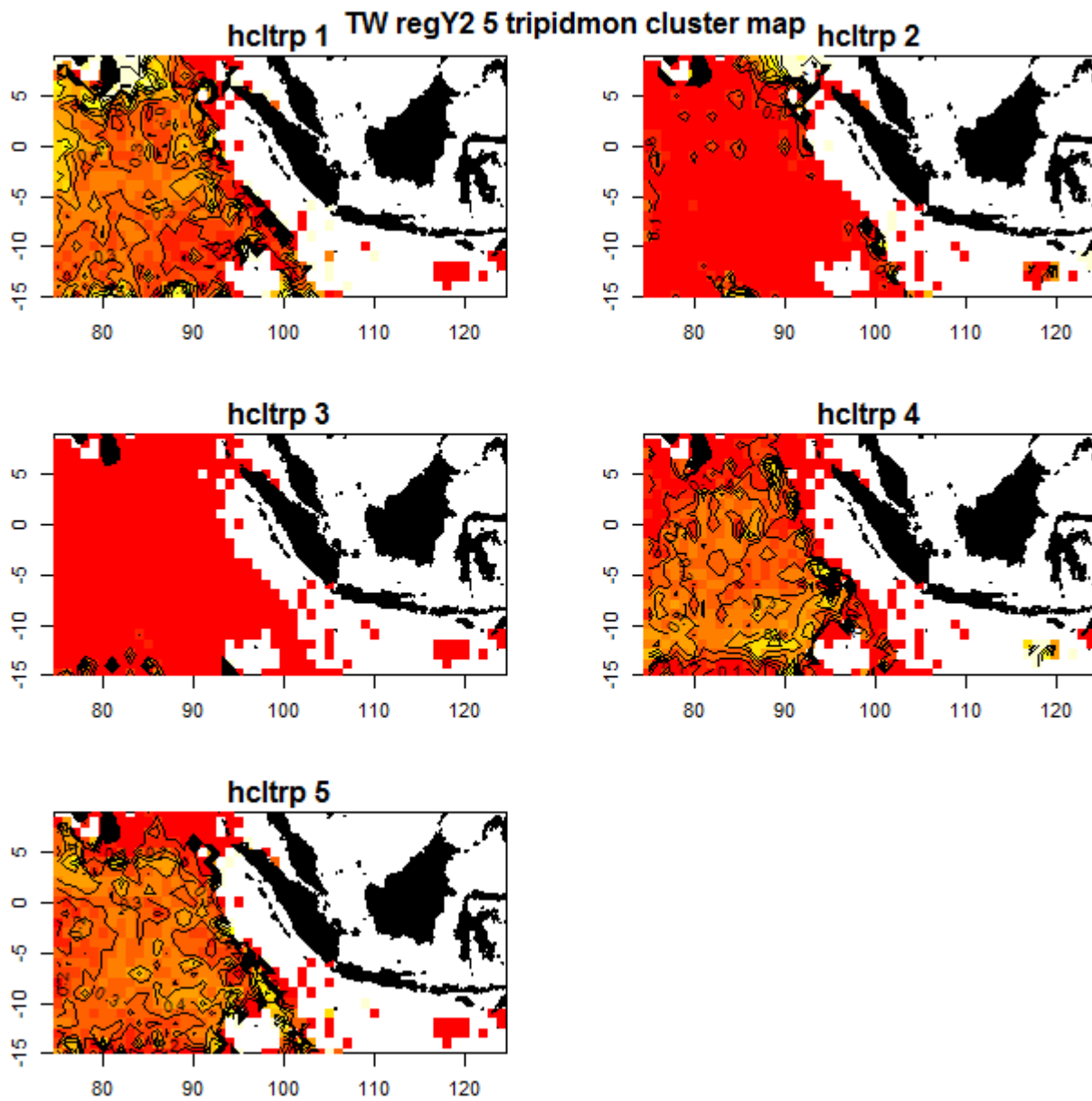


Figure 29. Maps of the spatial distributions of clusters in region 5 of Y2 for Taiwanese effort.

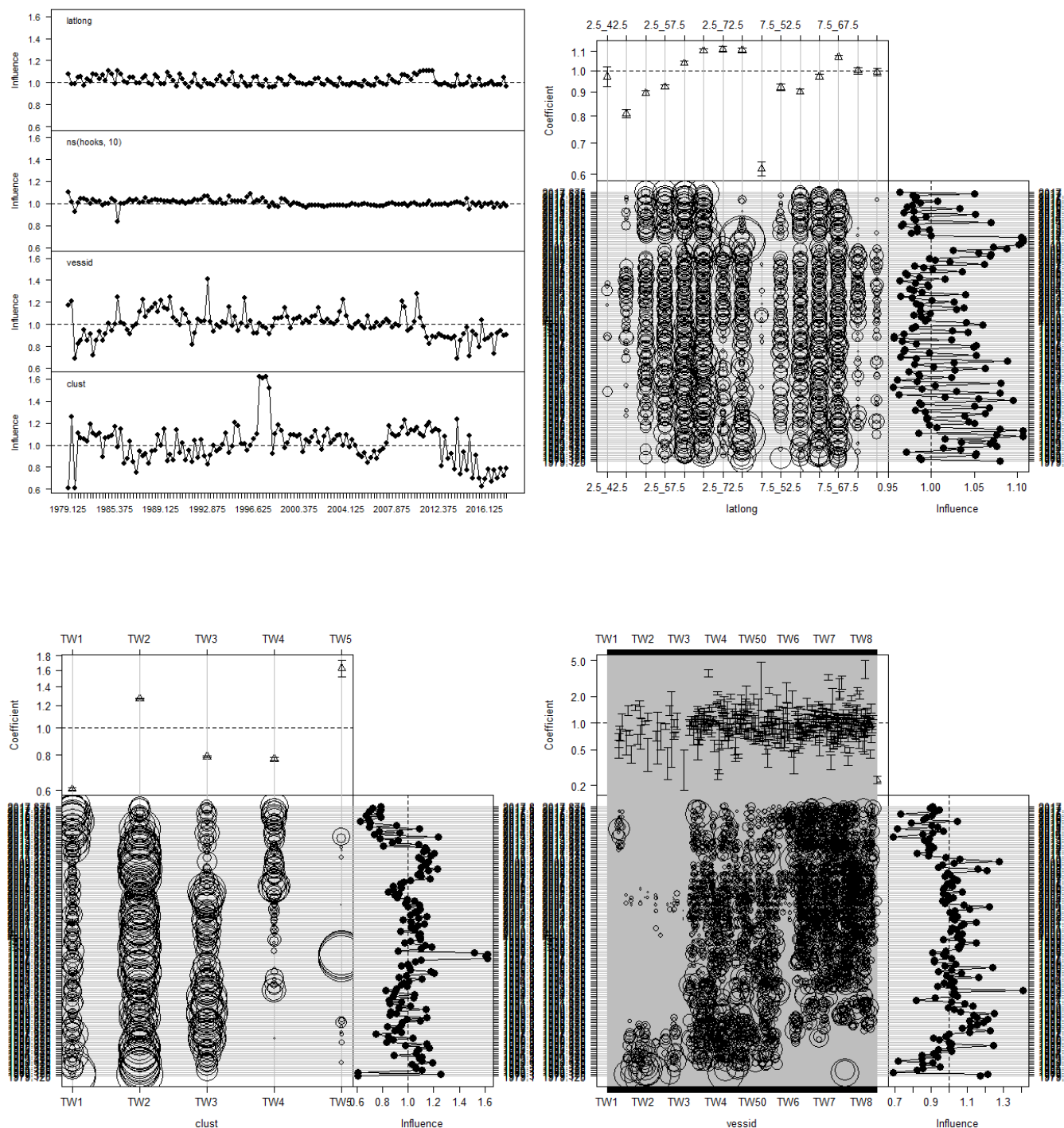


Figure 30. Influence plots for bigeye tuna CPUE in region 1N by the Taiwanese fleet. The top left plots shows the change in the CPUE time series caused by each covariate. The top right plot shows the influence of the latlong effect. The bottom left plot shows the influence of the cluster effect, and the bottom right plot shows the influence of the vessid effect.

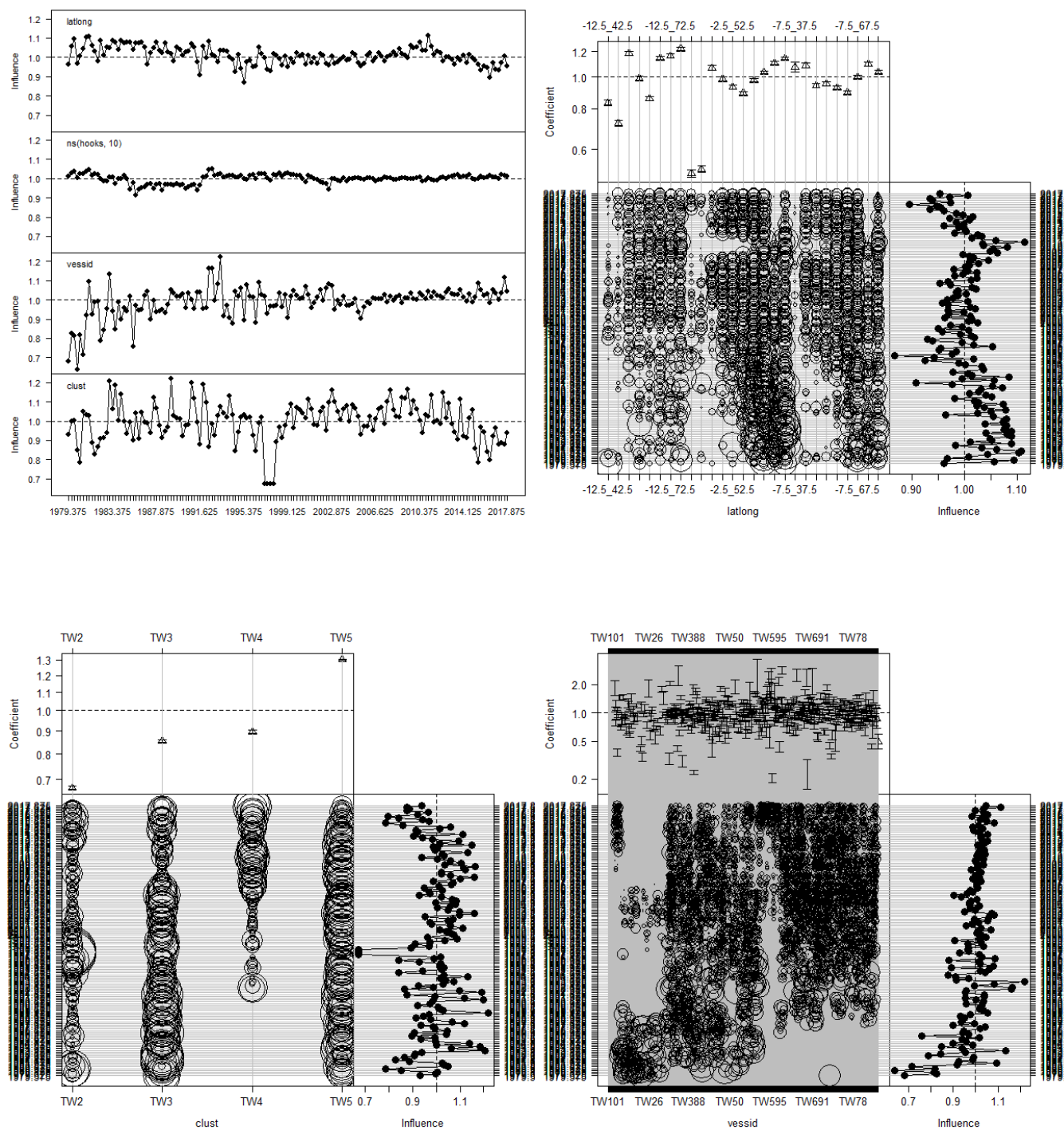


Figure 31 Influence plots for bigeye tuna CPUE in region 1S by the Taiwanese fleet. The top left plots shows the change in the CPUE time series caused by each covariate. The top right plot shows the influence of the latlong effect. The bottom left plot shows the influence of the cluster effect, and the bottom right plot shows the influence of the vessid effect.

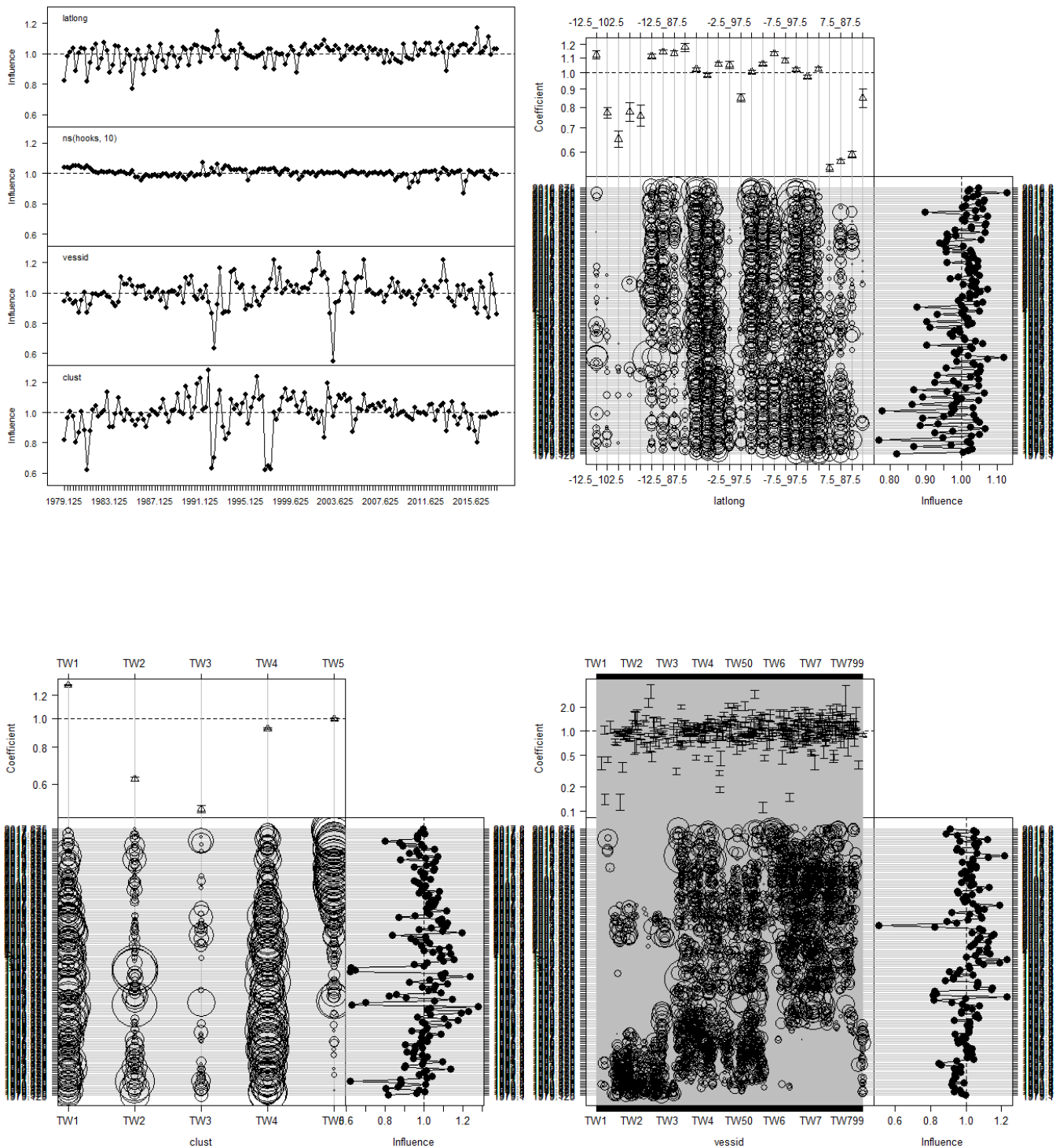


Figure 32 Influence plots for bigeye tuna CPUE in region 2 by the Taiwanese fleet. The top left plots shows the change in the CPUE time series caused by each covariate. The top right plot shows the influence of the latlong effect. The bottom left plot shows the influence of the cluster effect, and the bottom right plot shows the influence of the vessid effect.

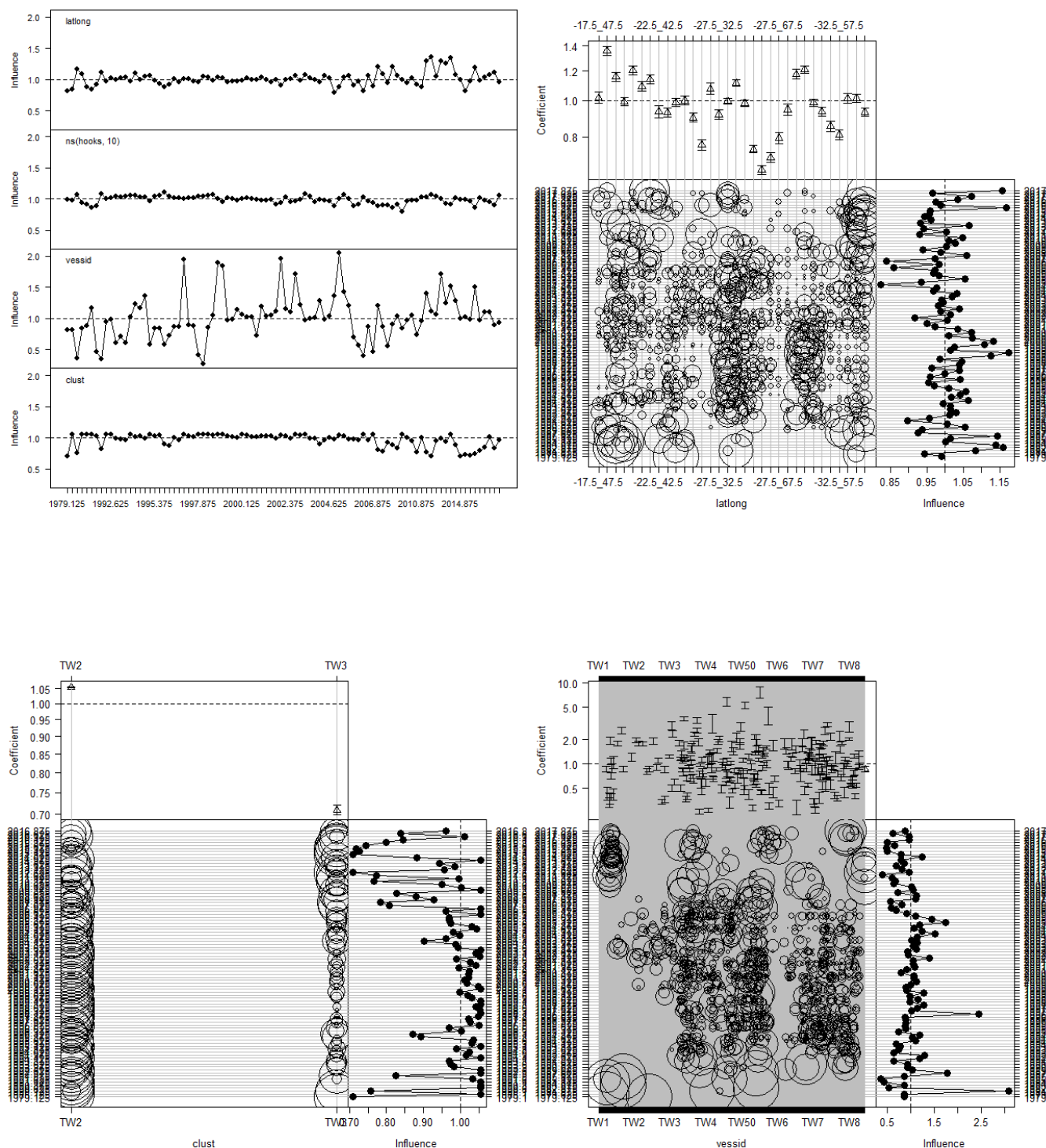


Figure 33 Influence plots for bigeye tuna CPUE in region 3 by the Taiwanese fleet. The top left plots shows the change in the CPUE time series caused by each covariate. The top right plot shows the influence of the latlong effect. The bottom left plot shows the influence of the cluster effect, and the bottom right plot shows the influence of the vessid effect.

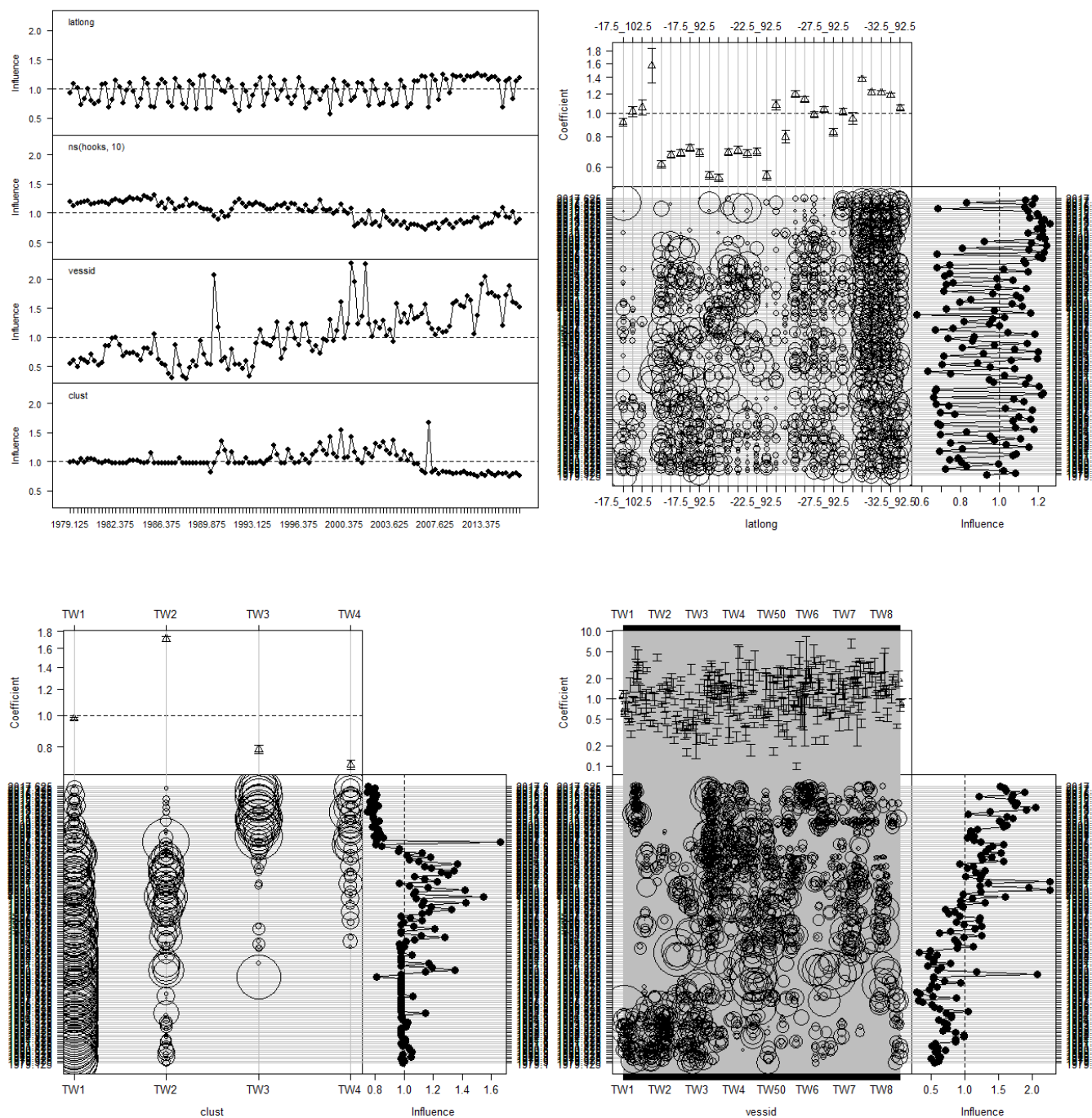


Figure 34 Influence plots for bigeye tuna CPUE in region 4 by the Taiwanese fleet. The top left plots shows the change in the CPUE time series caused by each covariate. The top right plot shows the influence of the latlong effect. The bottom left plot shows the influence of the cluster effect, and the bottom right plot shows the influence of the vessid effect.

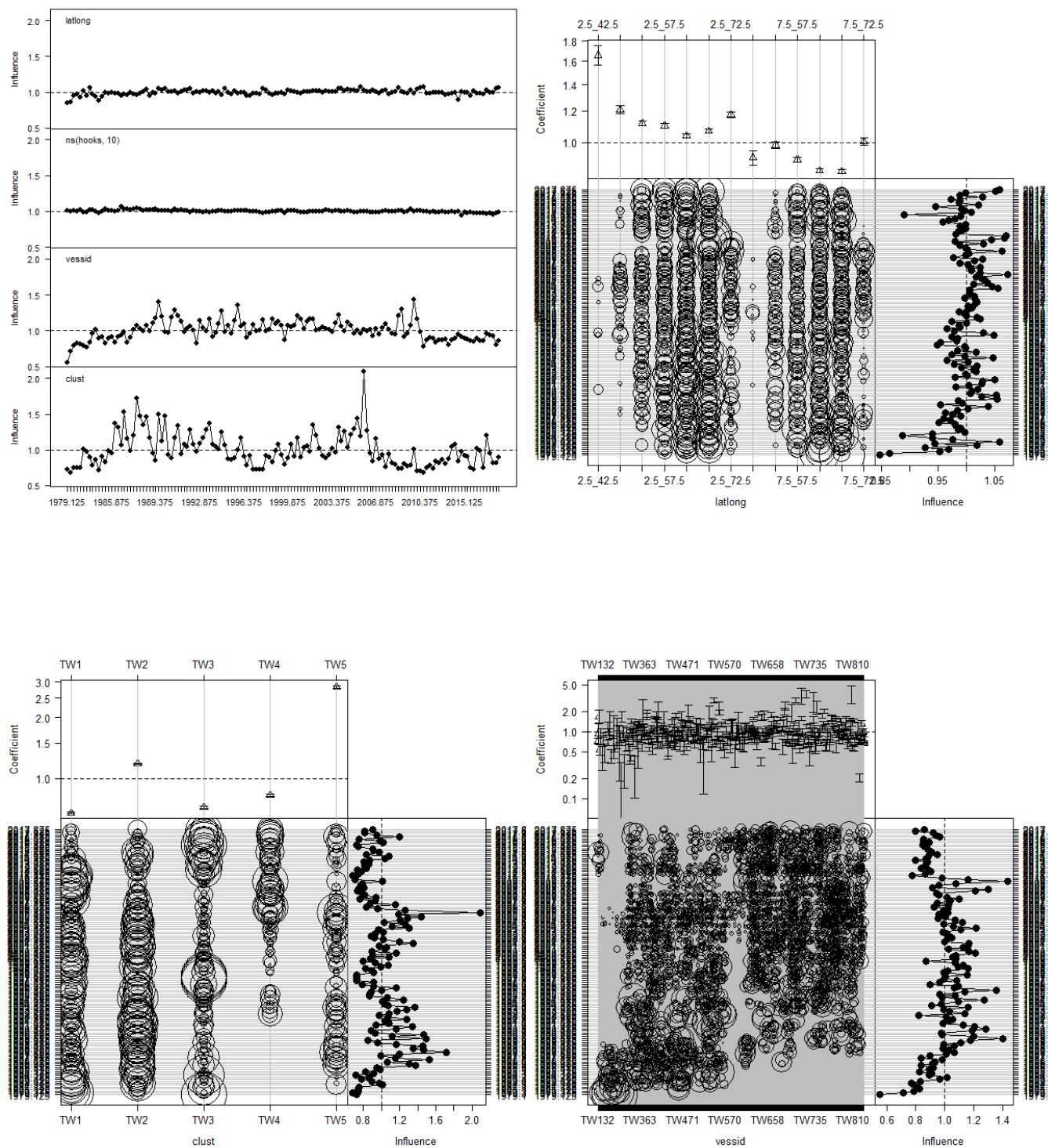


Figure 35 Influence plots for yellowfin tuna CPUE in region 2N by the Taiwanese fleet. The top left plots shows the change in the CPUE time series caused by each covariate. The top right plot shows the influence of the latlong effect. The bottom left plot shows the influence of the cluster effect, and the bottom right plot shows the influence of the vessid effect.

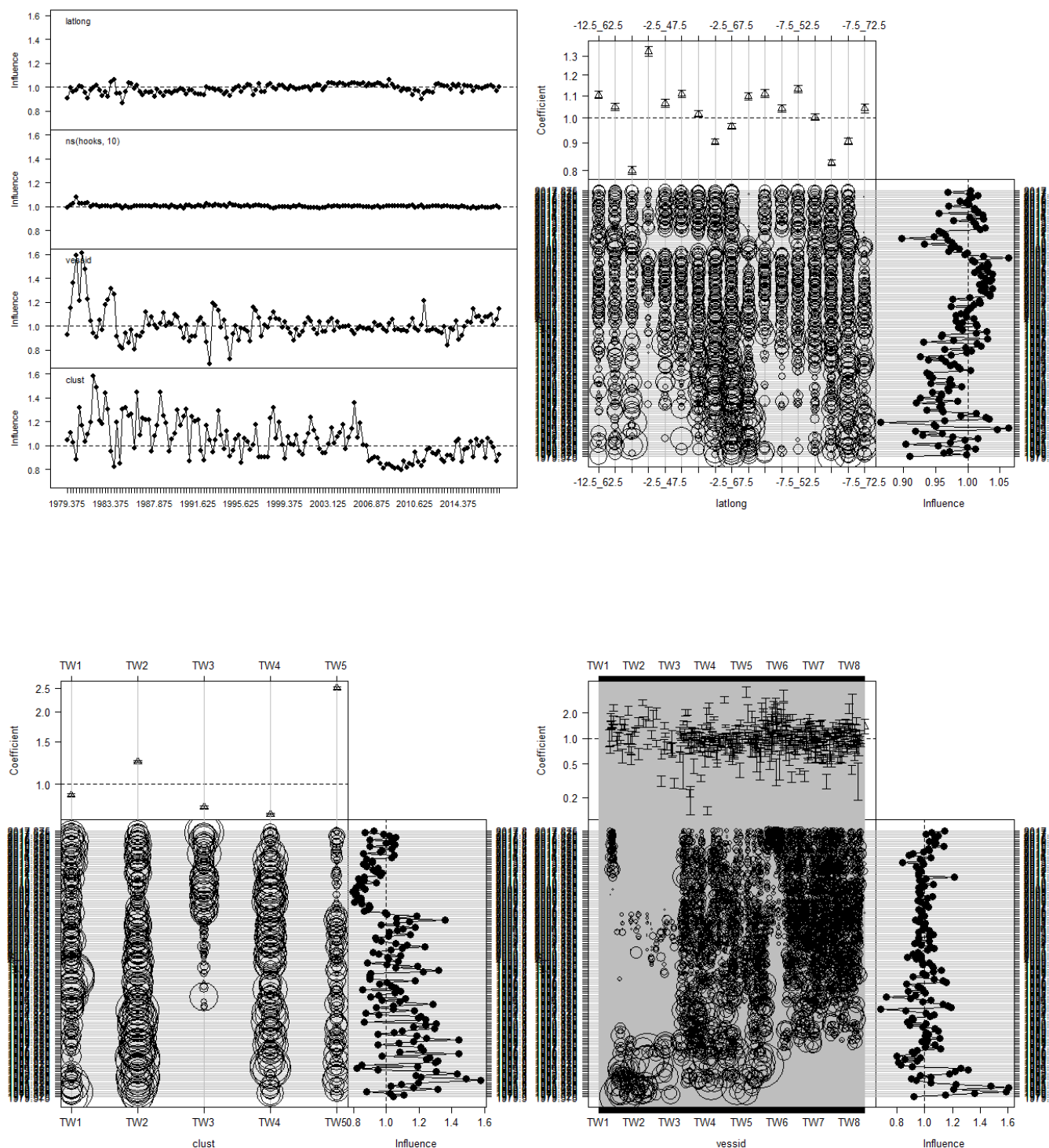


Figure 36 Influence plots for yellowfin tuna CPUE in region 2S by the Taiwanese fleet. The top left plots shows the change in the CPUE time series caused by each covariate. The top right plot shows the influence of the latlong effect. The bottom left plot shows the influence of the cluster effect, and the bottom right plot shows the influence of the vessid effect.

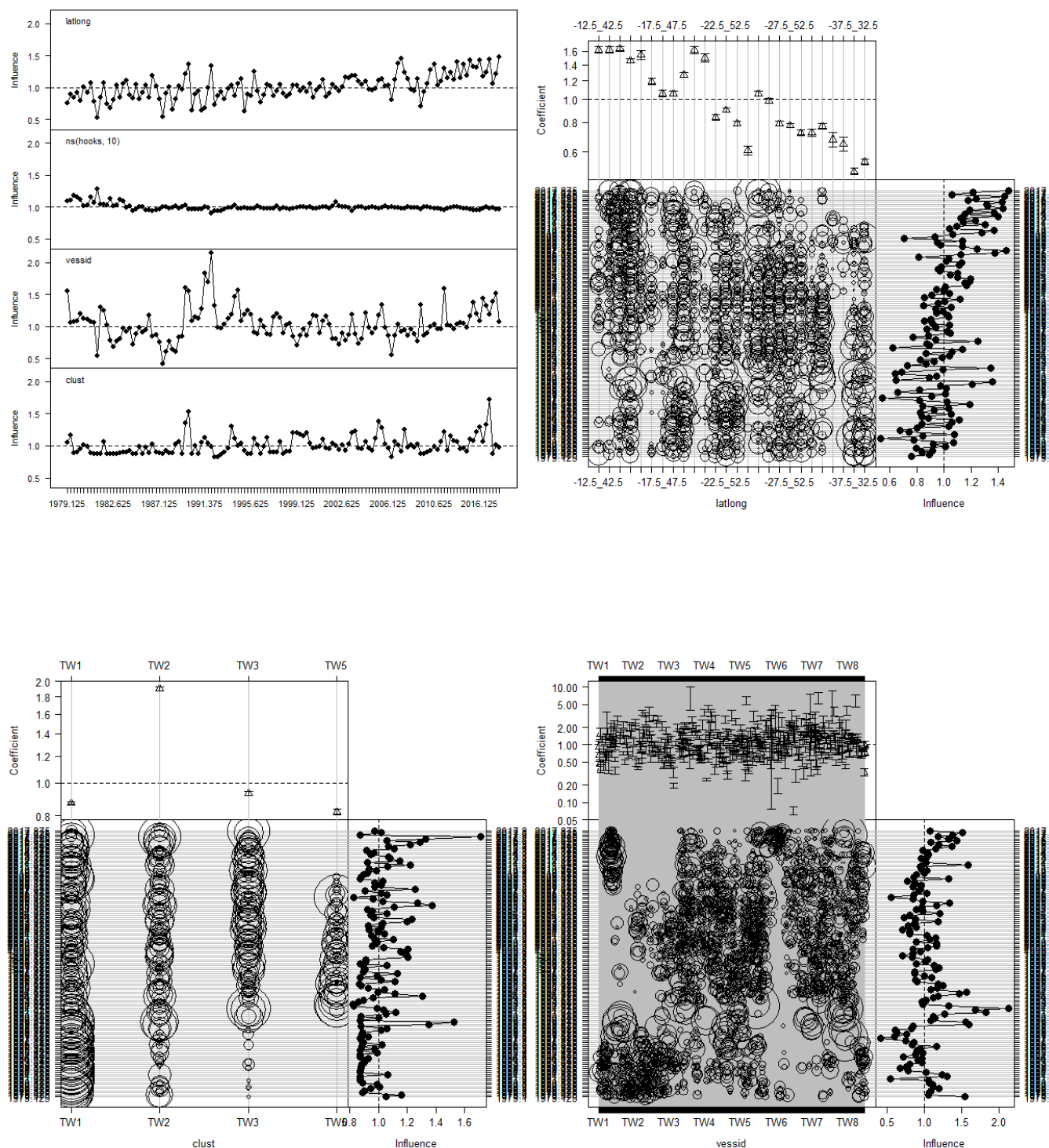


Figure 37 Influence plots for yellowfin tuna CPUE in region 3 by the Taiwanese fleet. The top left plots shows the change in the CPUE time series caused by each covariate. The top right plot shows the influence of the latlong effect. The bottom left plot shows the influence of the cluster effect, and the bottom right plot shows the influence of the vessid effect.

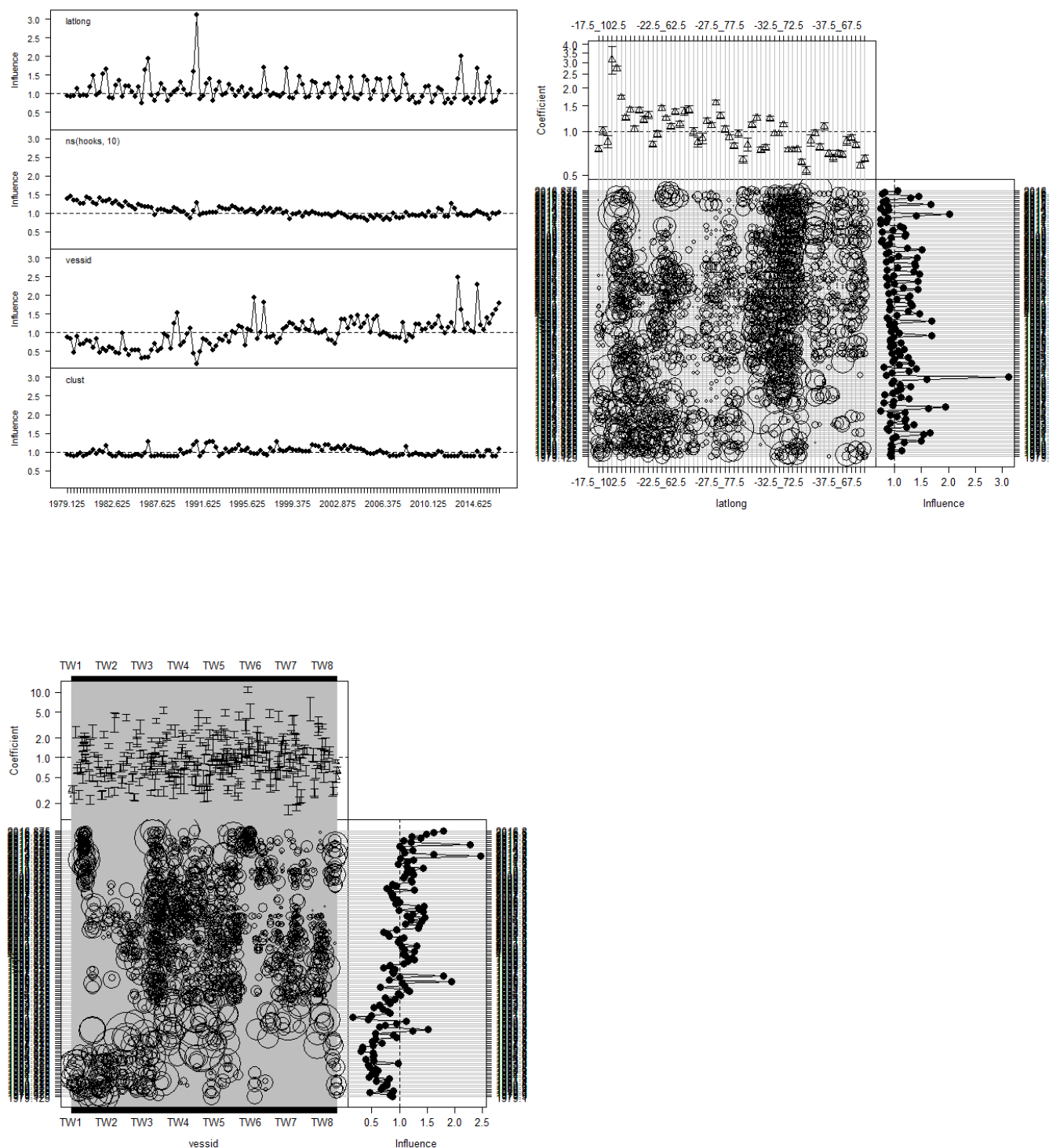


Figure 38 Influence plots for yellowfin tuna CPUE in region 4 by the Taiwanese fleet. The top left plots shows the change in the CPUE time series caused by each covariate. The top right plot shows the influence of the latlong effect. The bottom left plot shows the influence of the cluster effect, and the bottom right plot shows the influence of the vessid effect.

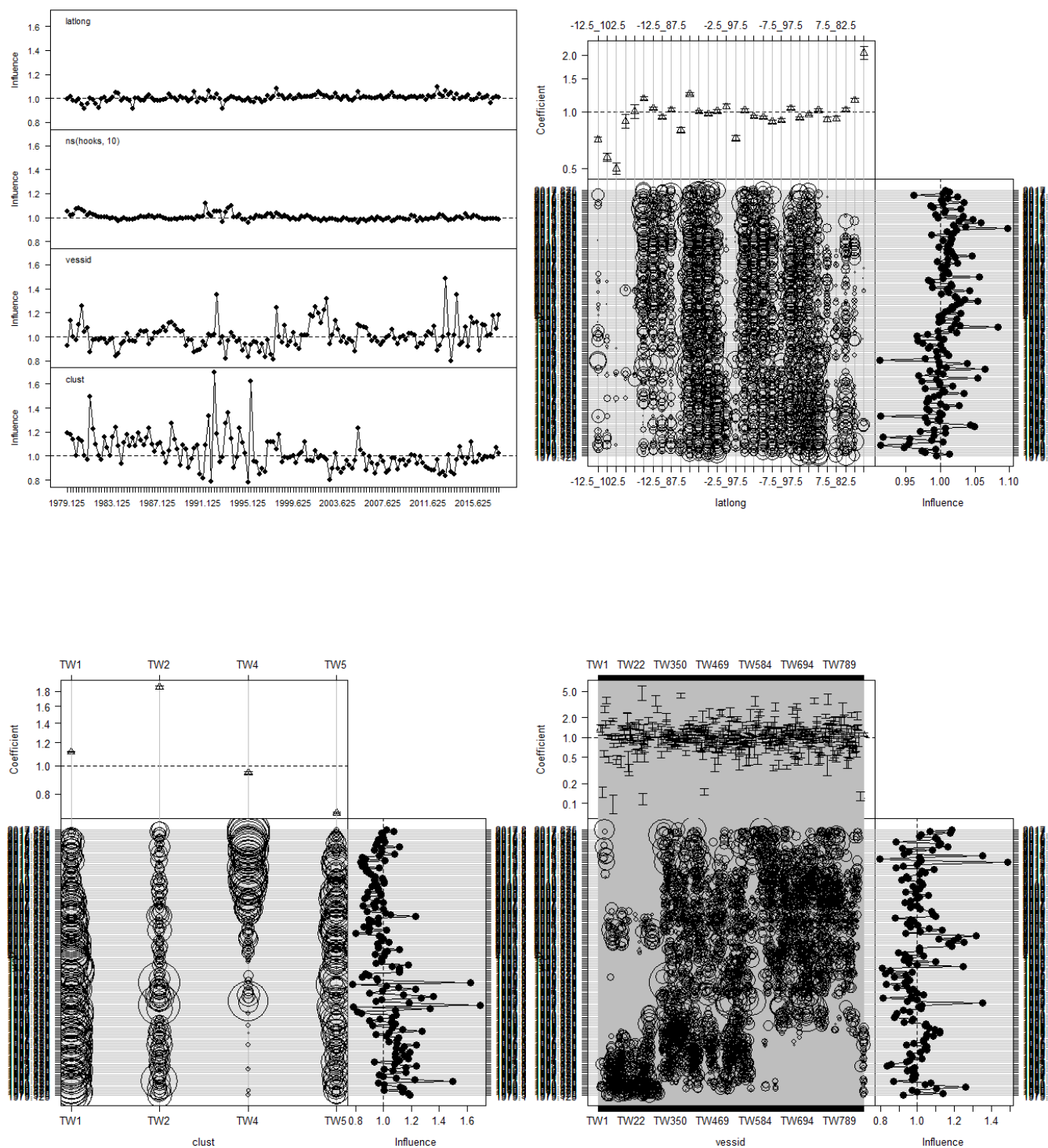


Figure 39 Influence plots for yellowfin tuna CPUE in region 5 by the Taiwanese fleet. The top left plots shows the change in the CPUE time series caused by each covariate. The top right plot shows the influence of the latlong effect. The bottom left plot shows the influence of the cluster effect, and the bottom right plot shows the influence of the vessid effect.

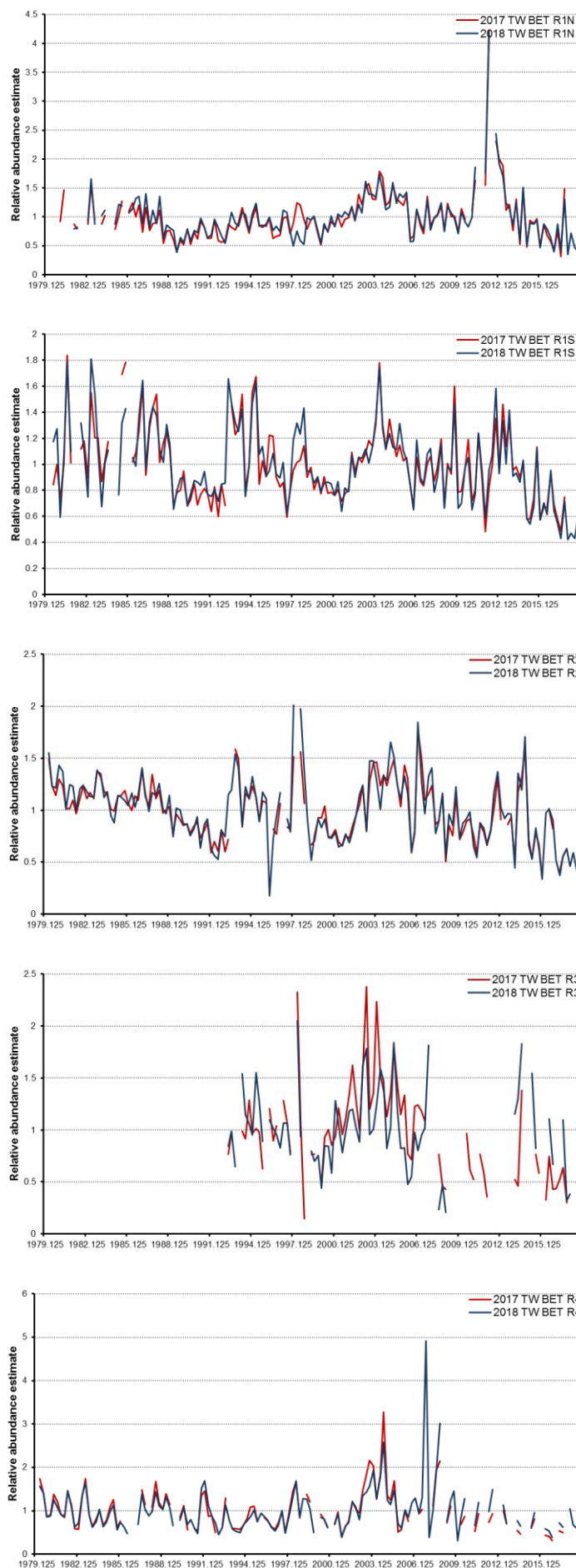


Figure 40. Comparisons of bigeye CPUE time series estimated in this analysis (blue) and estimated in 2017 (red)

by regions.

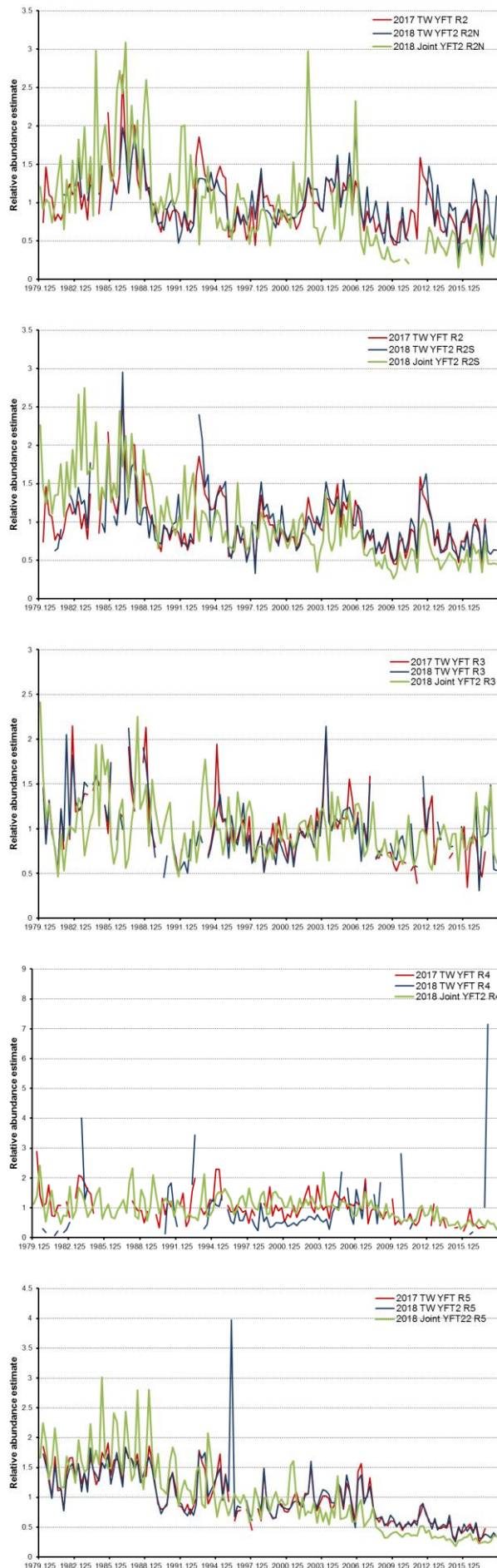


Figure 41. Comparisons of yellowfin CPUE time series estimated in this analysis (blue), estimated in 2017 (red)

and estimated in 2018 Joint work (green) by regions.

Region 1N

Region 1S

Region 2

Region 3

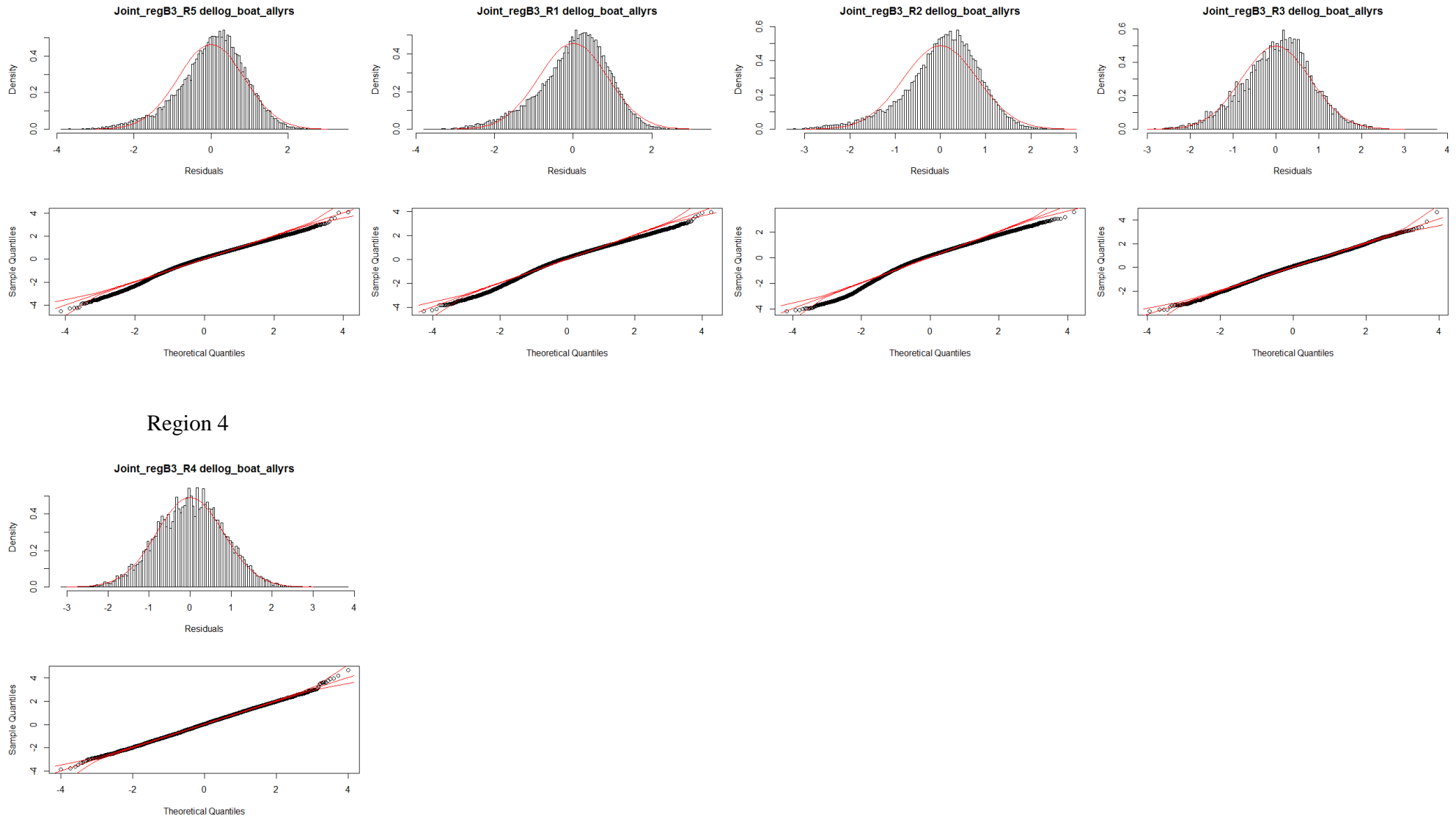
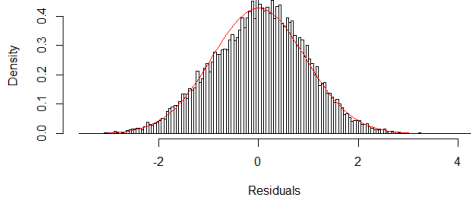


Figure 42. Residual diagnostics (as histogram and QQ plot) on bigeye tuna CPUE indices by regions.

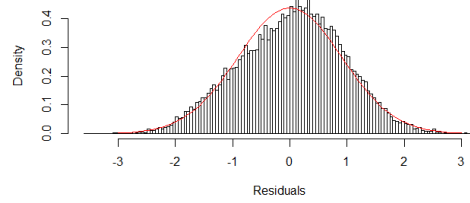
Region 2N

Joint_regY2_R7 dellog_boat_allyrs



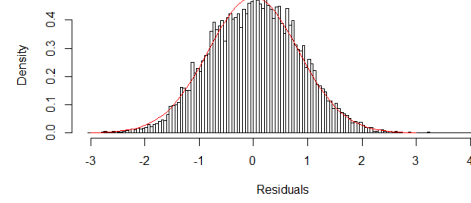
Region 2S

Joint_regY2_R2 dellog_boat_allyrs



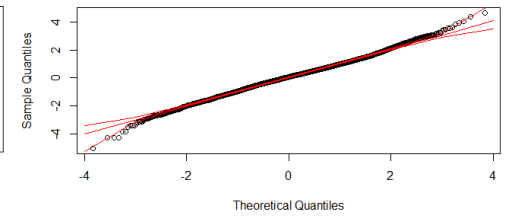
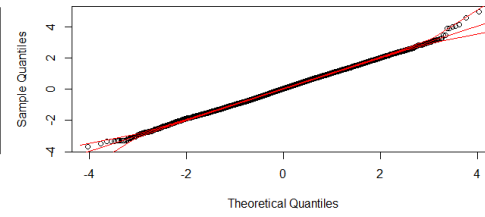
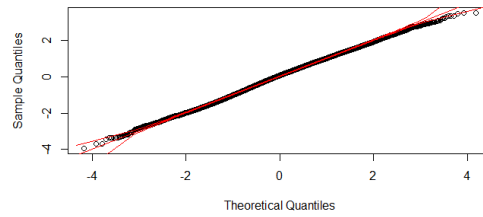
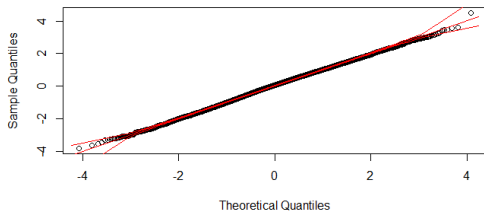
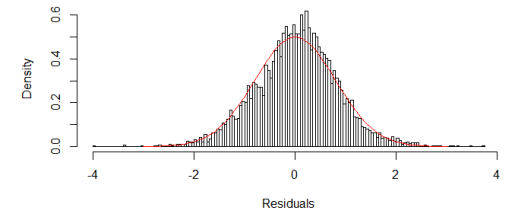
Region 3

Joint_regY2_R3 dellog_boat_allyrs



Region 4

Joint_regY2_R4 dellog_boat_allyrs



Region 5

Joint_regY2_R5 dellog_boat_allyrs

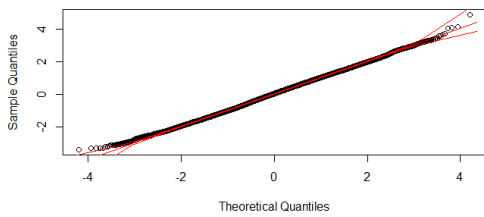
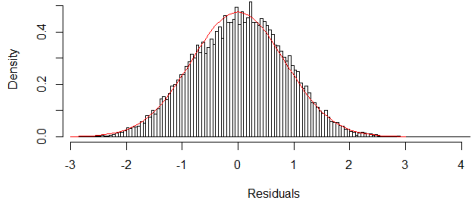


Figure 43. Residual diagnostics (as histogram and QQ plot) on yellowfin tuna CPUE indices by regions.

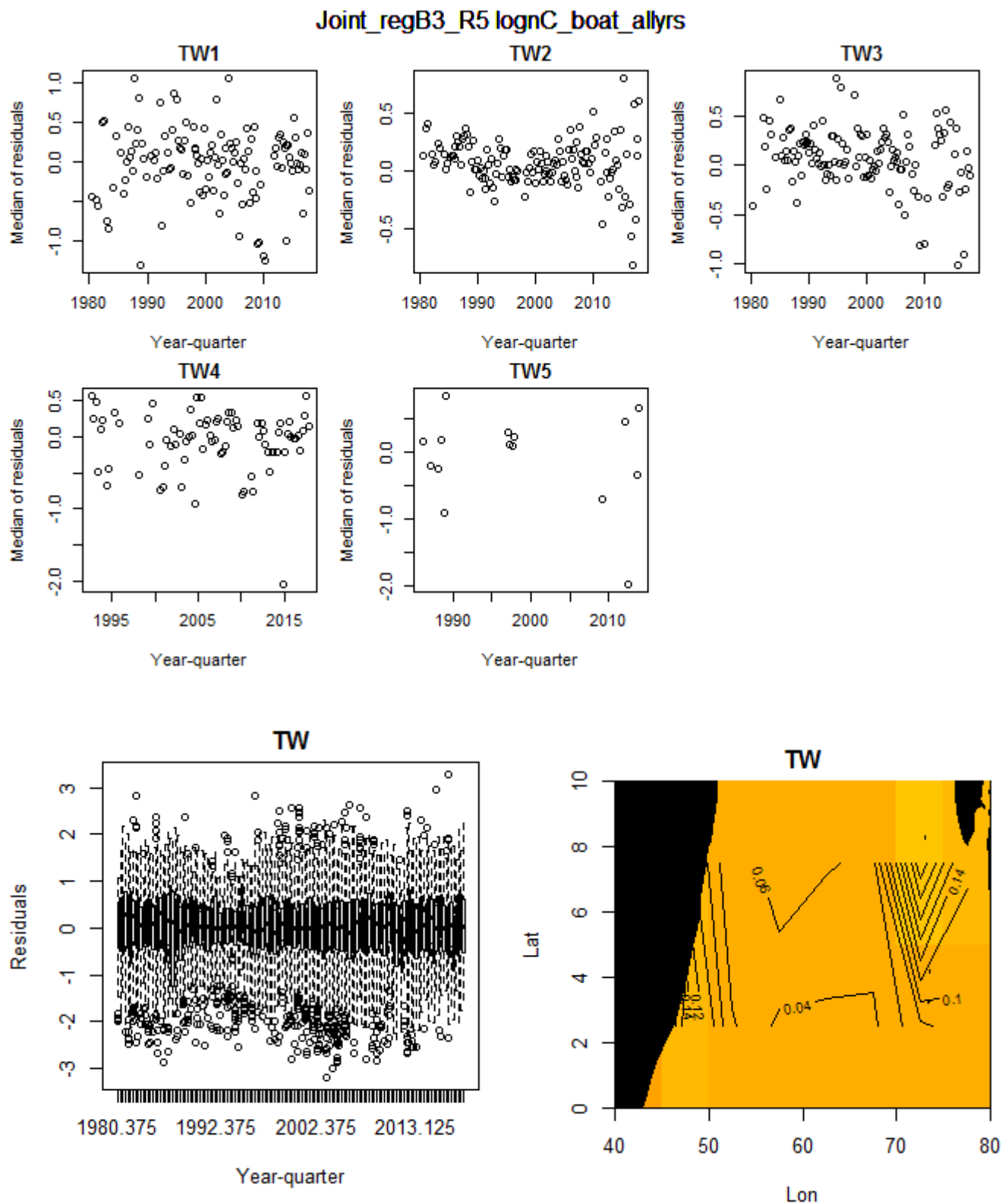


Figure 44. (Top) Median residuals from the lognormal constant model per year-quarter (x-axis), by cluster (subplots), for bigeye tuna in region 1N. (Bottom) Bigeye tuna residuals for regions 1N, median residuals are mapped by 5 cell (left) and plotted by year-quarter (right).

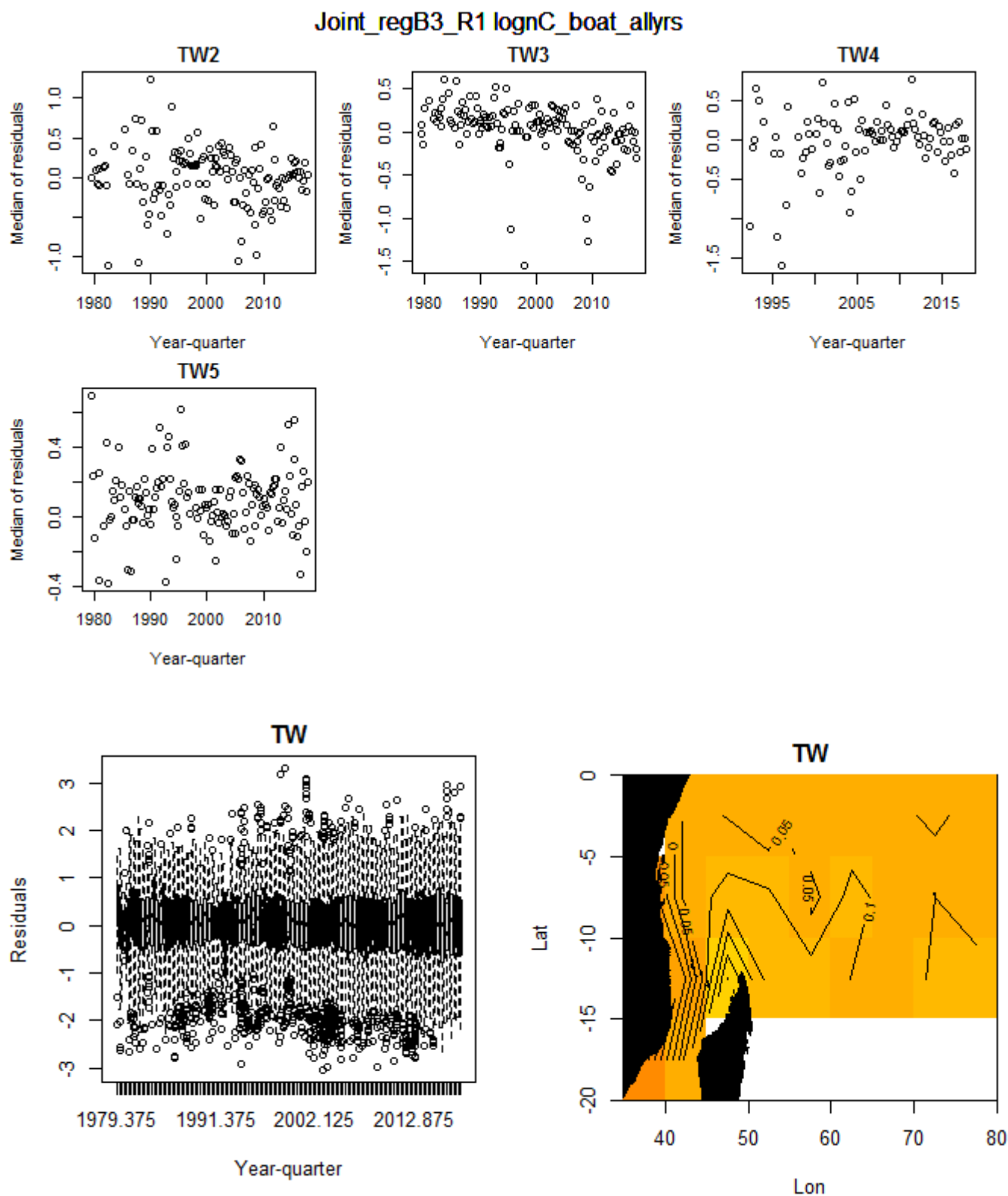


Figure 45. (Top) Median residuals from the lognormal constant model per year-quarter (x-axis), by cluster (subplots), for bigeye tuna in region 1S. (Bottom) Bigeye tuna residuals for regions 1S, median residuals are mapped by 5 cell (left) and plotted by year-quarter (right).

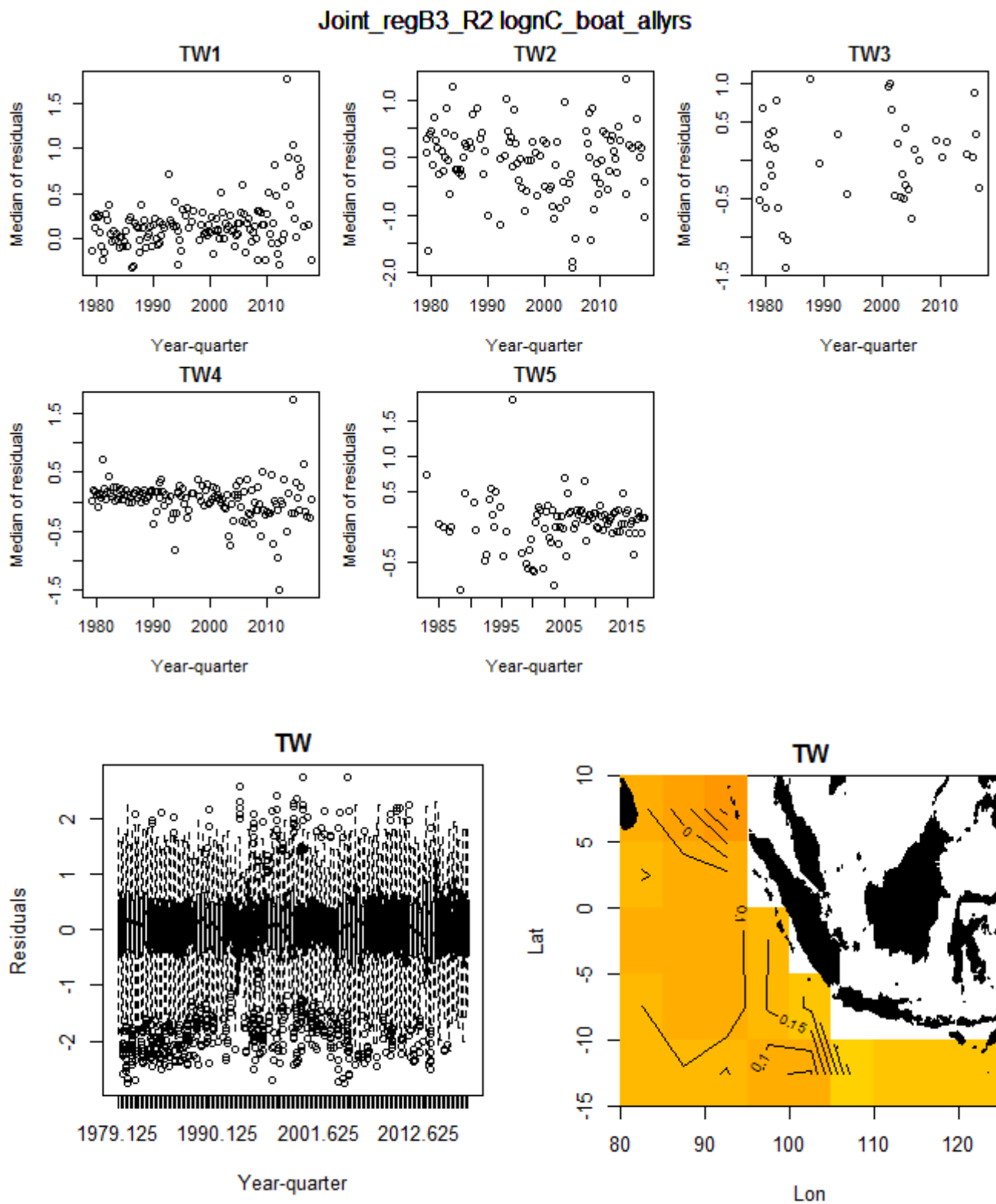


Figure 46. : (Top) Median residuals from the lognormal constant model per year-quarter (x-axis), by cluster (subplots), for bigeye tuna in region 2. (Bottom) Bigeye tuna residuals for regions 2, median residuals are mapped by 5 cell (left) and plotted by year-quarter (right).

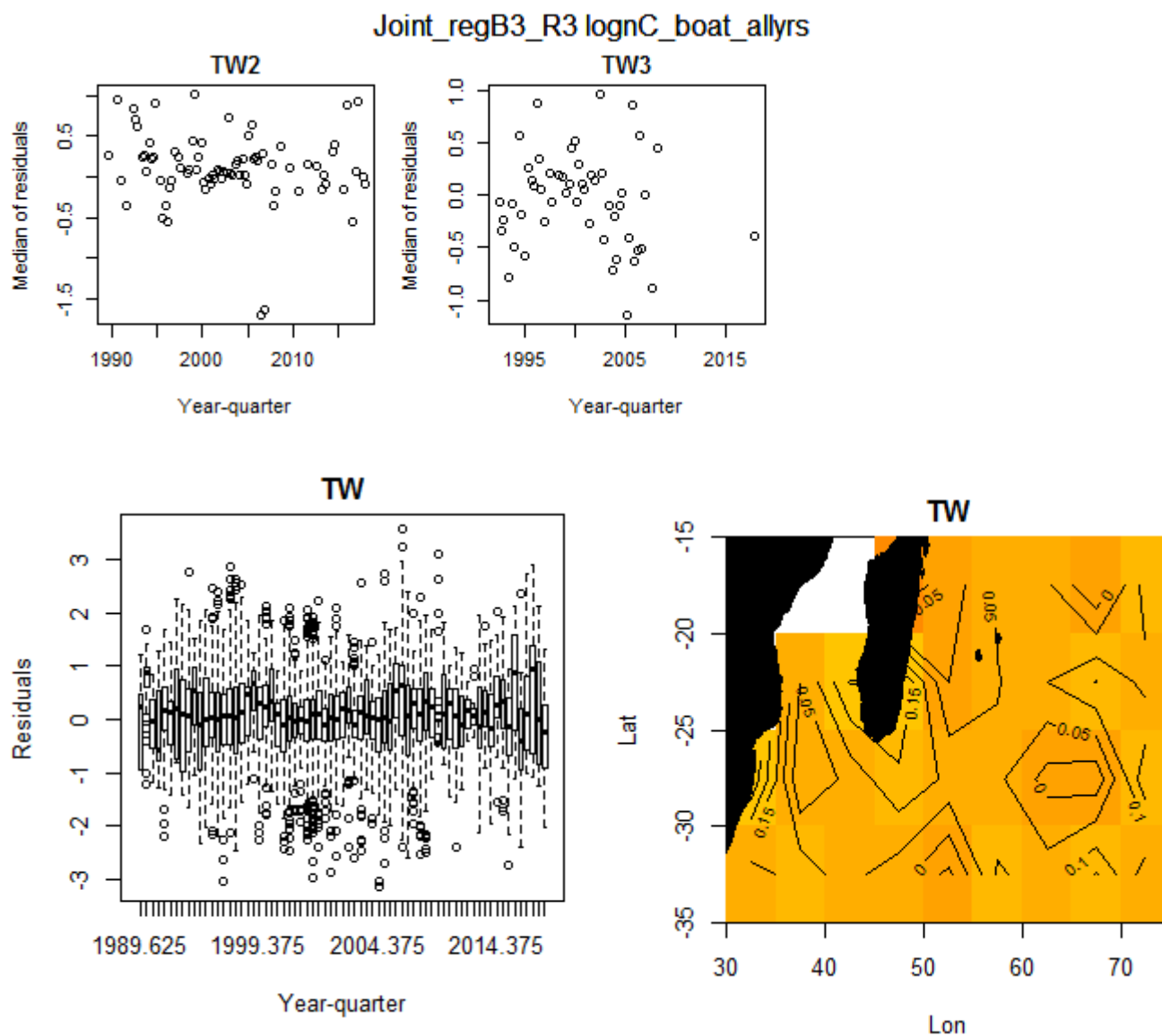


Figure 47. (Top) Median residuals from the lognormal constant model per year-quarter (x-axis), by cluster (subplots), for bigeye tuna in region 3. (Bottom) Bigeye tuna residuals for regions 3, median residuals are mapped by 5 cell (left) and plotted by year-quarter (right).

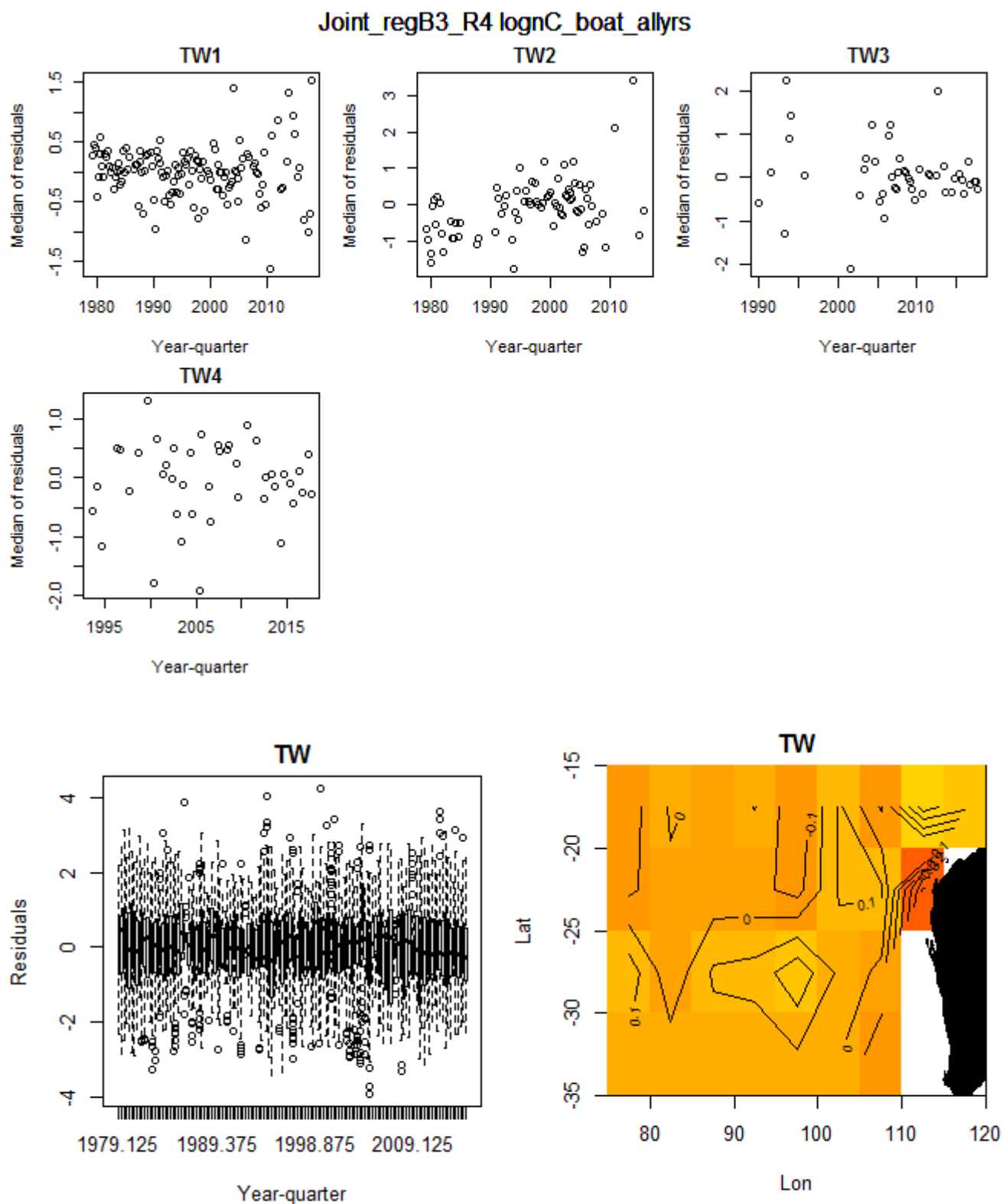


Figure 48. (Top) Median residuals from the lognormal constant model per year-quarter (x-axis), by cluster (subplots), for bigeye tuna in region 4. (Bottom) Bigeye tuna residuals for regions 4, median residuals are mapped by 5 cell (left) and plotted by year-quarter (right).

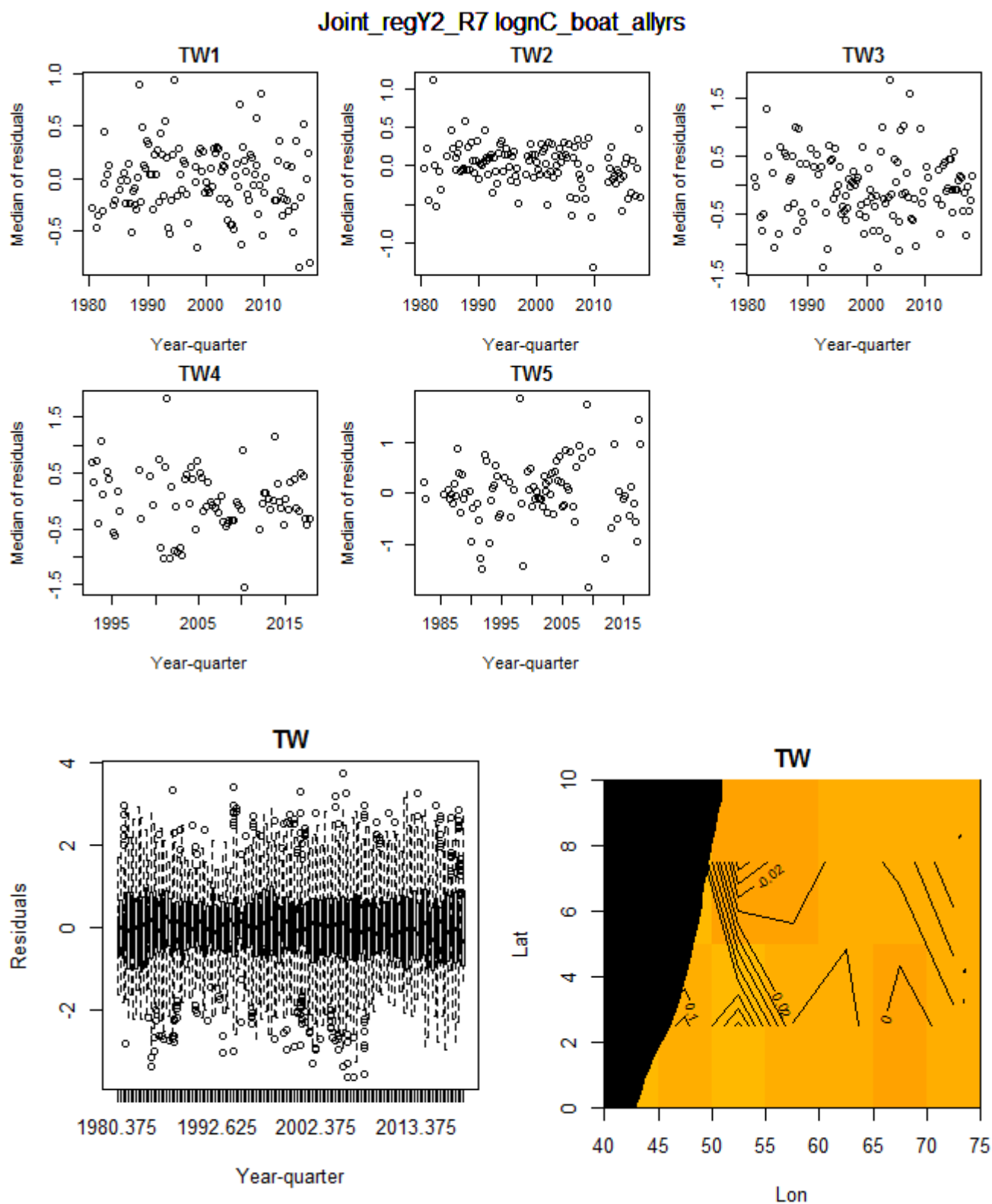


Figure 49. (Top) Median residuals from the lognormal constant model per year-quarter (x-axis), by cluster (subplots), for yellowfin in region 2N. (Bottom) Yellowfin tuna residuals for regions 2, median residuals are mapped by 5 cell (left) and plotted by year-quarter (right).

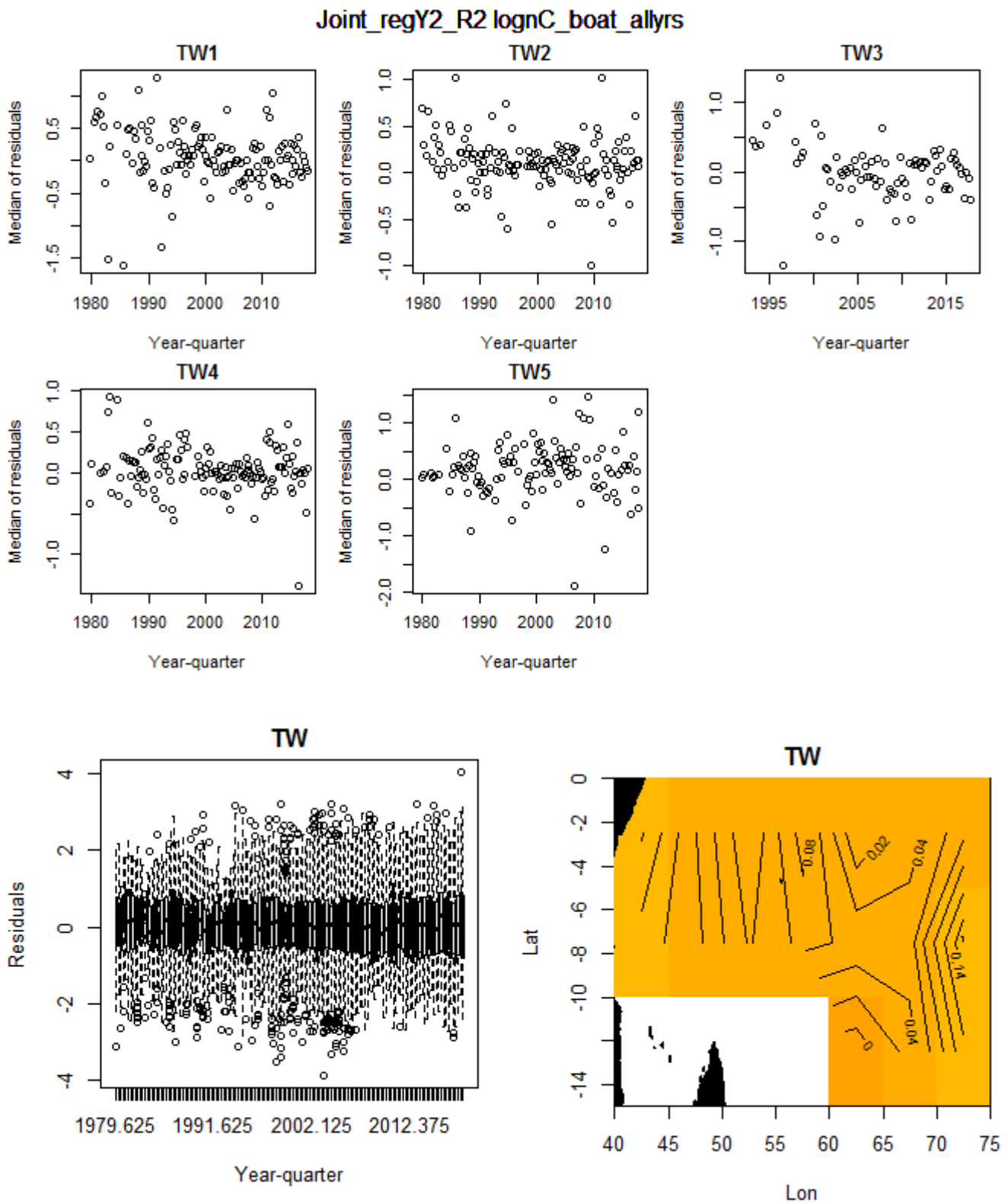


Figure 50. (Top) Median residuals from the lognormal constant model per year-quarter (x-axis), by cluster (subplots), for yellowfin in region 2S. (Bottom) Yellowfin tuna residuals for regions 2, median residuals are mapped by 5 cell (left) and plotted by year-quarter (right).

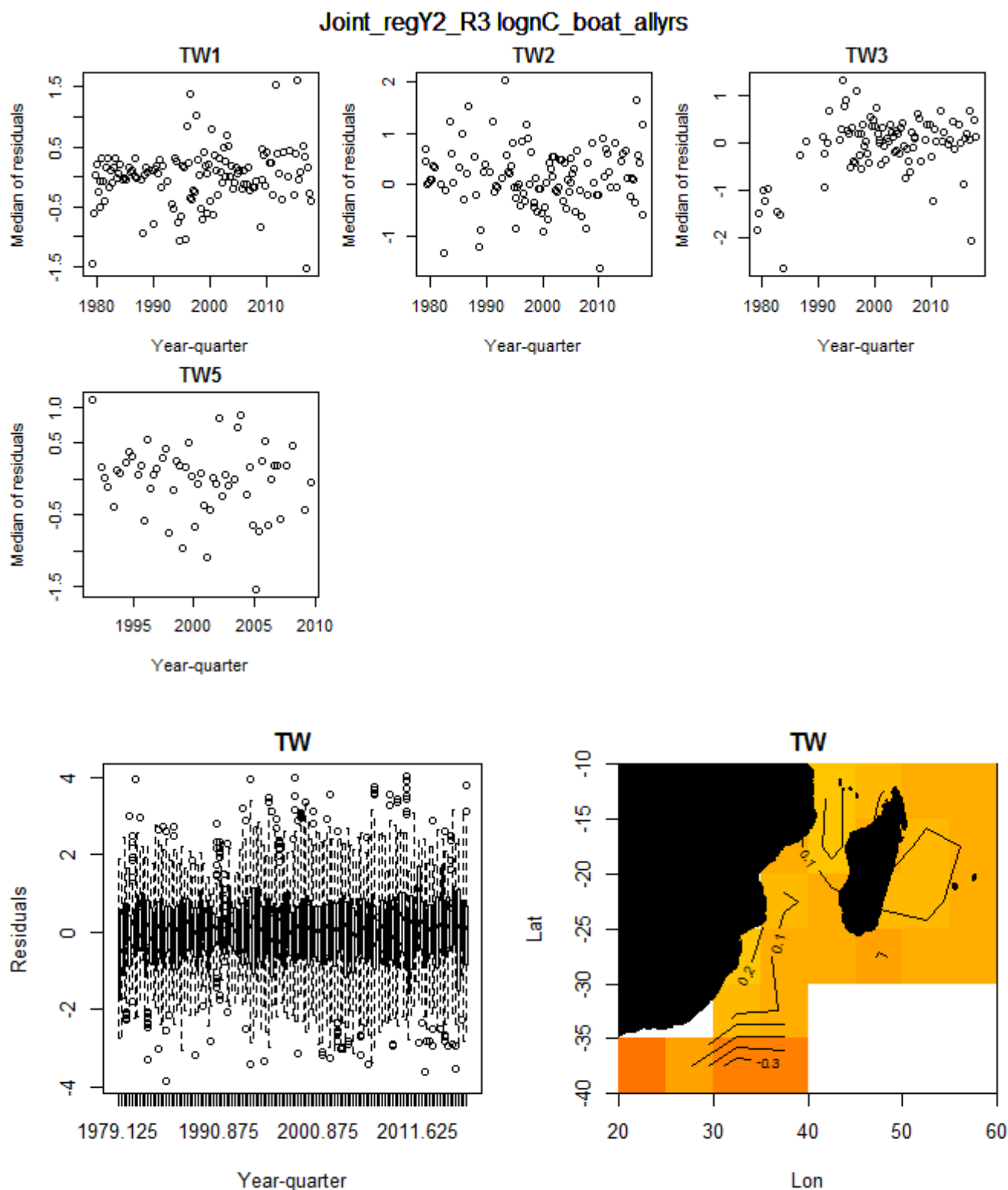


Figure 51. (Top) Median residuals from the lognormal constant model per year-quarter (x-axis), by cluster (subplots), for yellowfin in region 3. (Bottom) Yellowfin tuna residuals for regions 3, median residuals are mapped by 5 cell (left) and plotted by year-quarter (right).

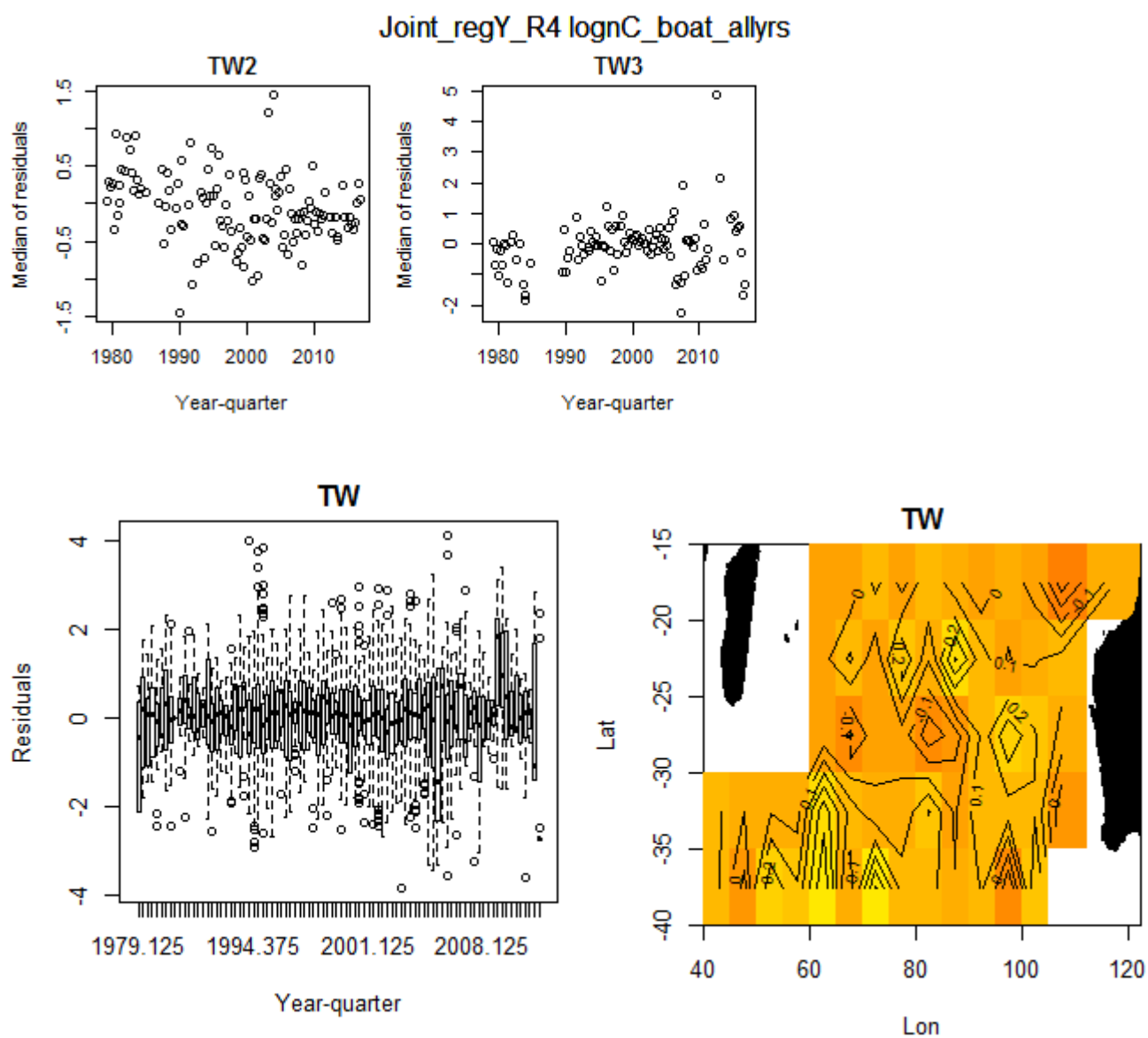


Figure 52. (Top) Median residuals from the lognormal constant model per year-quarter (x-axis), by cluster (subplots), for yellowfin in region 4. (Bottom) Yellowfin tuna residuals for regions 4, median residuals are mapped by 5 cell (left) and plotted by year-quarter (right).

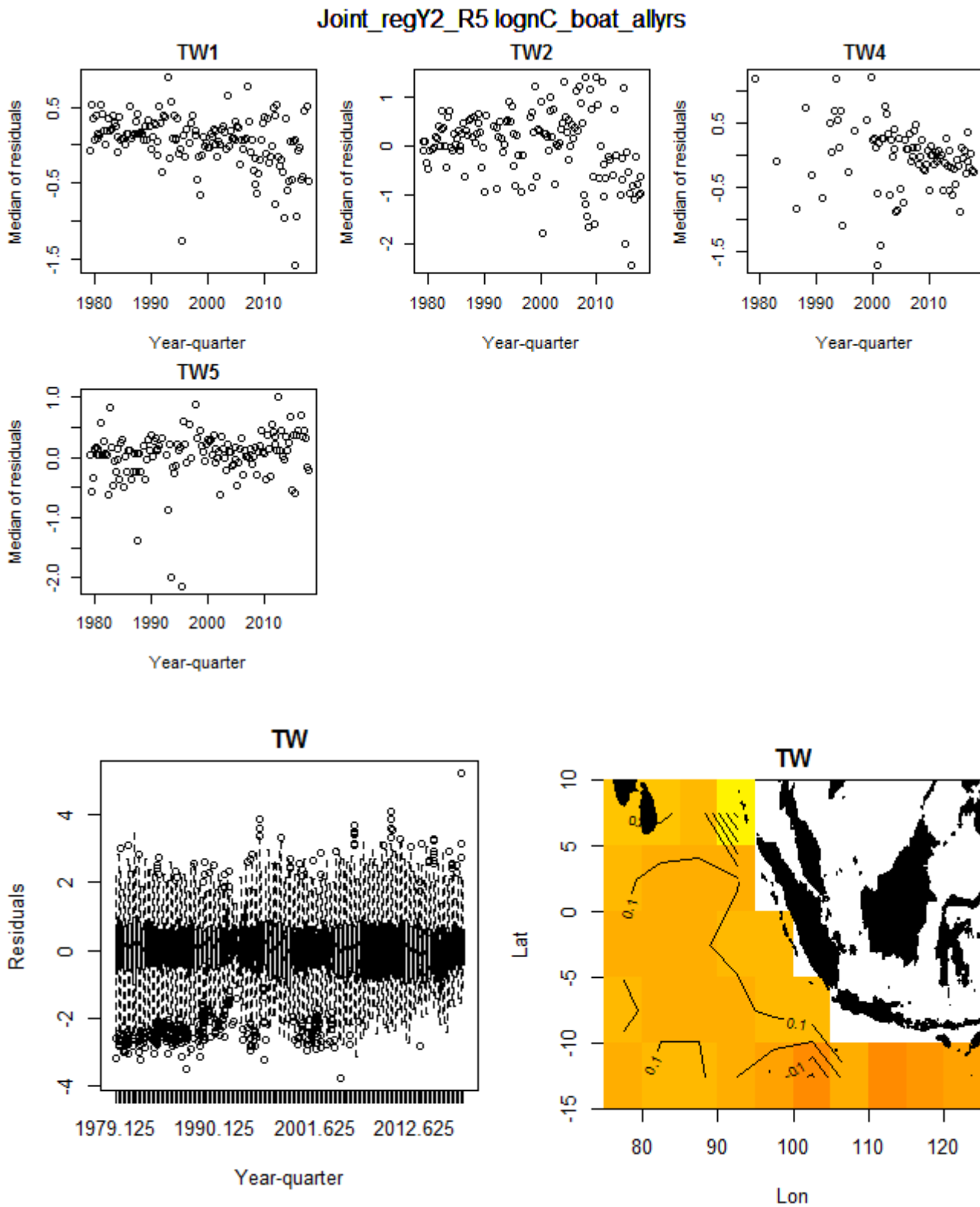


Figure 53. (Top) Median residuals from the lognormal constant model per year-quarter (x-axis), by cluster (subplots), for yellowfin in region 5. (Bottom) Yellowfin tuna residuals for regions 5, median residuals are mapped by 5 cell (left) and plotted by year-quarter (right).